Electrochemical removal of nitrate from waste water

PhD Thesis

Florina Maria CUIBUS (b. BĂLAJ)

Scientific Supervisors:

Prof. Univ. Dr. Ing. Petru ILEA
Prof. Univ. Dr. rer. nat. habil. Andreas BUND

Cluj Napoca

2012

urn:nbn:de:gbv:ilm1-2012000118

Acknowledgements

I feel emotionally moved when it comes to acknowledge after the task is accomplished. My mind is full of images of those who directly or indirectly helped me. I thank to all. First of all, I remember my parents who have contributed in making what I am today. Thank you for the support and concern given through all these years.

It is my privilege to express my sincere thanks and gratitude to Prof. Petru Ilea (Physical Chemistry, Babes Bolyai University Cluj Napoca) for his guidance, support and encouragement through the research work. He gave me a truly interesting topic to work in and sparked my interest for the electrochemistry. His dynamism and day-to-day monitoring of every detail were a constant source of inspiration to me. Besides, I thank him for giving me the opportunity to be part of a research project. I will always treasure his guidance and cooperation.

I express my great depth of gratitude to Prof. Andreas Bund (Elektrochemie und Galvanotechnik II, Technische Universität Ilmenau) for guidance, whole hearted support and encouragement in accomplishing the present work. I would like to thank him for giving me the opportunity to study in Germany, to obtain a DAAD scholarship, to be a member of the team and for having faith in me. Besides, I thank him for giving me the opportunity to participate in many national and international conferences.

I would like as well to thank my supervisors, for the appreciable help given within all these years and also for all the corrections and suggestions in writing articles and abstracts for conferences.

I would like to express my deep sense of gratitude to Lector Dr. Sorin Dorneanu (Physical Chemistry, Babes Bolyai University Cluj Napoca) for initiating me in the "nitrate world". I would like to thank him for his help in analyzing and interpretation of the data, without which it could not have been possible to complete the thesis. Besides, I thank him for all the helpful scientific discussions.

I highly appreciate the help and support given by my colleagues: Szabolcs, Codruța, Florica, Bianca, Mihaela, Vasile, Adriana, Romeo and Florin (Physical Chemistry, Babes Bolyai University Cluj Napoca).

I would like to express my gratitude to Dr. Adriana Ispas (Elektrochemie und Galvanotechnik II, TU Ilmenau) for the help and advices given during my research work.

I would like to thank to Dr. Udo Schmidt (Elektrochemie und Galvanotechnik II, TU Ilmenau) for the support and helpful discussions.

I highly appreciate the help extended by Dr. Svetlozar Ivanov (Elektrochemie und Galvanotechnik II, TU Ilmenau) and thank him for his friendly and ready help for carrying out some measurements. Besides, I thank him for the support and helpful discussions.

I would like to thank to my colleagues: Ralf, Cornel, Violeta, Magali and Yuze (Elektrochemie und Galvanotechnik II, TU Ilmenau) for the help and support given during my PhD.

I wish to place on record my deep sense of gratitude for the help given by faculty, department and supporting staff members of the both departments for their prompt help and co-operation at various phases of the research work.

Many thanks are addressed to Ellen Kern (Physical Chemistry, TU Dresden), Rolf Grieseler (ZMN, TU Ilmenau) for the SEM and EDX measurements and to Anneliese Täglich (Elektrochemie und Galvanotechnik II, TU Ilmenau) for the IC measurements.

This work was financially supported by the "Sectoral Operational Programme Human Resources Development 2007 – 2013, Priority Axis 1 "Education and training in support for growth and development of a knowledge based society", Key area of intervention 1.5: Doctoral and post-doctoral programmes in support of research, Contract SOPHRD/6/1.5/S/3, Project Title: „Doctoral studies: through science towards society". I thank SOPHRD for the financial support.

The Research Grant for Doctoral Candidates and Young Academics and Scientists (Forschungs-/ Studienstipendium) DAAD is greatly appreciated for the research stay at the TU Ilmenau.

The travel grant of the "Frauenförderung der TU Ilmenau" for the conference travel in Boston, USA is greatly appreciated.

I wish to extend my gratitude to my closer friends and I thank them for their encouragement and support through the work. And last, but certainly not least, I thank my husband Radu who was always there when I needed him and who was a great support through all this process.

Thanks to God for all His Blessings and wish for accomplishing this work.

Florina Maria Cuibus

TABLE OF CONTENTS

List of Abbreviations

ADI	Acceptable Daily Intake
ASTM	American Society for Testing and Materials
CA	Chronoamperometry
CE	Counter Electrode
CHV	Cyclic Hydrodynamic Voltammetry
CP	Chronopotentiometry
CV	Cyclic Voltammetry
DEMS	Differential Electrochemical Mass Spectrometry
DO	Dissolved oxygen
DSA	Dimensionally Stable Anode
ECSCF	European Commission's Scientific Committee on Food
EDX	Energy Dispersive X-Ray detector
EPA	Environmental Protection Agency
ER	Electrochemical Reactor
ERN	Electrochemical Reduction of Nitrate
FIA	Flow Injection Analysis
HER	Hydrogen Evolution Reaction
HPLC	High Performance Liquid Chromatography
IC	Ion Chromatography
LSV	Linear Sweep Voltammetry
MCL	Maximum Contaminant Level
OER	Oxygen Evolution Reaction
QCM	Quartz Crystal Microbalance
RDE	Rotating Disk Electrode
RE	Reference Electrode
RRDE	Rotating Ring Disk Electrode
SCE	Saturated Calomel Electrode
SEM	Scanning Electron Microscopy
SWV	Square Wave Voltammetry
USEPA	United States Environmental Protection Agency
WE	Working Electrode

Symbols

A	Electrode surface
α	Charge transfer coefficient
c_0	Bulk concentration
c	Concentration
C_t	Concentration of nitrate at time t
C_i	Initial nitrate concentration
D	Diffusion coefficient
Δε	Peak potential difference
ΔE_{step}	voltage step of the staircase voltage ramp
ΔE_p	amplitude of superimposed pulse (pulse height)
E	Potential
$E^{0'}$	Standard formal potential
E_{step}	Scan increment
ω	Electrode rotation rate
F	Faraday constant
f	Frequency
ϕ	Diameter
Ip,a	Anodic peak current
Ip,c	Catodic peak current
$\varepsilon_{p,a}$	Anodic peak potential
$\varepsilon_{p,c}$	Catodic peak potential
i	Current density
i_p	Peak current
I_L	Limiting current
k	apparent rate constant
n	Number of transferred electrons
ν	Kinematic viscosity
R	Universal gas constant
r_F	Current efficiency
S	Selectivity
t_{step}	Waveform period
V_R	Volume of the electrolyte
ν	Potential scan rate

W_s	Energy consumption
z	Number of transferred electrons
z_c	Number of electrons transferred in the rate determining step
Q_R	Flow rate

AIM OF THE THESIS

The electrochemical reduction of nitrate has a great importance mainly for environmental and analytical purposes. During the last years, the interest has been focused on the conversion of nitrate to the non-toxic nitrogen gas from wastes where the biological method cannot be applied. However, there are many types of waste water in which the biological method cannot be applied due to the toxic environment for the bacteria. Such waste waters are those containing toxic organic compounds, heavy metals, high concentration of nitrate or other salts at extremely high or low pH values and as well the low level nuclear wastes. Therefore, it is a major challenge to develop a complementary method for the treatment of wastes in which the biological method cannot be applied.

Two important factors must be recognized in discussing the influence of experimental conditions on the reduction of nitrate. Firstly, it must be stressed that the products, rate of reduction and mechanism can all depend on a large number of experimental parameters including the electrode material, the concentration of nitrate, pH, other deliberately added ions/molecules or impurities, electrode potential (or current density), mass transfer regime and passed charge. Secondly, the experiments carried out have been strongly influenced by the target application. For example the range of nitrate concentration when the objective is an analytical procedure or a water treatment is quite different from that for a synthesis or met in nuclear waste treatment. In this way, we have selected pH and electrode material as the principle parameters in this discussion.

The electrochemical method used within this doctoral thesis study was focused on the removal of nitrate from alkaline model nitrate solutions. The electrochemical methods offer a much broader application range in comparison to the biological method.

This thesis explains how the rising nitrate levels in groundwater come and where the danger lays when high nitrate concentrations are found in drinking water. The state of art and the literature regarding the variety of methods for removing nitrates from water has been described in detail here (Chapter 2). The literature reported to the nitrate reduction with benefits and problems of the used methods is also explained in Table 3.1.

A review of the methods, electrode materials and their combination with other metals (alloys) dealing with nitrate reduction has been reported (Chapter 2 and 3). By applying the electrochemical methods, the conversion of nitrate to nitrogen is a very difficult task due to the formation of toxic by–products; products which depend strongly on the nature of the electrode material (Chapter 3). Most extensive was described the study of the electrochemical reduction of nitrate (ERN).

The research performed within this doctoral thesis is divided in three parts. The first part of the study has been focused on synthesizing and characterizing of electrode materials which are suitable for ERN (Chapter 5). Most of the characterization measurements have been proposed to collect additional information which will be used to obtain a range of electroplating conditions in which adherent and uniform coatings can be produced. The deposits obtained will serve as an electrode material/electrocatalysts in ERN. A number of techniques, including scanning electron microscopy and X-ray spectroscopy were used to provide the information on these coatings development processes.

The second part of the study deals with an electrochemical method for monitoring / determining easy and quickly the species resulting from ERN (Chapter 6). Square-wave voltammetry and cyclic hydrodynamic voltammetry are known to be powerful analytical tools. In the same time, the rotating ring-disc electrode technique is also an important tool for the detection of reaction intermediates.

The last part of the thesis deals with the reduction of nitrates in an electrochemical flow reactor (Chapter 7). The cell was operated in a divided configuration, to remove possible interferences such as nitrite oxidation at the anode. Constant current electrolyses were performed using various cathode materials and a model nitrate solution. The concentration of nitrate and nitrite were monitored during the electroreduction process. The electrolytes were recirculated through the cells compartments with a double channel peristaltic pump, having a monitored flow rate. In order to analyse the nitrate and nitrite concentration, at specific time intervals, samples were withdrawn from the cathode compartment by using a syringe and were analysed by ion chromatography. Apparent rate constants, influence of flow rate, current efficiencies and energy consumptions were evaluated within this chapter. Moreover, a comparison of the two electrode materials was performed.

LITERATURE REVIEW

1. NITRATES AND THEIR PRESENCE IN THE ECOSYSTEM

1.1. Water – source of life

To obtain freshwater of high quality directly from the kitchen tap is something that many of us take for granted. We use it every day to prepare our food, to wash our clothes and for many other things. In some places, increasing environmental pollution has made many wells unsuitable as freshwater sources. Use of water treatment techniques is needed in order to meet society's need of high quality water. The regulations on the water quality are continuously getting stricter as new and better analytical instruments are developed, making it possible to detect lower levels of impurities. What is regarded as good water quality depends on the application. Potable water should be free from toxic and harmful substances. Ultrapure water on the other hand, is not considered as high quality drinking water, where some minerals are desirable. The taste, smell and visual appearance of the water are other important aspects of drinking water quality. Furthermore, there are some technical aspects of a suitable drinking water that are considered. For example, there are regulations on the pH and conductivity of the water in order to reduce corrosion problems in pipes. The definition of clean water in many industrial applications is completely different compared to the potable water. The microelectronic and pharmaceutical industries require extremely pure water in their processes. In power plants, ultrapure water is used to reduce problems with corrosion that could be a serious problem at the temperatures and pressures present in the heat exchanges. The production of this ultrapure water requires sophisticated water treatment systems. For many industrial processes, a zero waste target is on the agenda. Water treatment systems are used to reduce emission of e.g. heavy metals for environmental reasons. There might also be an economical advantage if chemicals used in the process can be recycled.

1.2. Sources of nitrate

The increase in nitrate (NO_3^-) level in water can be linked to several sources of human activity. Owing to agricultural and industrial activities, the nitrate concentrations levels in surface and groundwater have increased to such an extent that the admitted standards in drinking water have been largely exceeded in many regions in the world. Nitrate is a wide spread contaminant of ground and surface waters due to excessive use of nitrogenous

fertilizers in agricultural activities and disposal of untreated sanitary and industrial wastes [1, 2, 3]. Nitrates from fertilizers, decaying plants, manure and other organic residues are a common component of water and vegetarian food. Excessive use of natural or synthetic nitrogenous fertilizers and/or use of sewage water for crop irrigation lead to an accumulation of nitrates, particularly in the leaves. Usually plants take up these nitrates, but sometimes rain or irrigation water can leach them into groundwater or drain them to surface water. Common sources of nitrate include [4]:

- Excessive use of fertilizers;
- Municipal wastewater and sludge;
- Nitrogen fixation from atmosphere by vegetables, bacteria and lightning.

The problem of nuclear waste treatment represents another aspect of NO_3^- removal because this ion significantly increases the volume of waste and has a negative impact on the waste cohesion [5].

1.3. The nitrate health risk

The effects of nitrate on health are well known. Elevated nitrate concentrations in drinking water are linked to human and animal health problems. The US Environmental Protection Agency (EPA) has set the maximum contamination level (MCL) of nitrate to 45 mg/L in the United States, while the European Union legislation admits a maximum level of 50 mg/L of nitrates and 10 mg/L of nitrites for drinking water [6, 7]. Such contaminations represent high risks for public health causing serious diseases like bladder disorders and methemoglobinemia. Elevated nitrate levels in water are matters for concern, because plasma nitrate can interfere with blood-oxygen levels, leading to methemoglobinemia and gastric cancer [8]. Methemoglobinemia arises out of the excessive conversion of hemoglobin (containing ferrous ions) to methemoglobin (containing ferric ions), which is incapable of binding and carrying oxygen. Methemoglobinemia [9] was reported in all age groups consequent upon high nitrate ingestion. However, infants and those above 45 years old are most susceptible to nitrate poisoning. The causes, symptoms and treatment of methemoglobinemia are well studied. While methemoglobinemia may be due to anemia, and cardiac or pulmonary disease, it is more often caused by high concentration of chemical contaminants in food or water. Nitrates and nitrites are an important cause for methemoglobinemia, aggravated by congenital deficiencies of the enzyme nitrate reductase that effectively lowers nitrate concentrations. A visible symptom of methemoglobinemia is cyanosis, a grayish-blue

color of the skin, even when about 10 % of total hemoglobin is affected. Other symptoms are nausea, headache, weakness; abnormally rapid heartbeat (tachycardia), breathlessness (dyspnoea), chest pain and mental changes.

Excess quantities of nitrates are converted to nitrite in the gastro-digestive system. Nitrites are transformed into nitro-compounds, such as the nitrosamines, which adversely affect metabolic processes and hence cause health hazards. The European Commission's Scientific Committee on Food (ECSCF) fixed the acceptable daily intake (ADI) of nitrate at 3.65 mg/kg body wt/day. Certain substances such as vitamin C and E inhibit the transformation of nitrate to nitrite reducing nitrate related toxicity to some extent.

2. NITRATE REMOVAL METHODS

Various methods such as biological, physicochemical and electrochemical techniques have been proposed for the removal of nitrate from potable water and wastewaters. The physicochemical processes such as ion exchange [10], reverse osmosis [11] and electrodialysis [12] produce secondary brine wastes, because the nitrates are merely separated but not destroyed.

The ideal process for nitrate removal would be able to treat large volumes of water at a low cost. Furthermore it is desirable that the process adapts well to different feed loads and works without the addition of any chemicals.

The biological method for the removal of nitrate from waste water is the method of choice. In this method, bacteria convert nitrate to non-toxic nitrogen gas with a yield of about 99% [13]. However, there are many types of waste water in which the biological method cannot be applied due to the toxic environment for the bacteria. Such waste waters are those containing toxic organic compounds, heavy metals, high concentration of nitrate or other salts and extreme pH values. Examples of such waste waters are the low level nuclear wastes. Therefore, it is a major challenge to develop a complementary method for the treatment of wastes in which the biological method cannot be applied. This method must combine: high rate and high selectivity of conversion of nitrate to nitrogen, low operation costs and broad range of applications, regardless of the solution composition.

2.1. Biological denitrification

Biological denitrification [10, 14], is commonly used for treatment of municipal and industrial wastewater. Although the biological denitrification represents the most used method, it has several disadvantages e.g. it is slow, difficult to control, produces organic residues, requires intensive maintenance and a constant supply of the organic substrate [10]. A concern for bacterial contamination of the treated water has made the transfer to production of drinking water slow. The main advantage of using biological nitrate reduction is that the nitrate is turned into nitrogen gas reducing problems with waste solutions. Biological denitrification is however quite slow and thus large installations are required. Furthermore, the bacteria responsible for the transformation of nitrate into nitrogen are sensitive to changes in environmental conditions. Temperature and pH have to be kept within a narrow range. This together with the need for relatively large installations makes the biological methods expensive. Biological methods which, in

addition to being slow and difficult to control, cannot be used for nitrate concentrations larger than 1000 mg/L to avoid poisoning the bacteria. The biggest problem for biological denitrification is the presence of excess biomass (bacteria) or dead biomass. Therefore post-treatment, disinfection and oxygenation of the products are generally needed, making in this way the biological methods expensive.

2.2. Physico-chemical removal

The processes based on ion exchange [15], reverse osmosis [16] and electrodialysis have a lower efficiency if compared to biological denitrification, but they seem very interesting for medium and small applications or under emergency conditions [16]. Among physical-chemical methods for nitrate ions removal from water, ion exchange is most widespread. A major impediment to the removal of nitrate ions by ion exchange method is the presence of SO_4^{2-} ions, which compete with NO_3^- ions. To remove nitrate ions using the ion exchange method, highly basic anions should be used, as for example Cl^- ions. It should be noted that in the ion exchange process, the HCO_3^-anion is removed along with NO_3^-. Therefore, the acidity of water increases, requiring additional correction of pH from 7.0 to 7.5. The rate of nitrogen compounds removal using reverse osmosis method depends most from the pressure applied and the concentrations of dissolved substances. Under these conditions, reverse osmosis has some disadvantages:

- the method is expensive if the polluted water salinity is high, thus it requires a pre-treatment before being subjected to removal of nitrates;
- the membranes require periodic cleaning;
- the resulting concentrated solutions need further treatment.

Low costs, larger automation possibilities, process parameters control and no need of extensive post-treatment are advantages of these processes. But even so, reverse osmosis methods allow only a concentration of nitrogen compounds and not a conversion into less toxic compounds. Concentrated nitrate solutions are obtained and represent potential sources of pollution, hence additional methods of treatment and purification are required, which causes additional costs.

2.3. Electrochemical removal

Electrochemical reduction of nitrate has been studied extensively during last years in numerous works according to literature [17, 18, 19, 20, 21]. In this respect electrochemical

reduction catalysis could be advantageously applied to the treatment of potable and industrial wastewater, whereby nitrate species were transformed into harmless products at various cathode materials. Electrochemical methods do not require chemicals before or after the treatment, there is no sludge production, a small area is occupied by the plant and the investment costs are relatively low. Moreover, the increasing interest in the reduction of nitrate is connected with the increasing costs of the purification of drinking water [22].

The electrochemical techniques offer the following distinctive advantages for waste water treatment [23]:

- Environmental compatibility: the main reactant is the electron, which is a clean reagent.

- Versatility: electrolytic treatments can deal with solid, liquid, or gaseous pollutants to generate neutral, positively, or negatively charged inorganic or organic products, also inducing the production of precipitates, gaseous species, pH changes, etc. In addition, different reactors and electrode materials, shapes, and configurations can be utilized [24]. It is noteworthy that the same reactor can be used frequently for different electrochemical reactions with only minor changes, and that electrolytic processes can be scaled easily from the laboratory to the plant, allowing treatment of volumes ranging from mL to millions of litres, respectively.

- Safety: electrochemical methods are generally safe because of the mild conditions usually employed and the small amount and innocuous nature of the added chemicals.

- Energy efficiency: electrochemical processes are amenable to work at low temperatures and pressures, usually under ambient conditions. Up to now, the electrochemical methods did not meet industrial scale applicability because of the lack of highly efficient electrode materials [25]. Identification of a suitable electrode material will allow us to use the electrochemical methods for the treatment of wastewater.

Nitrate electroreduction leads to the coexistence of several products, more or less stable, like: nitrite, hydrazine, hydroxylamine, ammonia, nitrogen and other oxygen-containing nitrogen species [26]. From a practical and an environmental point of view, it is highly desirable that the electrochemical process transform nitrate efficiently and selectively into the harmless N_2 gas. Using the electrochemical reduction of nitrate (ERN), the final composition depends mainly on the pH, the applied potential and the used cathode material. On the other hand, electrochemistry provides promising solutions when it is combined with ion exchange, the last one being capable of NO_3^- selective removal from the waste water. The electrochemical alternative represents an attractive and promising solution for the removal of nitrate ions [23].

2.4. Conclusions

The electrochemical method used in this doctoral thesis was focused on the removal of nitrate from alkaline model nitrate solutions. According to this method, nitrate can be converted to the non-toxic nitrogen and nitrous oxide with a yield of 92% [13] which is in the same order with that of the biological method. In addition, the removal of nitrate is not affected by the presence of salts, toxic compounds and heavy metals. Based on the above discussion this method is the most advantageous among all the proposed alternative methods. The electrochemical method offers a much broader application range in comparison to the biological method.

3. SPECIFIC ASPECTS OF ELECTROCHEMICAL PROCESS USED FOR NITRATE REMOVAL

Literature concerning the topic of electrochemical removal offers important amount of data. In Table 3.1 (see page 28) an overview on specific parameters of electrochemical reduction of nitrate processes is presented. As presented in the introduction part, the electrode material plays an important role in the removal of nitrates. The materials used for nitrate reduction are described below.

3.1. Materials used in electrochemical reactors for nitrate reduction

3.1.1. Cathode electrode materials

A comparative study was performed to classify the materials used in cathodic reduction of nitrates. Previous investigations showed that the reduction efficiency of nitrate ions depends strongly on the nature of the material used to modify the electrode surface. The suggested criteria to differentiate the materials are as follows:

- carbon electrodes;
- monometallic electrodes, which are composed entirely of a single metal component;
- multimetallic electrodes, which are composed of two or more metal components.

3.1.1.1. Carbon electrodes

Electrodes based on carbon are in widespread use, because of their good electrical conductivity, low cost, chemical inertness and rich surface chemistry. The electron-transfer rate observed at carbon surfaces is often slower than that observed at metal electrodes. The most common carbon electrode materials are glassy carbon, carbon paste, carbon fibres, screen-printed carbon strips, carbon films, and other carbon composites. They differ in the relative density and orientation of the edge and basal planes at their surfaces.

Glassy (or vitreous) carbon is widely used for the electrochemical reduction of NO_3^- because of its mechanical and electrical properties (obtained by a controlled heating program of a phenol-formaldehyde resin in an inert atmosphere over 300-1200°C temperature range). An impregnating procedure is not required, because of its high density

and small pore size, but to create an active and reproducible surface a pre-treatment is usually applied by polishing to a shiny "mirror-like" appearance [27, 28].

The carbon-paste contains graphite powder blended with various water immiscible organic pasting liquids, including mineral oil, paraffin oil, silicone grease and bromo-naphthalene. In the absence of binder, the graphite electrode yields very rapid electron-transfer rates, similar to metallic electrodes. Carbon-paste electrodes offer an easily renewable surface, the disadvantage being the tendency of the organic binder to dissolve in solutions containing organic solvents [27, 28]. Generally, the carbon materials are often used as substrates for current collectors for cathodes in ERN.

3.1.1.2. Monometallic materials

The materials consisting entirely of a single metal are called monometallic electrodes. A series of cathode materials were investigated to establish their performance towards the electrochemical reduction of NO_3^- ions in aqueous solutions, such as palladium [29, 30, 31], platinum [32], rhodium [33, 34, 35], ruthenium [30], gold [36], silver [37], copper [38, 39], cobalt [40], nickel [41], zinc [41], tin [42], lead [41], and iridium [43, 44].

These coinage and transition metals have very different electrochemical properties. There are differences in the electrocatalytic activity, number of intermediates, nature of intermediates, influence of anions and efficiency towards selective formation of N_2. The electrochemical reduction of the nitrate ions was also studied (by cyclic voltammetry) at Pt in perchloric acid solution [32], which indicates that in the adsorbed hydrogen region the electrocatalytic nitrate reduction is inhibited by adsorption of hydrogen.

The electrochemical reduction of nitrate ions was investigated at Rh-modified monometallic electrodes by Brylev *et al*. [33]. The results clearly demonstrate that Rh/pyrolytic graphite electrodes obtained by potentiostatic electrodeposition are more efficient for NO_2^-reduction than for NO_3^- at room temperature. In this case N_2 is also produced, but its content is negligible; ammonia was found to be the main product of the reduction process.

Copper has the highest electrocatalytic effect among transition-metal monometallic electrodes for the cathodic reduction of nitrate ions in acid and in alkaline media [38]. The results seem to confirm that the adsorption-controlled reduction of nitrate anions to nitrite corresponds to the rate determining step. Nitrite is subsequently reduced to hydroxylamine, which appears as a short-life intermediate, because it is immediately reduced to ammonia. The competitive hydrogen adsorption reaction and the adsorption of

nitrate reduction products block the electrode surface and inhibit the overall electroreduction process.

The electroreduction of nitrate to nitrite and ammonia has been investigated using a polycrystalline Au electrode in acidic and basic NO_3^- containing electrolytes [36]. It was observed that the reduction process strongly depends on the solution pH: in strongly acidic solutions with pH lower than 1.6 the current efficiency for the NO_3^- reduction is less than 5%, but in basic solutions the reduction of NO_3^- occurs and the current efficiency is in the range from 80 to 99%. Other reports show that the reduction of nitrate at gold electrodes is characteristically slow and hardly detectable, making Au not a good monometallic electrocatalyst for the reduction of nitrate [36].

Studies carried out by Katsounaros *et al*. [42], indicated that tin is an efficient electrocatalyst for the reduction of nitrate. The percentage of the removed nitrate that was converted to nitrogen is approximately 85%, at -2.8 V vs. Ag/AgCl. The yield of N_2O production was about 5%, and small amounts of NO were also detected. The disadvantage of this material is the corrosion, which increases the concentration of tin ions, unacceptable in potable water.

3.1.1.3. Multimetallic materials

A wide range of multicomponent electrode surfaces have been investigated, the most relevant are: copper-tin [45], copper-palladium [46], palladium-tin [47, 48], platinum-tin [49], palladium-rhodium [31], copper-zinc [50], palladium-indium [48], palladium-platinum-germanium [51], palladium-cobalt [52], palladium-cobalt-copper [52], palladium-gold [53], copper-thallium [54].

The importance of investigation of multicomponent electrodes is the result of high catalytic activity of noble metals in hydrogenation processes, the first choice for reducing nitrates. The reduction mechanism of the NO_3^- and NO_2^- ions at multi- and monometallic electrode surfaces is very similar, except for the fact that the activity and selectivity of mixed composites strongly depends on the preparation methods.

The Pt/Sn bimetallic electrode material deposited on Au(111) exhibited a very high catalytic activity for the reduction of nitrate. Shimazu and coworkers [49] reported that the reduction current increased almost linearly with increasing Pt/Sn ratio, the maximum value of -2.7 mA cm^{-2} is comparable to those of the Sn/Pt and Sn/Pd electrode materials. The selectivity towards the formation of ammonium ions reached 0.97, small amounts of

NO_2^- being also indicated. In comparison with other Pt based alloys, the quantity of Pt deposited on the electrode is small, the maximum value of Pt/Sn ratio being 0.3.

Information obtained from cyclic voltammetry and exhaustive electrolysis measurements indicate that a Cu/Pd nanostructured cathode composite, with 15% (w/w) Cu, exhibit appreciable activity towards the formation of ammonia as main product of the reduction process. It was also observed by de Vooys *et al*. [46] that with increasing copper content, the activity increases but the selectivity towards the formation of N_2 decreased and only traces of N_2O could be detected. The reduction was strongly dependent on coexisting anions and pH.

In comparison with pure Cu and Tl, the alloy $Cu_{45}Tl_{55}$ has higher electrocatalytic activity in alkaline medium towards the reduction of nitrate species [54]. The thallium particles are efficient promoters of NO_3^- and NO_2^- ions adsorption on the electrode surface, with subsequent accumulation on the copper catalytic centres.

Addition of Sn to Cu as a base cathode material in the composition region up to 10 wt. % Sn has a positive effect on electrocatalytic activity [45]. The selectivity of the reduction process towards the formation of N_2 as the final product is affected only at potentials more cathodic than -1.40 V versus SCE (saturated calomel electrode). However, there are two important problems that require further treatment: (a) the efficiency is low, because of the hydrogen evolution reaction and (b) re-oxidation of NO_2^- on the anode surface in case of undivided cells. Copper and tin alloys are mostly considered as efficient catalytic electrode materials. At the same time, co-deposition of tin with another metal makes it possible to obtain coatings with additional properties. The group of Polatides et al. [55] claimed that, by using a CuSn electrode at very negative potentials (E = -2 V *vs*. Ag/AgCl), nitrate can be removed up to 97%, with a selectivity of 35% for N_2 as a final product. This represents an important finding for the nitrate removal process.

3.1.2. Anode materials

Two requirements should ideally be met by potential anode materials: first, the material should be stable under actual electrolysis conditions and second, it would be an advantage if the anode reaction did not interfere with the reduction process so that the cell may be operated in an undivided configuration. Genders *et al* [56] studied the influence of three anodes in an undivided flow cell. When a stainless steel anode was used, a large amount of rust coloured solids was obtained in the solution. No solids where observed in the solution when a nickel anode was used, but the anode was coated with precipitate and

showed a slight weight loss. The platinum anode did not show physical evidence of corrosion, but gave much poorer destruction efficiency. Negative destruction efficiencies seen early in the experiment reflect a net oxidation of nitrite to nitrate. Thus, from all the anode materials tested only nickel may be suitable for the direct reduction of nitrate in an undivided cell [56].

3.1.3. Ion exchange membranes

The exchange membrane plays an important role on the removal of nitrate. A cation exchange membrane brings about a significant improvement for nitrate reduction. The membrane isolates the catholyte from interfering with nitrite (and other reduction products) oxidation at the anode. Without the membrane, the destruction efficiency of nitrate is poor or even negative, suggesting that a membrane should be included, in order to remove nitrate from solution at good efficiencies. For a feasible reduction process in a divided cell, the cation exchange membrane must not be destroyed by the presence of other trace amounts of compounds presented in the treated waste water.

3.2. Analysis methods of the nitrate products

Products expected during nitrate reduction are summarized in Table 3.2 Moorcroft *et al.* [57] reviewed the strategies for determination of nitrate and nitrite and also suggested the reaction pathways which may be the basis of all detections and determinations (Scheme 1).

Table 3.2 Products arising from reduction of nitrate

Oxidation states	Products	Remarks
+4	nitrogen dioxide (NO_2)	possible intermediate
+3	nitrite (NO_2^-)	known intermediate
+2	nitric oxide (NO)	probable intermediate
+1	nitrous oxide (N_2O)	known intermediate
0	nitrogen (N_2)	known product
-1	hydroxylamine (NH_2OH)	known product
-2	hydrazine (N_2H_4)	no information
-3	ammonia/ammonium (NH_3/NH_4^+)	known product

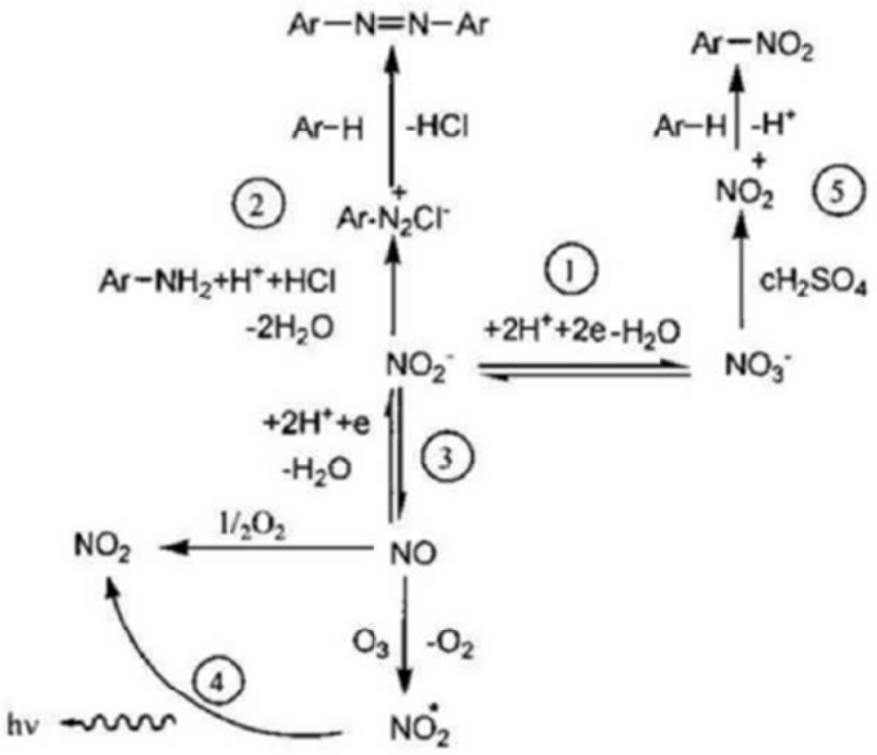

Scheme 1 Common reaction pathways that form the basis of nitrate detection strategies [57]

Different techniques and tests have been used for the analysis of products formed during electro-reduction of nitrate. One approach is to collect the products and the subject them to analysis. Differential electrochemical mass spectrometry (DEMS) has been successfully used for product analysis along with isotopic labelling [58, 59, 60, 61]. Tada *et al.* [62,63] determined the concentrations of the nitrate, nitrite and ammonium ions in a solution by flow injection analysis (FIA). Electrolyte product samples were analysed for electro-reduction of nitrate in some papers by UV-VIS spectrometry [34, 38, 64]. In some other works reaction components were analyzed by the high performance liquid chromatography (HPLC) [60].

The determination of nitrate and nitrite was performed by ion chromatography by Katsounaros *et al.* [42], Wang*et al.* [65]. Moreover, as reported by Piao *et al.* [66] product analysis was carried out by quartz crystal microbalance (QCM) measurements; concentrations of the nitrate, nitrite and ammonium ion in a solution were determined by ion chromatography. Li *et al.* [67] used a variety of techniques for product analysis; the nitrate was determined by a standard colorimetric method using a spectrophotometer and the nitrite was analyzed by ion chromatography. According to Badea *et al.* [68], the

electrolysis product of nitrate reduction was analyzed with Nessler reagent. Nitric oxide and nitrogen dioxide were detected using an Environment S.A. (AC 30M) NO_x analyzer [69]. Nitrate and nitrite were separated by a cation exchange column and were detected by a conductivity detector by Polatides *et al.* [69].

As a conclusion, the reliable and rapid analysis of nitrate is important in many fields. Analytical procedures that distinguish nitrate are particularly attractive although in many practical situations the nitrite level is much lower than that of nitrate.

3.3. Electrochemical reactors for nitrate reduction

Electrochemical reactors have become an established unit process for synthesis of materials and pollution control applications. Such reactors are often operated under mass transport controlled reaction conditions in order to maximize their productivity in which flow conditions in the reactor play a dominant role [70]. Both in the laboratory and in the industry, the electrochemical reactor is a key component of an electrochemical process and special attention must be paid in its design to achieve a high conversion rate of reactant to product as well as a high current efficiency for the desired reaction. In view of the diverse applications of electrochemistry, a wide range of different electrochemical reactor designs is possible, varying from traditional plate-in-tank configurations to more sophisticated designs.

Hobbs [71] emphasized the need for the construction of electrochemical reactors for the destruction of nitrates from liquid and mixed waste for the development of the electrochemical technology. Technology description, optimal conditions, advantages, applications and reactor models were discussed in the report.

3.3.1. Types of electrochemical reactors

Several types of electrochemical reactors (ER) are used for nitrate destruction. The electrochemical process for removal of nitrate can be operated in either undivided or membrane-divided cells. Each mode has advantages and disadvantages that are summarized below. Both types of cells share the following characteristics:

- capable of destroying >99% of nitrate;
- compatible with caustic recycle processes;
- when no chromate is present, best results are obtained with a nickel cathode and a nickel anode;

- presence of chromate inhibits nitrate reduction at high current density;

- ammonia gas generated at the cathode requires further treatment before release to the environment.

Undivided cell advantages:

- simpler design;

- lower power consumption due to the lower resistance between electrodes;

- membrane lifetime is not an issue.

Undivided cell disadvantages:

- wasted current due to cycling of nitrate (nitrite reaction at anode and cathode);

- mixing of anode and cathode product gases (hydrogen, ammonia, oxygen, etc.);

- longer induction period required before net nitrate destruction begins.

Divided cell advantages:

- destruction of nitrate at cathode begins immediately with power application;

- anodic and cathodic gases are collected separately;

- higher electrical efficiency by preventing re-oxidation of reduced nitrogen species.

Divided cell disadvantages:

- higher power consumption resulting from higher cell resistance across the membrane;

- first batch requires added caustic as anolyte;

- reactor complexity introduces more potential problems (e.g., membrane fouling, breakage and disposal; feed and product streams for both anolyte and catholyte).

The types of ER used in the denitrification were tested with continuous mixing and circulation with membrane separator in order to prevent oxidation of nitrite species and to keep the anode separate from the gaseous products. Synthetic nitrate solution is passed through the cathode side of the cell and through the anode an alkaline solution is circulated. Another type of ER would be to build a very long reactor. But this option is not practical because it increases significantly the ohmic resistance of the cell. A combination between circulation, reactor length and optimal operating parameters was established for the present studies.

3.3.2. Applications of electrochemical processes for ERN

The various applications of the electrochemical processes are detailed as follows:

- In the electrochemical destruction of sodium nitrate, sodium hydroxide is the major liquid phase product of the process. If the sodium hydroxide could be recovered and

recycled significant reduction in the quantity of waste requiring disposal would be realized. Immediate use of sodium hydroxide included neutralization of fresh waste and as a corrosion inhibitor in the waste storage and evaporation facilities [71];

- Electrochemical processes are used for the production of a variety of industrial chemicals like ammonia, nitrogen, hydroxylamine, ammonium hydroxide, sodium hydroxide and oxides of nitrogen;

- Electrochemical methods are also useful for the treatment of waste streams and waters prior to disposal and release to the environment;

- The electrochemical reactions are easily controllable; they can be shut down instantaneously by shutting off the power to the electrochemical reactor;

- Moreover no additional chemicals are necessary to be added in the process, and therefore there is minimal or no secondary wastes generated by the process.

3.4. Literature review regarding the reduction of nitrates

As has been shown at the beginning of this chapter, Table 3.1 shows an overview on specific parameters of electrochemical nitrate reduction processes. This table contains information about the electrochemical reactors used in different measurements, detailed aspects of electrode materials, electrolyte composition, pH, electrochemical parameters (current density, electrode potential), etc. From literature analysis and based on data contained in Table 3.1, some conclusions about the performance of different electrode materials and the performance of ERN process were formulated:

• Application of the ERN method using cathodes of different metals is effective only at high concentrations of nitrate ions (about 1000 mg/L);

• By applying electrochemical methods, nitrates can be reduced to several intermediary or final products like: nitrite, hydroxylamine, ammonia and molecular nitrogen;

• In terms of kinetic mechanisms proposed for ERN the following steps are involved:

1) Adsorption of NO_3^- which is rapid and reversible. Since the reaction is under kinetic control, NO_3^- is weakly adsorbed on the surface, leading to a competitive adsorption reaction type;
2) Reduction of nitrates through the transfer of electrons. This step is strongly influenced by the nature and structure of electrode material;
3) Desorption of products from the electrode surface.

• For each metal or alloy used as electrode material for ERN a number of specific parameters, such as pH, applied potential range, have impact on the selectivity of nitrate reduction to N_2 or NH_3.

• The more efficient cathodes used in the conversion of NO_3 to N_2 were Al and alloy $Sn_{85}Cu_{15}$, allowing a removal of nitrate from waste water of 88.6% for Al and 55% for the $Sn_{85}Cu_{15}$ alloy [55];

• The Cu electrode has high catalytic activity. Reduction of nitrate at a copper cathode is characterized by two distinct peaks in the corresponding region of the potential [39];

• Fe electrodes are unsuitable for these processes due to low efficiency of nitrates removal. Electrodes like Fe and Zn cannot be used to reduce nitrate because of their corrosion in alkaline environments [72];

• Hydrogen storage alloys can participate directly in the reduction and increase the catalytic activity of electrode. These electrodes have many advantages such as high selectivity, excellent power efficiency and good stability in the reduction of nitrate to ammonia [73];

• In comparison with Tl, Cu and alloys like Cu-Tl present an increased electrocatalytic activity. Electrochemical reduction can be successfully applied to wastewater treatment where nitrates are converted into products which are not harmful [54];

• NO_3^- reduction kinetics is faster for the bronze electrode containing 10% Sn and the electrocatalytic activity for reduction of NO_3^- is four times higher than the corresponding Cu electrode. An alloy containing 10% Sn showed the best properties (no hysteresis, low sensitivity) and the Koutecky-Levich analysis showed good electrocatalytic activity to reduce NO_3^- [45];

• An ion exchange membrane (Nafion 417) used with a Pb cathode shows a good stability and efficiency over 1000 hours destructive testing [56].

Table 3.1 Overview on specific parameters of electrochemical reduction of nitrate processes

Nr. crt.	Electrode material			Electrolyte	pH	T (^{0}C)	Techniques	Results Mechanism, efficiency, yield, rate constant	Ref.
	Cell setup	Cathode	Anode						
1	3 anodes 2 cathodes	Cu, Ni, Graphite Pt	Ti rods	$NaHCO_3$ 84 g/dm^3 NaCl 0.4 g/dm^3 Na_2SO_4 0.4 g/dm^3 $NaNO_3$ 1 g/dm^3 $NaNO_2$ 1 g/dm^3	Weakly alkaline	20	Hydrodynamic voltammetry (cyclic voltammetry on a rotating ring disc electrode) Batch electrolysis	On copper cathode: Efficiency r_F=43%; NO_3^- concentration decreases from 1g/dm^3 to 170 mg/dm^3; On nickel cathode: Efficiency r_F=7%; [NO_3^-] decreases from 1g/dm^3 to 824 mg/dm^{3}occurred.	[39]
2	6 anodes 5 cathodes Plane parallel reactor Fluidized bed reactor	Cu	Activated Ti	$NaHCO_3$ 84.0 g/dm^3 NaCl 0.4 g/dm^3 Na_2SO_4 0.4 g/dm^3 $NaNO_3$ 1.0 g/dm^3	Weakly alkaline	20	Hydrodynamic voltammetry	$NO_3^- \rightarrow NO_2^- \rightarrow NH_3$ For plane parallel setup mass transfer coefficient : k_{NO3}= 3.4×10^{-6} ms^{-1}; Applied limiting current density for NO_3^- reduction: i_{NO3}= 42Am^{-2}.	[74]
3	Plane parallel reactor	TiO_2 Fe	Graphite	$NaNO_3$ 1-5 mg/l NaCl 1500-3000 mg/l NH_3 5-20 mg/l	≈7	16-32	Batch electrolysis Electrochemical oxidation	Iron → low removal efficiency. TiO_2 cathode and graphite anode increase the removal efficiency. Conductivity and current input has the strongest influence on electrochemical process.	[72]

4	Divided cell setup Nafion ion exchange membrane	-	Mm(NiAlMnCo)$_5$ Mm–alloy with La, Ce and Pr	0.5 M KOH+ 0.05 M KNO_3	Alkaline	22	Galvanostatic and potentiostatic electroreduction	The electrolysis on the fully hydride electrode in the solution produced ammonia with a current efficiency of 90% at E=1.2 V *vs.* SCE. The dissolved hydrogen atom presented in the alloy electrode participates directly in the reduction process and enhances the catalytic activity.	[73]
5	Bioelectrochemical reactor 10 cathodes 1 anode	Immobilized denitrifying bacteria on carbon	Carbon electrode	Synthetic solution with nitrate and organic matter	-	36-38	Batch electrolysis	Denitrification rate was increased by applying electric current. Removal of nitrate and COD occurred simultaneously.	[75]
6	Divided cell setup Cation membrane Porous cathode plane anode Gas-liquid separator	Porous Ni foam	Stainless steel plane anode	Alkaline wastewater 0.6 M $NaNO_2$ 1.95 M $NaNO_3$ 1.33 M NaOH	Alkaline	32	Batch electrolysis	Using porous cathodes for nitrate and nitrite destruction indicate definite advantages at a cell current of 0.25 A cm^{-2} the porous cathode needed one-third the time and energy required to destroy 95% of the nitrates and nitrites compared to the planar cathode.	[76]

7	Divided cell setup	CdS	-	Nitrate solution Na_2SO_4	Alkaline	-	Photoelectrochemical reduction Cyclic voltammetry	The oxidation and the reduction reactions take place separately, thus, decreasing the electron–hole recombination and enhancing the yield of ammonia production.	[77]
8	Biofilm reactor	Stainless steel cathode with denitrifying Bacteria	Amorph. carbon electrode	K_2HPO_4 9.4 mg/l KH_2PO_4 11.1 mg/l NaCl 5.1 mg/l $CaCl_2$ 6.0 mg/l $FeCl_2*6H_2O$ 10 mg/l $MgSO_4*7H_2O$ 21 mg/l Cl^- 7-9 mg/l NO_3^- 3-5 mg/l SO_4^{2-} 4-5 mg/l	7 – 8	-	Denitrification and neutralization	Continuous denitrification of nitrate–contaminated groundwater containing dissolved oxygen (DO), $SO_4^{2-}$was carried out in with 3 identical electrochemically activated biofilm reactors. By applying current, denitrification and neutralization occurs simultaneously. Sulphate reduction and nitrite accumulation were not observed.	[78]

9	Divided cell setup	Poly-crystalline Au	-	0.5 M $NaNO_3$ 0.5 M $CsNO_3$	1-3 10-13	-	Galvanostatic electroreduction Cyclic voltammetry	The reduction of NO_3^- does not occur significantly in the strongly acidic solutions with pH between 1.4 to 1.6;r_F= less than 5%.	[36]
10	Biofilm reactor	Stainless steel	Carbon	Groundwater with NO_3^-, NO_2^-, SO_4^{2-}, Cl^- ,PO_4^{3-}, HCO_3^-, NH_4^+,Na^+, K^+, Ca^{2+},Mg^{2+}	-	20-30	Denitrification and neutralization	Denitrification occurred as function of the applied currents. r_F= [53% - 100%]	[79]
11	3 electrode cell setup	Modified vitreous carbon	-	-	1- 4	25	Hydrodynamic voltammetry	Electrocatalytic reduction and oxidation of $NO_2^-$by a mixture of copper(II) and iron(II) complexes with the same or different ligands. The results show that HNO_2 is reduced to N_2O through Cu(I) complex species, while HNO_2or NO_2^- is oxidized to NO_3^- through Fe(III) complex species.	[80]
12	Glass cell	Pd-[Cu-In-Sn]on carbon	-	Synthetic solution 100 ppm NO_3^- (pH = 5) Inhibitors: NO_2^-, SO_4^-	5-7	100-200	Batch electrolysis	NO_2^-selectivity (S) = 90%; Feasibility of catalyst usage for nitrate reduction on carbon electrode.	[51]

13	Divided teflon cell setup Nafion 117 cation membrane	Sn plate	Platinated Pt plate	Synthetic electrolyte 2 M NaCl 0,5 M $NaNO_3$	7	-	Cyclic voltammetry Potentiostatic electrolysis	Main product: N_2 (r_F= 85,7%) H2N2O2 and hydroxylamine have been identified as intermediary products.	[81]
14	Divided cell setup w/o exch. membrane	Pd-Co, Pd-Cu, Pd-Co-Cu on Ti	Ti/Pt-Ir	Synthetic solution 268 mg/L $NaNO_3$ 0,1 M $NaClO_4$ $5*10^{-4}$ M $CuSO_4$	-	22	Cyclic voltammetry Exhaustive electrolysis	W_s = 6,62 kWh/kg NO_3^-; NO_3^-concentration drop from 200 to 50 mg/L.	[52]
15	3 electrode cell setup	Graphite with Rh	Pt	0,1 M $NaNO_3$ 0,1 M $NaNO_2$ 1 M NaCl	-	20	Cyclic voltammetry Potentiostatic electrolysis SEM	Efficient NO_2 reduction. Main products $NO_2^-$and NH_3.	[35]
16	Undivided and divided cell cation membrane	Poly-crystalline Cu	Pt rod	0,1 M $NaNO_3$ 1 M NaOH 0,1 M $NaNO_2$	-	22	Cyclic voltammetry RDE EQCM	Products: NO_2^-, NH_3, NH_2OH Adsorption on Cu occurs at-0.6 V which is reduced to nitrite at -0.9 V. At -1.1 V nitrite is reduced to hydroxylamine and NH_3.	[38]
17	Undivided cell setup	Pd-Cu	-	$HClO_4$ NaNO3 0.1 M KOH H_2SO_4	0-14	-	Cyclic voltammetry RDE RRDE EQCM	Products: N_2, N_2O, NO_2^-, NH_3 N_2 selectivity S=60% Alloy fabrication highly impacts the process.	[46]
18	3 electrode cell setup	Glassy carbon Cu-Tl	Pt plate	1 -8 mM NO_3^- 10 Mm NaOH NO_2^-	>7	22	Cyclic voltammetry	Detection limits : NO_3^-=190µM; NO_2^-=250 µM.	[54]

19	Divided Glass cell	Pt, Ir, Pt-Ir	Pt	0,1 M $NaNO_3$ 0,5 M $HClO_4$ 0,5 M H_2SO_4	-	30	Cyclic voltammetry	Nitrate reduction occurs at less negative potential on Ir Product: N_2O.	[44]
20	Divided PP 3 electrode cell setup	Rh on Ti	Ru-Ti	Synthetic solution: 0,3 M KNO_3 0,2 M KOH 0,2 M KCl	>7	-	Cyclic voltammetry SEM TEM	Investigation of the electro-chemical activation of Rh on titanium. Reduction activation energy reduction from 47 to 20 kJ mol^{-1}. Reduction leads to N_2.	[34]
21	Divided and undivided 3 electrode cell setup	Cu-Sn	Pt	Synthetic electrolyte 1 g/L $NaNO_3$ 1 g/L $NaNO_2$ 84 g/L $NaHCO_3$ 0,4 g/L Na_2SO_4 0,4 g/L NaCl	>7	20	Cyclic voltammetry RRDE Batch electrolysis	Sn (10%) enhances reduction process. Overall efficiency is low thanks to hydrogen evolution reactions presence at nitrate reduction potential. Results: N_2, NH_3	[45]
22	Teflon Divided cell setup	Pt, Rh, Pt-Rh pe Au	Pt plate	Synthetic electrolyte 3 M HNO_3 0,5 M H_2SO_4	<<7	-	Cyclic voltammetry DEMS FTIR	Pt exhibits higher activity than Rh modified electrode. Products: NO_2^-, NH_3, NH_2OH, N_2, N_2O, NO	[31]
23	3 electrode cell setup	Pd-Ge, Pd-Pt-Ge on Pt	-	Synthetic electrolyte 0,1 M KNO_3 10 mM KNO_2 0,5 M H_2SO_4	<7	-	Cyclic voltammetry DEMS RDE	Pd/Ge shows selectivity (100%) towards N_2O formation.	[61]

24	-	Pt, Pd, Rh, Ru, Ir, Cu, Ag, Au on Pt	Pt plate	Synthetic electrolyte 0,1 M $NaNO_3$ 0,5 M H_2SO_4 0,5 M $HClO_4$	<7	23	Cyclic voltammetry RDE DEMS	Comparative study of NO_3^- reduction on different modified electrodes. Activity decreases :Cu>Ag>Au Rh>Ru>Ir>Pd>Pt; Products: NO, NH_3, NH_2OH.	[30]
25	Teflon Divided/Un cell setup cationic membrane	Pd, Zn, Pb, $Cu_{60}Zn_{40}$ $Sn_{85}Cu_{15}$	Pt foil	Synthetic electrolyte 0,05 M KNO_3 0,1 M K_2SO_4	-	-	Cyclic voltammetry Potentiostatic electrolysis	Products: NO_2^-, NH_3, N_2 Selectivity for N_2:35,3-43 % In case of $Cu_{60}Zn_{40}$alloy, r_F=99% for NO_3^-destruction.	[55]
26	Glass cell setup	Cu	Pt	Synthetic electrolyte 5-80-0,1 mM $NaNO_3$ 0,1 M NaOH	12	297	Cyclic voltammetry Potentiostatic electrolysis	Reduction of the N_2O_2intermed. to N_2at -1.3 V.	[68]
27	Divided cell setup Anionic membrane	Cu, Ni	Pt, RuO_2, Ti	Synthetic solution 0,01-0,1 M $NaNO_3$ 1 M HCO_3^-/CO_3^{2-}	8-9	-	Ion exchange Electrodialysis	2 step removal: reduction at the cathode to NH_3, at the anode NH_3 oxidized to N_2.	[82]
28	Divided Teflon cell setup	Sn	Pt	0,05 M KNO_3 0,1 M K_2SO_4	-	20	Cyclic voltammetry Potentiostatic electrolysis	Study on NO_3^- reduction at high cathodic potentials. .r_F=60%. N_2 selectivity 92%, E= -2.9 V.	[83]
29	3 electrode cell setup	Sn/Pd on Au	Pt	0,01-0,1 M $NaNO_3$ 0,1 M $HClO_4$ $PdCl_2$	-	-	Cyclic voltammetry EQCM, FIA, XPS	Main product: N_2O Sn(0.65)/Pd(1.3)/Au alloy shows the highest catalytic activity.	[84]

30	Divided glass cell setup	Cu-Zn [30% 35%, 41%]	Ti	$NaHCO_3$+NaCl+Na_2SO_4+$NaNO_3$$NaHCO_3$+NaCl+$Na_2SO_4$+$NaNO_2$	-	-	RRDE Batch electrolysis	Linear dependence of electrocatalytic activity with Zn content in the cathode material. Highest electrocatalytic activity for Cu with 41% Zn.	[50]
31	-	Pd-Al_2O_3 Pd-Cu	-	1.95 M $NaNO_3$, 0.60 M $NaNO_2$, 1.33 M NaOH	-	-	HPLC, Chromatography	Nitrate reduction selectivity towards N_2 formation (99,9%)	[85]
32	Industrial scale cell	Pd/$Rh_{1.5}$ on Ti	-	Na_2SO_4, NaCl, $NaHCO_3$, $NaNO_3$	-	-	Cyclic voltammetry Electrolysis	At 20 mA cm^{-2} r_F=100% NO_3^- removal. Pd/$Rh_{1.5}$/ Ti shows high stability after 1000 hours of usage.	[86]
33	3 electrode cell setup	Pt/Sn on Au	-	0.1 M $HClO_4$ KCl_6 $SnCl_2$	-	-	Cyclic voltammetry, QCMX (XPS)	Pt/Sn shows high electrocatalytic activity with mainly NH_3formation.	[49]
34	Divided glass cell setup	Pb Ni	Pt	1.95 M $NaNO_3$ 0.60 M $NaNO_2$ 1.33 M NaOH	-	70-80	HPLC Galvanostatic electroreduction	Pb has been identified as optimal cathodic material in long and batch (short) reduction processes.	[56]
35	3 electrode divided cell setup	Co-DIM	-	NaBr 0.1 M KNO_3	>10	21	Cyclic voltammetry Potentiostatic electrolysis	Co-DIM improves NO_3^- reduction to NH_3. Intermediates:$NO_2^-$and NH_2OH.	[40]
36	Divided cell setup Cationic membrane	Cu, Zn, Ag Alloys: Cu-Zn	Pt, Ir, Pd	H_3PO_4 HClO	10	-	Electrolysis	On Cu, after 80 min NO_3^-reducti-on from 10 mg/l to 5.8 mg/l occurs. On Cu-Zn reduction from	[87]

		Cu-Fe Cu-Ni Cu-Al	Carbon					10 mg/l la 3.2 mg/l. $NO_3^- \rightarrow NO_2^- \rightarrow NH_3$.	
37	Divided cell setup Cationic membrane	Cu, Fe, Ni, Zn, Al, Au, Ag, Pt, Pd , C	IrO_2on Ti Pt oxide covered by Ti	$NaNO_3$ NaOH	Acid Alkaline	0-120	-	$NO_3^- \rightarrow NO_2^- \rightarrow N_2$ Intermediary products: NO, NO_2 On copper electrode at pH = 4.8 r_F=74.5 %.	[88]
38	Batch reactor	Pd,Rh, Cu,Pd-Cu, Pd / Al_2O_3	-	100 ppm NO_2^-	Acid	10	Catalytic reduction	After 20 min of electrolysis r_F=99.7% NO_3^- conversion occurred. C_{final}= 0.3 ppm.	[89]
39	2 electrode undivided reactor	Pt Pt-Ir	Noble metal	KCl NO_3^- Cl^-	-	22	Galvanostatic electrolysis Denitrification	Through 14 h of electrolysis high efficiency of the reduction process is noted. NO_3^- to N_2conversion occurs in 6 hours.	[90]
40	Divided cell stup with membrane	Cu, Pt, Ni, Pb, C	Ni, Pt, Ti, Nb.	NaOH $NaNO_3^-$	-	45-55	Electrolysis	2 Step reduction process : First step: r_F=76% Second step : r_F=24%	[91]
41	Divided cell setup Cationic exchange membrane	Cu Pt	Graphite	EDTA 345 mmolL NH_3 50 mmol/L NO 600 mmol/L Br^- sau 600 mmol/L Cl^-	-	60	Galvanostatic electrolysis (500 mA)	C_{init} =345 mmol/l, Electrolysis duration: 4 hours C_{final}=314 mmol/l.	[92]

42	Divided cell setup	Pt on Ti, Carbon	-	65 ppm NO_2^- 108 ppm NO_3^- 35 ppm NH_3 29,6 ppm PO_4^{3-}	-	-	Galvanostatic electrolysis (10 A)	NO_3^- şi NO_2^-removal with r_F= 100% after 120 minute of galvanostatic electrolysis.	[93]
43	Divided cell setup	Ni Co Fe Cd Cu	Ni Co Fe Cd	NaOH $NaNO_3$ Na_2CO_3	-	-	Electrolysis	Products: NH_3, N_2 Cd anode: $NH_3 \rightarrow N_2$ r_F=36.9%. Ni catode:$NO_3^- \rightarrow NH_3 r_F$= 59%	[94]

PERSONAL CONTRIBUTIONS

4. EXPERIMENTAL DETAILS

4.1. Experimental Techniques

Cyclic voltammetry (CV), chronoamperometry (CA) chronopotentiometry (CP), square wave voltammetry (SWV) measurements were carried out with a computer controlled potentiostat/galvanostat (EG&G model 263A, SUA, COMPACTSTAT Bipotentiostat, Ivium Technologies, Germany and Biologic BiStat). CV, CA and CP measurements were carried out using a Pt/Pt (Tacussel, France) as a disk-ring electrode and Cu (Methrom, Swizerland) as a disc electrode. SWV measurements were performed using a Pt/Pt (Tacussel, France) or Pt/Cu (EG&G PARC, USA) as a rotating ring-disk electrode. A standard glass cell with three electrodes was used. Electrochemical measurements were carried out under controlled hydrodynamic conditions. The counter electrode (CE) was a Pt wire (ϕ = 0.8 mm, L = 15 mm) and a $Ag/AgCl/KCl_{sat}$ electrode was used as reference electrode (RE). The pH values of the solutions were recorded by a pH/Cond 340i (WTW, Germany) pH-meter. All measurements were performed at room temperature (298±1 K). Before use, the surface of the ring-disk electrode was polished with alumina slurry (Al_2O_3, Struers AP-Paste SQ, Copenhagen, Denmark).

4.1.1. Rotating Disk Electrode

The rotating disk electrode (RDE) is one of the few convective electrode systems for which the hydrodynamic equations and the convective-diffusion equation have been solved rigorously for the steady state. This electrode is simple to construct and consists of a disk of the electrode material imbedded in a rod of an insulating material. For example, a commonly used form involves a platinum wire sealed in glass tubing with the sealed end ground smooth and perpendicularly to the rod axis. More frequently, the metal is imbedded into Teflon, epoxy resin, or another plastic (see Figure 4.1). The rod is attached to a motor directly by a chuck or by a flexible rotating shaft or pulley arrangement and is rotated at a certain frequency [21].

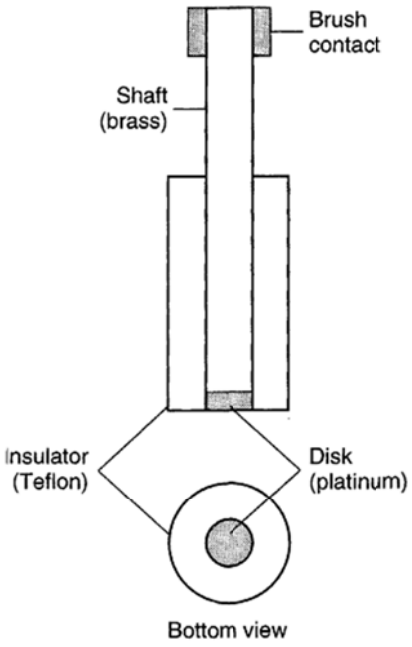

Figure 4.1 Schematic representation of the rotating disc electrode [21]

Electrical connection is made to the electrode by means of a brush contact; the noise level observed in the current at the RDE depends on this contact. Details of the construction and application of RDEs are given in several reviews [95].

In a rotating disk electrode, the electrolyte flows past the electrode by convection. The Levich equation (4.1) [27] predicts the current observed at a RDE and shows that the limiting current is proportional to the square root of rotation speed.

$$I_L = 0.62nFAD^{2/3} \cdot v^{-1/6} \cdot \omega^{1/2} \cdot c_0 \qquad (4.1)$$

where: A is the geometric electrode area surface, c_0 is the bulk concentration, D is the diffusion coefficient, ω is the electrode rotation rate, I_L is the plateau current, n is the number of transferred electrons and v is the kinematic viscosity.

4.1.2. Rotating Ring-Disk Electrode

Reversal techniques are obviously not available with the RDE, since the product of the electrode reaction is continuously swept away from the surface of the disk. Information equivalent to that available from reversal techniques at a stationary electrode is obtained by the addition of an independent ring electrode surrounding the disk (Figure 4.2) [21].

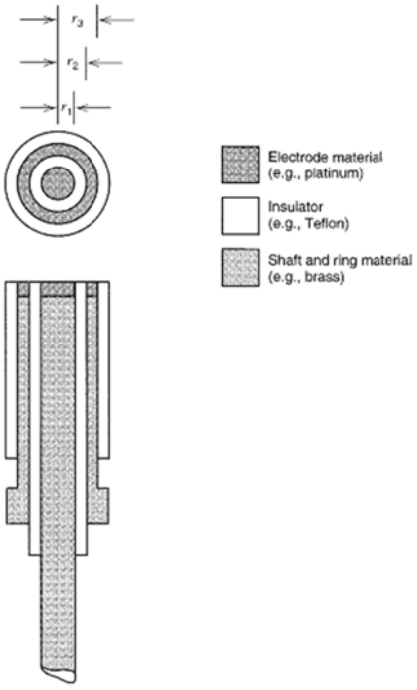

Figure 4.2 Schematic representation of the rotating ring-disc electrode [21]

By measuring the current at the ring electrode, some information about the processes occurring at the disk electrode surface can be obtained. The ring can also be used alone as an electrode (the rotating ring electrode), such as when the disk is disconnected. The rotating ring-disk electrode (RRDE) is also an important technique for the detection of reaction intermediates [96]. The capability of a ring electrode to detect species generated at the disc electrode provides an elegant and powerful procedure for elucidating electrochemical reactions.

Electrochemical measurements were carried out under controlled hydrodynamic conditions using a Pt/Pt RRDE (Radiometer, France; Tacussel, France; EG&G PAR, USA; ring: ϕ_{inner} = 4.4 mm, ϕ_{outer} = 4.8 mm; disk: ϕ = 4 mm). The experimentally determined collection efficiency for the RRDE assembly was 0.22 which compares well to the theoretical value of 0.21 [21].

4.1.3. Cyclic voltammetry

Sweep voltammetry is the most used electrochemical method of investigation, providing information about the electroactive species involved in electrochemical processes (intermediate, product), adsorption phenomena and other kinetic data [97]. The method is

based on tracking the current response given by the electrode and the potential in time, that can be changed linearly (linear sweep voltammetry) or cyclic (cyclic voltammetry). The signal response is the current recorded during the potential sweep (voltamogramm) [97].

The important parameters that can be calculated, corresponding to a reversible system are:

- peak current (anodic, cathodic), $I_{p,a}$; $I_{p,c}$;
- peak potential (anodic, cathodic), $\varepsilon_{p,a}$; $\varepsilon_{p,c,}$.
- standard formal potential $E^{0'}$:

$$E^{0'} = \frac{\varepsilon_{p,a} + \varepsilon_{p,c}}{2} \tag{4.2}$$

- distance between peak potentials ($\Delta\varepsilon$)

$$\Delta\varepsilon = \varepsilon_{p,a} - \varepsilon_{p,c} \cong 0{,}059 / z \tag{4.3}$$

Cyclic voltammetry (CV) can reveal the behavior of homogeneous chemical reactions coupled with heterogeneous transfer reaction by building diagram like $I_{p,a}/ I_{p,c} = f(v)$ [98].

The presently named cyclic hydrodynamic voltammetry (CHV) method represents an original combination between the cyclic voltammetry at relative high scan rate (500 $mV \cdot s^{-1}$) and the controlled hydrodynamic mass-transport using a Pt/Pt RRDE. Commonly such experiments are also referred as (R)RDE experiments.

4.1.4. Square wave voltammetry

Square-wave voltammetry (SWV) [99, 100, 101, 102] is known to be another versatile analytical tool. Compared to CV, according to the literature [27], there are several advantages by using SWV:

- greater speed in analysis;
- lower consumption of electroactive species;
- reduced problems with blocking of the electrode surface.

A general scheme of the square wave voltammetric signal is presented in Figure 4.3.

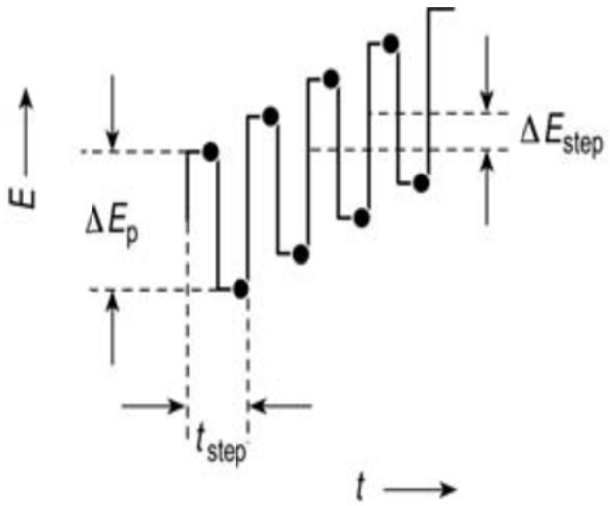

Figure 4.3 Measurement technique of square-wave voltammetry: ΔE_{step} = voltage step of the staircase voltage ramp, ΔE_p = amplitude of superimposed pulse, t_{step} = waveform period [103].

Since the current is sampled during the positive and the negative going pulses, peaks corresponding to the oxidation or reduction of the electroactive species at the electrode surface can be obtained in the same experiment. Subtraction also means that the difference in current is zero for a species at a potential corresponding to the region of mass-transport limited current. In data analysis, this can be very useful, particularly for removing the current due to reduction of dissolved oxygen [104]. It should be emphasized that the quality of the response is strongly influenced by the experimental parameters chosen; thus, the symmetrical square wave and current measurement scheme rejects background currents and the choice, nE_{SW} = 50 mV (ΔE_p), generally yields a good sensitivity with reasonable resolution [104].

For the SWV measurements, a Datronix DXC 240 (Romania) computer controlled multichannel Potentio-/Galvanostat and a BioLogicBistat (France) were used. Labview 8.5 and EC-Lab® software were employed for the experimental control and data acquisition. A similar philosophy was applied for the SWV measurements, where the variable potential is also applied to the ring electrode. During the present work, the following parameters have been used: pulse height, ΔE_p = 50mV; pulse width, t_{step} = 10 ms; step height, E_{step} = 5mV; rotation speed, ω = 1000 rpm.

4.1.5. Scanning Electron Microscopy

Scanning Electron Microscopy (SEM) is a technique for imaging surface morphology. Besides grain size and shape which can be obtained from surface morphological studies, the texture of the deposits (defined as preferred distribution of grains) is also important. Basically, SEM instruments consists in an electron source (electron gun), magnetic lenses for focusing the electron beam, a detector for the secondary electrons emitted by the bombarded specimen and a monitor where the image produced by the secondary electrons is displayed. A detailed description of the SEM technique can be found [105, 106]. Surface morphology and microstructure of the samples were characterized by using SEM. A DSM 982 Gemini (Zeiss Oberkochen, Germany) and ESEM XL30 (Philips) with EDX and EBSD (FEI) were used to study the surface morphology of the deposits.Energy of incident electron beam was kept between 5 to 30 kV for all experiments.

4.1.6. Energy Dispersive X-Ray

The Energy Dispersive X-Ray (EDX) detector is usually incorporated in the SEM device, because whenever an electron beam interacts with matter, as it happens in SEM, X-rays are produced. A detailed description of the EDX technique can be found in [107].

The EDX analyses were performed with a EDX model Voyager III 3200 (SUS Pioneer) in order to get information about the chemical composition of the deposited layers.

The SEM and EDX analysis were performed by Ms. Ellen Kern (TU Dresden, Institut für Physikalische Chemie und Elektrochemie) and Rolf Grieseler (TU Ilmenau, ZMN).

4.1.7. Ion chromatography

Ion chromatography (IC) is a well-established technique for the analysis of ionic species and many organizations, such as ASTM (American Society for Testing and Materials), AOAC (Association of Official Analytical Chemists), and USEPA (United States Environmental Protection Agency), have standard or regulatory methods of analysis based upon IC. Despite the diverse range of solutes and sample types currently analyzed by IC, environmental analysis continues to be the largest application area in terms of new instrument sales and the total number of samples analyzed. In terms of the solutes analyzed in

environmental applications of IC, inorganic anions are by far the most important. Consequently, the simultaneous analysis of the common inorganic anions in drinking water and wastewater remains the most important routine application of IC. More information about the IC technique can be found [108].

A Dionex DX 100 IC with an anion column for AG 14A/AS14 A (4mm) and 4.2 mM Na_2CO_3 / $NaHCO_3$ 1.0 mM eluent was used. The reagent was 0.05 N H_2SO_4 (2 L). The internal standard contains: 0.12 M trifluoroacetic acid: $C_2HF_3O_2$ [CF_3COOH]. A flow rate of 1.2 mL / min was used for the eluent. The Turbochrom 4 software was used for data evaluation.

The IC analysis were performed by Ms. Annelise Täglich (TU Ilmenau, Fachgebiet Elektrochemie und Galvanotechnik I).

4.2. Experimental Setup and Electrolytes

4.2.1. Experimental set-up for the synthesis of cathode materials

Tin sulphate (Merck), copper (II) sulphate pentahydrate (Grüssing) and sulphuric acid (Merck) were of analytical grade and used for the deposition of tin, copper and copper-tin coatings. The plating bath parameters are described in Table 4.1.

Table 4.1 Plating bath selection for copper, tin and copper-tin alloy

Parameters			
Concentration	**Copper bath**	**Tin bath**	**Copper-tin bath**
$CuSO_4 \cdot 5\ H_2O$ (M)	0.1	-	0.1
$SnSO_4$ (M)	-	0.1	0.1 ÷ 0.8
H_2SO_4 (M)	1	1	1
HBF_4 (M)	-	-	0.2
Anode	Pt		
Temperature (^oC)	Room temperature		
Agitation (rpm)	0 ÷ 2000		

4.2.2. Experimental Set-up for electrochemical nitrate detection

Sodium nitrate (Merck), sodium nitrite (Merck), hydroxylammoniumsulfate (Riedel de Häen), ammonium sulphate (J. T. Baker), sodium sulphate anhydrous (J. T. Baker), copper (II) sulphate pentahydrate (Grüssing), sodium hydroxide (Merck) were of analytical grade and used without further purification. The solutions were prepared using Millipore Milli-Q®, double-distilled water. The conductivity was 0.5 μS cm^{-1} at 25^0C. More specifications about the used Milli-Q® Direct 8 Water purification system can be found in [109]. For all measurements 1 M Na_2SO_4 was used as supporting electrolyte. All the measurements were performed in the presence of dissolved oxygen. In order to explain some results (for example the stability of the Cu electrode), measurements were performed also in deaerated electrolytes. High purity argon (99.999%) from ALPHAGAZ™ was used for purging the solutions.

Before use, the surface of the ring-disk electrode was polished with alumina slurry (Al_2O_3, Struers AP-Paste SQ, Copenhagen, Denmark). For each set of measurements, the working disk electrode (Pt covered with Cu or Cu-Sn) was polarized at a constant potential value. After the polishing, the ring-disk electrodes were pre-treated by repeated cycling between hydrogen and oxygen evolution regions -1.5 and +2.0 V vs. $Ag/AgCl/KCl_{sat}$. After the pre-treatment reproducible current-voltage curves were obtained. The counter electrode (CE) was Pt wire (ϕ = 0.8 mm, L = 15 mm) and a $Ag/AgCl/KCl_{sat}$ electrode was used as reference electrode (RE).

4.2.3. Experimental set-up for direct reduction in electrochemical flow cell

An electrochemical flow cell as presented in Fig.7.1 (see Chapter 7) was used for the electroreduction of nitrates. The cell was operated in a divided configuration, to remove possible interferences such as nitrite oxidation at the anode. A model electrolyte mixture (0,1M $NaNO_3$, 1M NaOH) was used for the catholyte compartment. The cathode and anode chambers were separated by a Nation ® 324 (DuPont) cation selective – membrane (separator). An oxygen evolving DSA (Dimensionally Stable Anode) was used as anode. The anodic and cathodic compartments were of equal volumes (10 mL). Electrolyte was recirculated through the cells with a double channel peristaltic pump with a monitored flow rate. In order to analyse the nitrate and nitrite concentration, at specific time intervals, samples

were withdrawn from the catholyte by a syringe and were analyzed, after the appropriate dilution. The determination of nitrate and nitritewas performed by ion chromatography (Dionex DX 100 with an anion column for AG 14A/AS14 A) (see Chapter 4.1.7). The tightness of the cell was achieved by rubber frames specially designed for the reactor. The geometrical area of the cathode and the anode was 10 cm^2 and the distance between the two electrodes was 1 cm.

5. SYNTHESIS OF ELECTRODE MATERIALS

This part deals with the synthesis of the electrode materials that were then used for ERN. Previous investigations (see Chapter 3.1) showed that the reduction efficiency of nitrate ions depends strongly on the nature of the electrode material. Different electrode materials for the ERN process were described in Chapter 3. The interest for copper-tin alloys coatings increased for the last years due to their better corrosion and mechanical properties compared with those of pure copper or tin coatings. There is a worldwide tendency in substitution of cadmium and lead that are intensively used in ERN process, due to their toxicity.

Copper has the highest electrocatalytic effect among transition-metal monometallic electrodes for the cathodic reduction of nitrate ions in acid and also in alkaline media [38]. Tin represents an efficient electrocatalyst for the reduction of nitrate as described by Katsouranos et al. [42]. Also, Sn has positive effect on electrocatalytic activity when is added to Cu as a base cathode material in the composition region up to 10 wt.% [45]. The group of Polatides [55] claimed that by using a CuSn electrode at very negative potentials (E = -2 V *vs*. Ag/AgCl) nitrate can be removed 97% with a selectivity of 35% N_2 as a final product. Based on the literature study, we consider that copper, tin and copper-tin alloy have to be further studied due to their properties and applications in ERN process (see Chapter 3 and Table 3.1).

5.1. Electrochemical thermodynamically aspects

The available information concerning the electrodeposition of copper-tin alloy is confined to the literature [110, 111, 112, 113, 114, 115, 116, 117, 118, 119, 120]. Later claims concerning Cu-Sn alloy plating, however, have been based upon the use of both alkaline and acid sulfate electrolytes. The effect of the plating variables on the composition of electrodeposited alloys is of great interest, since the composition of the alloys must be controlled within narrow limits to obtain the alloys with the optimum properties.

Electroplating of tin has been known for more than 150 years. There are two main types of solutions for tin electroplating, alkaline stannate based solutions and acidic stannous salt based solutions. Tin has been generally applied as a coating to increase corrosion resistance, enhance appearance or improve solderability. Compared to aluminum, cadmium and steel [121, 122] there is an increasing interest in tin used as a substitute for conventional coatings because it has less environmental impact.

5.1.1 Values of standard electrode potentials for metals deposition

The simultaneous deposition of two or more metals without regard to the physical nature of the deposit is a relatively simple matter, for it is necessary only to electrolyze a bath of the mixed metal salts at a sufficiently high current density. Thus, deposits obtained are usually loose, spongy, non-adherent masses, contaminated with basic inclusions and are not the type of the deposit of interest. Thus, the use of a high current density is not a means of solving the problem of alloy deposition.

Depending on the concentration of the species present in the bath, the equilibrium potential varies. According to the literature [123], the standard reduction potentials for acidic solution of the Cu and Sn metals, are presented in Figure 5.1.

The most important practical consideration involved in the co-deposition of two metals is that their deposition potentials be fairly close together.

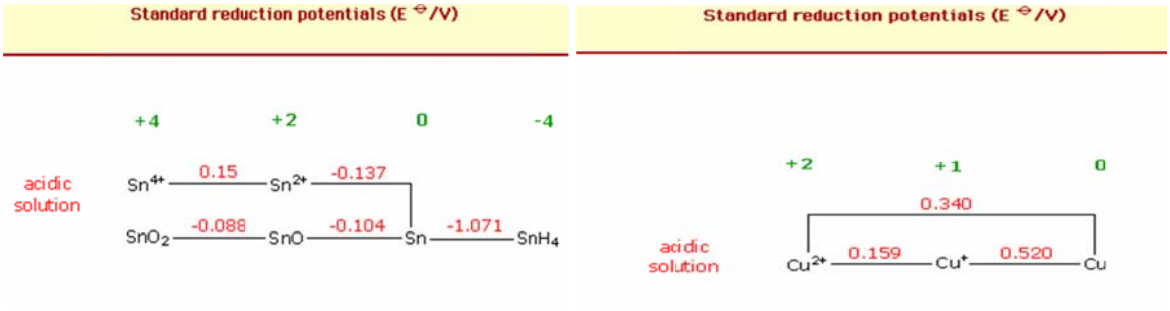

Figure 5.1 Standard reduction potentials for tin and copper in acidic solution [123]

The analysis of the data in Figure 5.1 raises the question of how far apart the standard electrode potentials of metals may be and yet permit satisfactory co-deposition. No general answer can be given because this depends on the nature of the bath. However, satisfactory alloys have been obtained from metals with potential differences about 0.5 V [124].

5.1.2. Potential - pH equilibrium

For the electrodeposition of metals and alloys, the electrolyte and deposition conditions are chosen so that deposits have uniform composition and properties over the course of the deposition process. Based on potential-pH equilibrium diagrams [125] for the systems Cu-

H_2O and Sn-H_2O (see Figure 5.2) electroplating can be performed either in acid or in alkaline solutions.

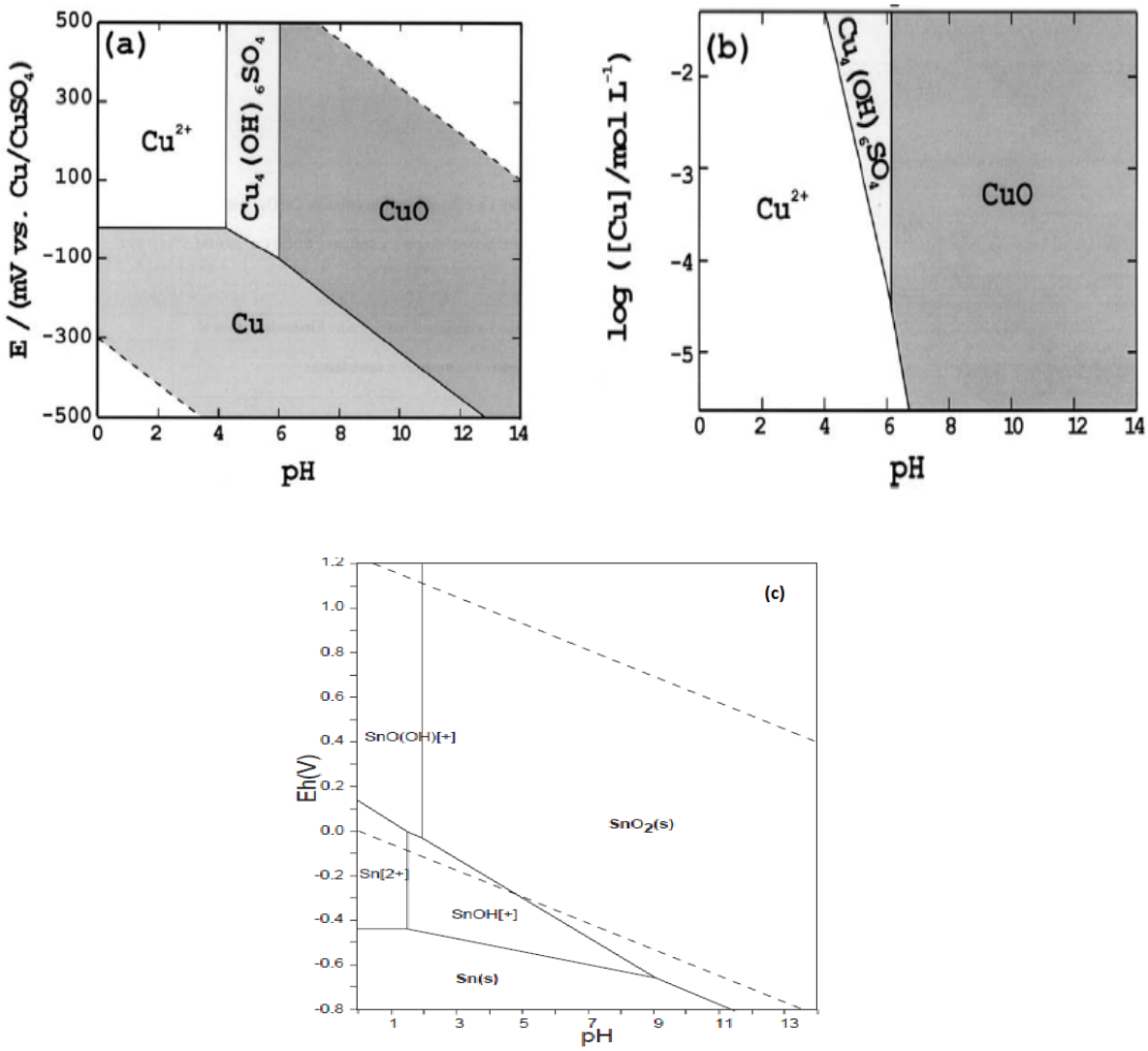

Figure 5.2 Equilibrium diagrams for Cu-H_2O system: (a) potential - pH diagram, (b) log Cu^{2+} - pH diagram,(c) Sn-H_2O system at 25^0C [125]

Possible species in the copper - water system were first examined by constructing the equilibrium potential - pH diagram of copper in water, as given in Fig.5.2(a) for 25^0C. According to the potential-pH diagram, the cupric ion area is confined by the metallic Cu and Cu ion sulphate complex ($Cu_4(OH)_6SO_4$) in the pH range between 0 and 4.2. The solubility - pH diagram (see Fig.5.2(b)) was constructed to determine the equilibrium concentration of cupric ions in the entire pH range.

For the potential-pH diagram of Sn^{2+} (see Figure 5.2(c)) the stannous ion area is confined by the Sn^{2+} ions in the pH range between 0 and 1.5. The stability of the Sn^{2+} ions is ensured

for a pH range < 2. Consequently, the experiments in this investigation were limited to pH region in which copper and tin were soluble.

5.1.3. System selection for metal depositions

5.1.3.1. Alkaline electrolyte systems

Deposition of copper from alkaline solution is disadvantaged due to the limited solubility of copper ions. Electrodeposition of copper from this solution might result in copper powder adherence to substrate.

The alkaline stannate solutions contain sodium stannate or potassium stannate and the corresponding alkali metal hydroxide. These solutions are non-corrosive and do not require other additives. Potassium stannate is more soluble than sodium stannate and it allows operation at high current densities with higher current efficiency. Alkaline stannate solutions must be heated, however, and have a low maximum plating current density and a restrictive anode current density range. In addition, the tin contained in stannate solutions is in the tetravalent form, so twice as much electrical charge is required to plate the same mass of tin compared with plating from stannous salt solutions [126].

Kremann and co-workers [127] investigated an alkaline bronze plating bath. They studied this bath and the properties of the deposit and they came to the conclusion that the cyanide type bath was preferable. Another study from an alkaline pyrophosphate bath was made by Vaid [128]. The bath was operated at 60^0C with a rotating cathode. The deposits obtained were of good quality.

The types of baths which are most used commercially for deposition of copper - tin alloys is a mixed bath containing copper as the complex cyanide and tin as stannate. Although the deposition of copper - tin alloys from the mixed cyanide-stannate bath was brought to a commercially successful stage by the work done after 1936, there is a strong need for alternative process due to their high level of toxicity [129].

5.1.3.2. Acidic electrolyte systems

The most used solutions for Cu deposition are the acid copper sulphate. Electrodeposition of copper from acid solutions is extensively used for different applications. Focusing on the

acid copper electroplating process, critical parameters of the acid copper bath include electrical, mechanical, physical, and chemical variables. Electroplating of tin from acidic stannous solutions consumes less electricity than alkali stannate solutions. In acidic solutions, tin (II) and tin (IV) are equally stable, and tin (II) can be easily oxidized to tin (IV) by atmospheric and anodic oxidation (see Fig. 5.2(c)). Furthermore, Sn (IV) forms fine colloidal particles which may be incorporated in the deposits causing surface roughness and degradation of solderability [124].

A sulphate CuSn alloy plating bath has been developed, which has the advantage of low toxicity and relative ease of handling [130, 131]. The characteristics of the sulphate acid electrolyte are its high cathode (100%) and anode current efficiencies under normal operating conditions. It is low initial cost chemistry and it is relatively easy to maintain and control.

A general comparison of some parameters of different methods of CuSn electrodeposition is given in Table 5.1.

Table 5.1: Comparison of typical properties of CuSn acidic and alkaline electrolytes

Properties	**Acidic electrolyte**	**Alkaline electrolyte**
Temperature	Room temperature	Close to boiling
Voltage needed	Low	Relatively high
Cathodic current density	Under proper conditions the cathodic current density may be very high	Very low current density
Current efficiency	90%	70%
Time needed for depositing 3 µm layer	Seconds	Minutes

From the comparison made between acidic and alkaline bath, the alkaline bath represents not such a good choice for copper-tin electroplating. This is due to the low current density, high voltage, time and the limited solubility of copper ions. From our point of view, the acidic system should be investigated in more detail. One of the aims of this study was to develop a simple, environmentally friendly cupric-stannous plating solution containing a minimum of components, which can be electroplated at reasonable rates at room temperature and can be applied to ERN.

5.2. Cu and Sn electrodeposition

5.2.1. Cyclic voltammetry analysis

Cyclic voltammetry studies were carried out at a platinum disc electrode. The cyclic voltammograms were performed in order to find the region where the Cu and Sn depositions take place. The electrode potential was linearly swept from +0.1V to −0.8V *vs.* $Ag/AgCl/KCl_{sat}$ then the sweep direction was reversed at various potential sweep rates (10, 20, 40, 80 and 160 mVs^{-1}). Three different types of copper and tin concentrations were used in this study. Figure 5.3 shows the cyclic voltammogram of copper at a platinum surface from a sulphuric acid electrolyte. The forward sweep from +0.1V to −0.8V *vs.*$Ag/AgCl/KCl_{sat}$ shows a single reduction peak for copper (Eq. 5.1) and tin (Eq. 5.2) deposition corresponding to a two-electron step:

$$Cu^{2+} + 2e^{-} \rightarrow Cu^{0} \quad (5.1)$$

$$Sn^{2+} + 2e^{-} \rightarrow Sn^{0} \quad (5.2)$$

Hydrogen evolution could occur as a secondary reaction:

$$2H^{+} + 2e^{-} \rightarrow H_2 \quad (5.3)$$

A small amount of current is used for dissolved oxygen reduction:

$$O_2 + 4e + 4H^{+-} \rightarrow 2H_2O \quad (5.4)$$

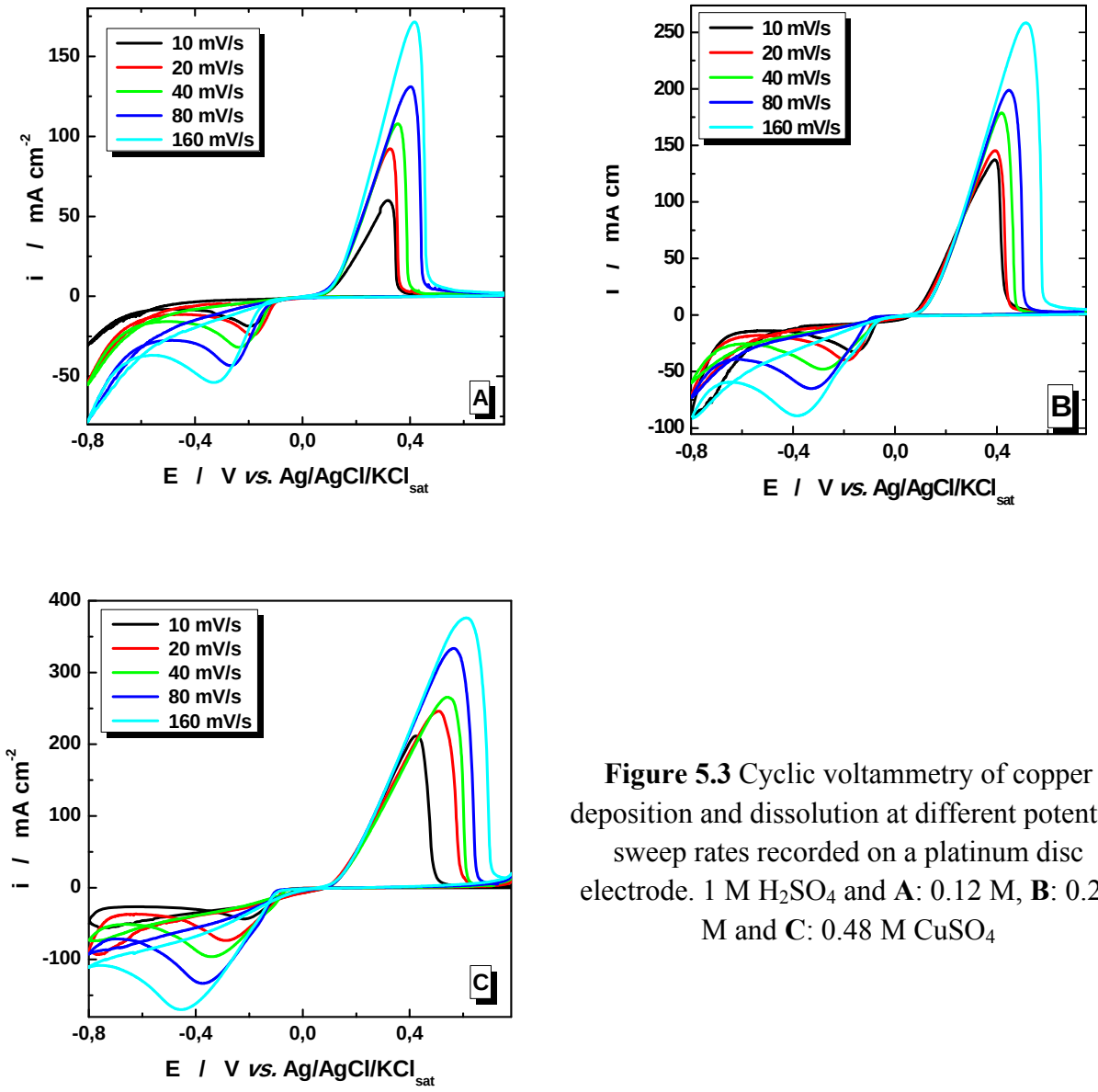

Figure 5.3 Cyclic voltammetry of copper deposition and dissolution at different potential sweep rates recorded on a platinum disc electrode. 1 M H_2SO_4 and **A**: 0.12 M, **B**: 0.24 M and **C**: 0.48 M $CuSO_4$

In a similar series of experiments Sn deposition was investigated. The influence of the scan rate on tin deposition is presented in Figure 5.4.

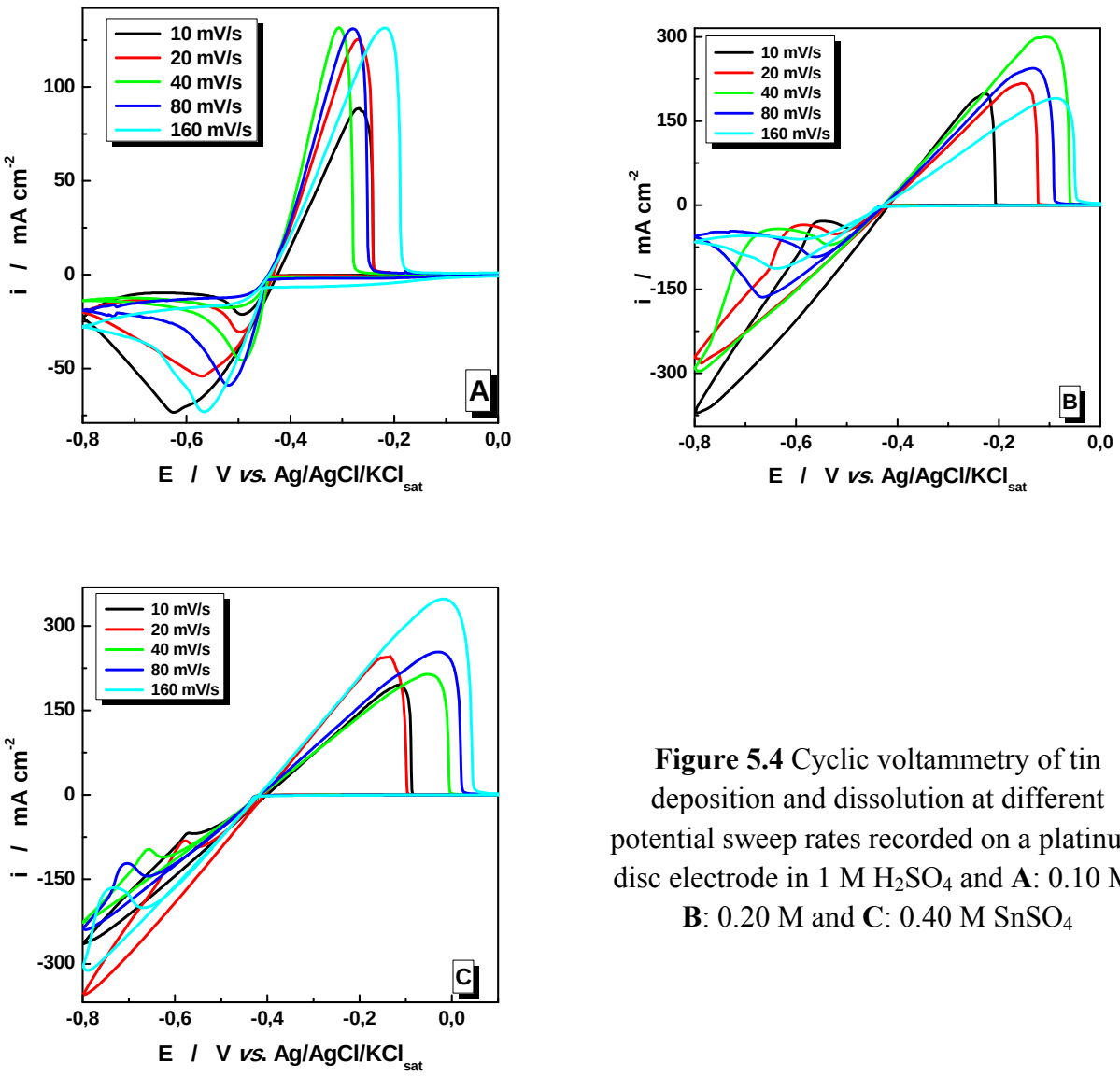

Figure 5.4 Cyclic voltammetry of tin deposition and dissolution at different potential sweep rates recorded on a platinum disc electrode in 1 M H_2SO_4 and **A**: 0.10 M, **B**: 0.20 M and **C**: 0.40 M $SnSO_4$

The peak current density is associated with the complete consumption of cupric ions (Fig. 5.3) and stannous ions (Fig. 5.4) at the electrode surface under mass transport control. On reversing the potential sweep from −0.8V to +0.1V *vs.* Ag/AgCl/KCl_{sat} a single stripping peak was observed, confirming the two-electron oxidation of metallic copper to cupric ions (see Fig. 5.3) and oxidation of metallic tin to stannous ions (see Fig. 5.4) via the reverse of the reactions 5.1 and 5.2. The deposition of copper and tin at the platinum surface is evidenced by the sharp rise in the current at a potential of approximately −0.30V *vs.* Ag/AgCl/KCl_{sat} (for copper deposition) and at about −0.5V *vs.* Ag/AgCl/KCl_{sat} (for tin deposition).

At potentials more negative than -0.5V vs. Ag/AgCl/KCl_{sat} (in the case of Cu) and -0.7V vs. Ag/AgCl/KCl_{sat}(in the case of Sn) water decomposition occurs. This reaction implies the

occurrence of hydrogen evolution and of the OH^- species on the cathode surface. As a consequence, metal hydroxides can be formed that can precipitate on the electrode and together with the hydrogen evolution will block the electrode surface and inhibit further depositions. After the region where the water decomposition occurs, the probability of forming oxide inhibiting species is higher, therefore, the deposition will be retarded when the sweeping of the potential is made in the anodic direction.

Cyclic voltamogramms were performed at different concentrations of Cu and Sn in the bath solution.

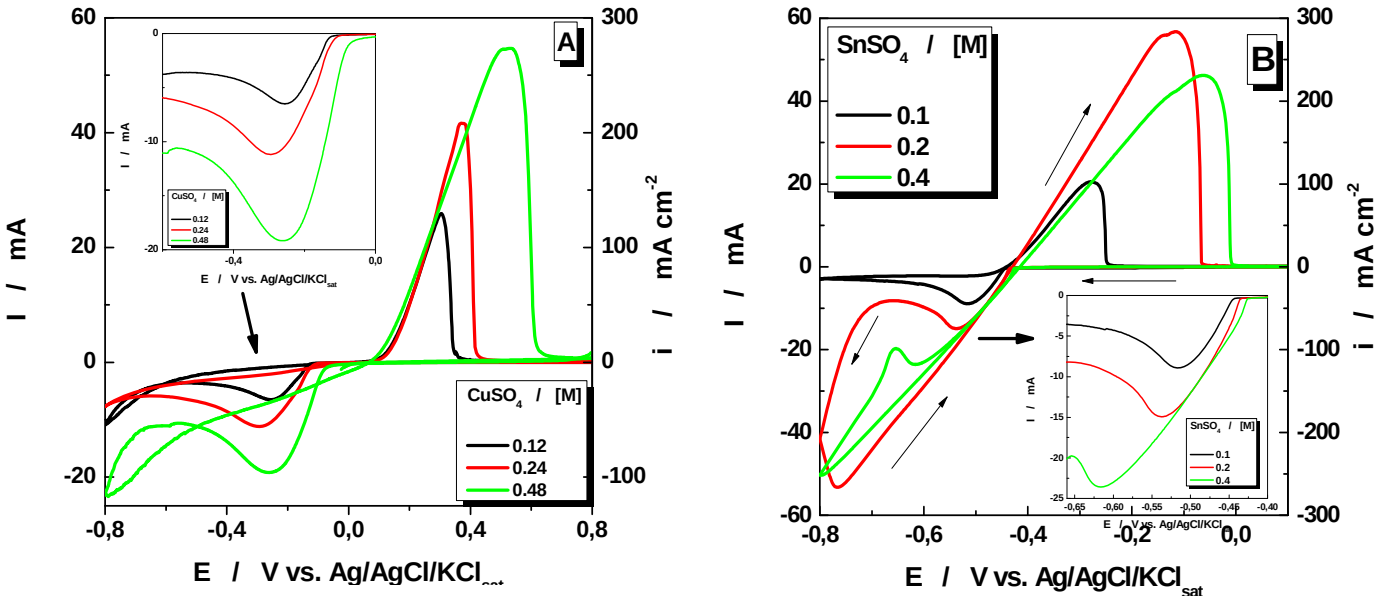

Figure 5.5 Influence of copper (**A**) and tin (**B**) concentrations on the corresponding peak currents. Experimental conditions: platinum disc electrode (S = 0.2 cm^2), scan rate: 50 mV s^{-1}. The electrolyte was prepared at 296 K and contains 1 M H_2SO_4

Analyzing the voltamogramms (Fig. 5.5) and the data from Table 5.2 we can conclude that the anodic and cathodic copper peaks (Fig. 5.5A) and tin peaks (Fig. 5.5B) do not represent the mirror image one to each other, they characterize a quasi-reversible process. The cathodic peaks are shifted to more negative potentials as the concentration and the scan rate increases. The peak potential difference, $\Delta\varepsilon$, ranged between 126 and 156 mV for copper ions.

Table 5.2: Electrochemical parameters corresponding to voltammetric response of the electrode (experimental conditions as in Fig.5.5)

Electrolyte	$E^{0'}$ (mV *vs.*Ag/AgCl)	Δε(mV)	I_{pa}/I_{pc}
$CuSO_4$ 0.12 M	320	126	2.88
$CuSO_4$ 0.24 M	349	130	2.97
$CuSO_4$ 0.48 M	534	156	2.20
$SnSO_4$ 0.10 M	398	238	2.30
$SnSO_4$ 0.20 M	327	422	3.80
$SnSO_4$ 0.40 M	339.5	555	1.96

The number of electrons involved in the reduction peak can be determinated by [43]:

$$i_p = 0.496 \cdot (\alpha z_c)^{1.5} \cdot n \cdot F \cdot A \cdot c \cdot [(F \cdot D \cdot v)/RT]^{0.5} \quad (5.5)$$

where:

i_p is the peak current, n is the number of electrons involved in the electrode reaction, α is the charge transfer coefficient, z_c is the number of electrons transferred in the rate determining step, A is the electrode area surface, D is the diffusion coefficient of stannous ions, $v$is the potential scan rate and c is the concentration. From the literature data, the diffusion coefficient of stannous ions was estimated to be $6.5\times10^{-10} m^2\ s^{-1}$ [116] and for cupric ions was estimated to be $0.72\times10^{-9}\ m^2 s^{-1}$ [97].

A plot of the peak current i_p as a function of the square root of the scan rate $v^{1/2}$ is shown Fig. 5.6. This plot yields a straight line and from the slope, the number of electrons involved in the reaction was estimated.

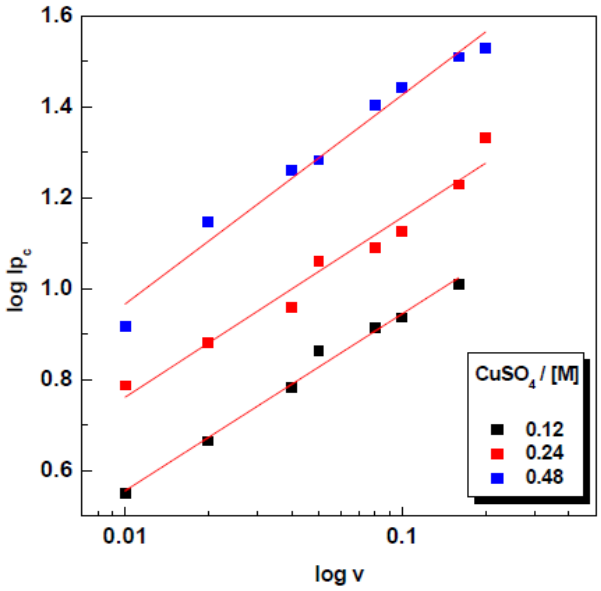

Figure 5.6 Dependence of the log I_p vs. log v extracted from cyclic voltammograms at a Pt electrode for different concentration of $CuSO_4$.

The reduction slopes log I *vs.* log v obtained from Figure 5.6 were ranged between 0.3 ÷ 0.5 (Table 5.3). For a kinetic control the values should be close to theoretical value 1. In our case, the values are close to 0.5 suggesting that the process is diffusion controlled [21].

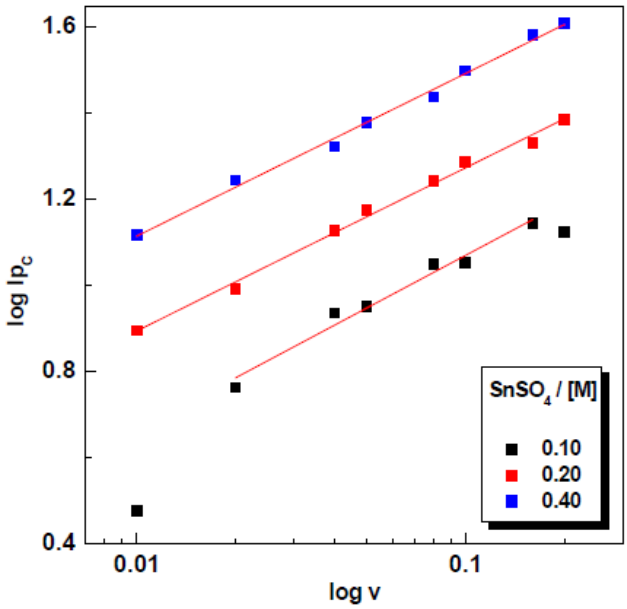

Figure 5.7 Dependence of the log I_p vs. log v extracted from cyclic voltammograms at a Pt electrode for different concentration of $SnSO_4$.

Table 5.3 Corresponding linear regression parameters of log I vs. log v for different concentrations of $CuSO_4$ and $SnSO_4$. Experimental conditions: see Fig. 5.3 and 5.4.

Concentration (M)	Slope reduction	R / nr. of points reduction
$CuSO_4$ in H_2SO_4 1M		
0.12	0.39 ± 0.01	0.987 / 7
0.24	0.40 ± 0.03	0.960 / 8
0.48	0.46 ±0.02	0.974 / 8
$SnSO_4$ in H_2SO_4 1M		
0.10	0.41 ± 0.03	0.971 / 6
0.20	0.38 ± 0.01	0.994 / 8
0.40	0.38 ± 0.01	0.993 / 8

The CV studies allow establishing the adequate potential and current density parameters for the Cu and Sn electrodeposition. These informations will be further used for the synthesis of the electrode material in galvanostatic and potentiostatic conditions.

5.2.2. Rotating disk electrode experiments

In order to investigate the electrodeposition of Cu and Sn in hydrodynamic conditions, rotating disk electrode experiments were performed. Fig. 5.8 shows the polarisation curves of copper and tin electrodeposited under controlled rotation speeds from 0.1 M $CuSO_4$ and 1M H_2SO_4. Electrode rotation speeds from 250 to 2000 rpm were investigated; polarisation curves in the background electrolyte were also carried out. The electrode potential was swept from 0.0 to −0.8V *vs.* $Ag/AgCl/KCl_{sat}$ at 10 mVs^{-1}.

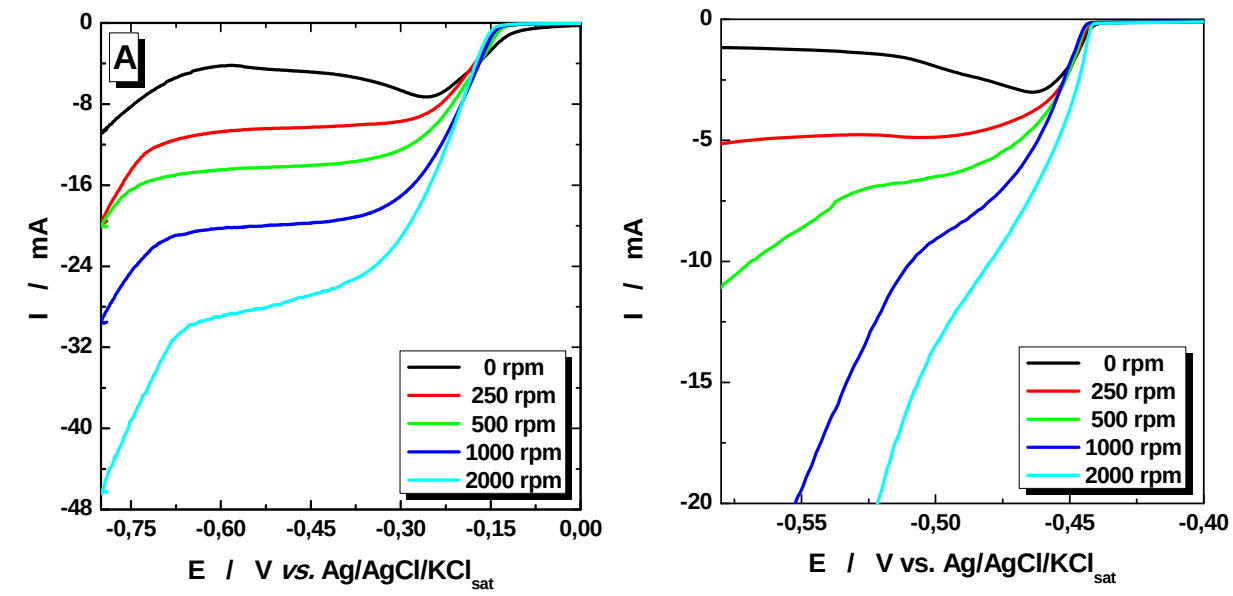

Figure 5.8 Influence of electrode rotation rate on Cu (A) and Sn (B) deposition. The electrolyte contains 0.1 M $CuSO_4$ and 1 M H_2SO_4 (A) and 0.1 M $SnSO_4$ + 1M H_2SO_4 (B). Electrode scan rate: 10 mVs^{-1}.

In contrast, the intensity of the plateau current (I_L) observed in the presence of copper and tin ions (see Fig. 5.8.) clearly depends on the electrode rotation speed (ω). In addition, the hydrogen evolution reaction induces a high increase of the current below -0.7 V vs. $Ag/AgCl/KCl_{sat}$for copper ions and below -0.5V vs. $Ag/AgCl/KCl_{sat}$ for tin ions. From Fig. 5.9 Levich plots (I_L vs. $\omega^{1/2}$) were constructed according to the following equation [27]:

$$I_L = 0.62nFAD^{2/3} \cdot v^{-1/6} \cdot \omega^{1/2} \cdot c_0 \qquad (5.6)$$

where: A is the geometric electrode area surface, c_0 - is the bulk concentration, D - the diffusion coefficient, ω - the electrode rotation rate, I_L - the limiting current, n - the number of electrons involved at the considered reaction and v - the kinematic viscosity.

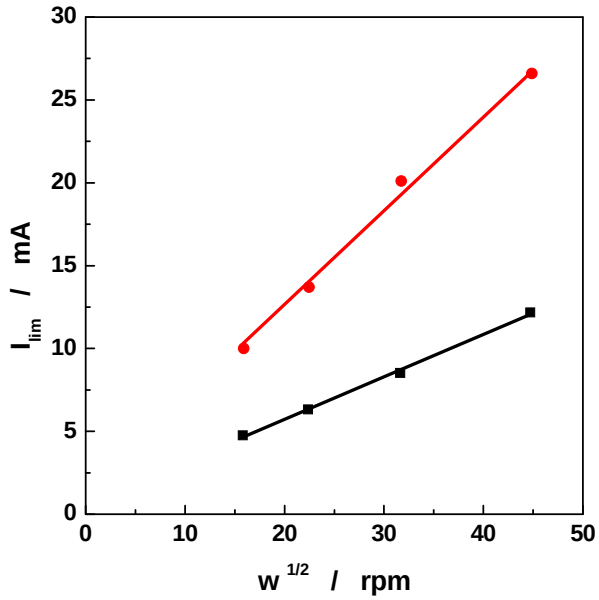

Figure 5.9 The corresponding Levich plots I_L for copper ions (red line) and for tin ions (black line) vs. the square root of the rotating rate $\omega^{1/2}$. Experimental conditions as in Fig. 5.8

The Levich plots (I_L vs $\omega^{1/2}$) in presence of copper ions (red line) and for tin ions (black line) are presented in Fig. 5.9. In both cases, this representation yields a straight line passing through the origin, confirming that the processes are transport controlled.

The obtained results allowed us to see the limiting current for copper and tin electrodeposition, which will help us in the future choosing of the galvanostatic parameters for obtaining the electrode material in an intensified mass transport regime and economic as well.

5.2.3. Morphological studies

5.2.3.1. Study of copper deposits

All the SEM analyses were performed in order to give informations about the surface morphology and the crystalline structure of the investigated deposits. Moreover, with the SEM data a correlation between the uniformity and composition of the deposits could be established. In this stage of researches it was followed that the substrate used for the preparation of the electrode material to be entirely covered and to obtain uniform deposits with a high Sn content in the case of CuSn alloy.

In order to study the electrodeposition of the copper (as standard electrodeposition process), deposits were obtained galvanostatically from a 0.1 M $CuSO_4$ in 1M H_2SO_4 bath. The SEM images obtained for copper deposits are presented in Figure 5.10.

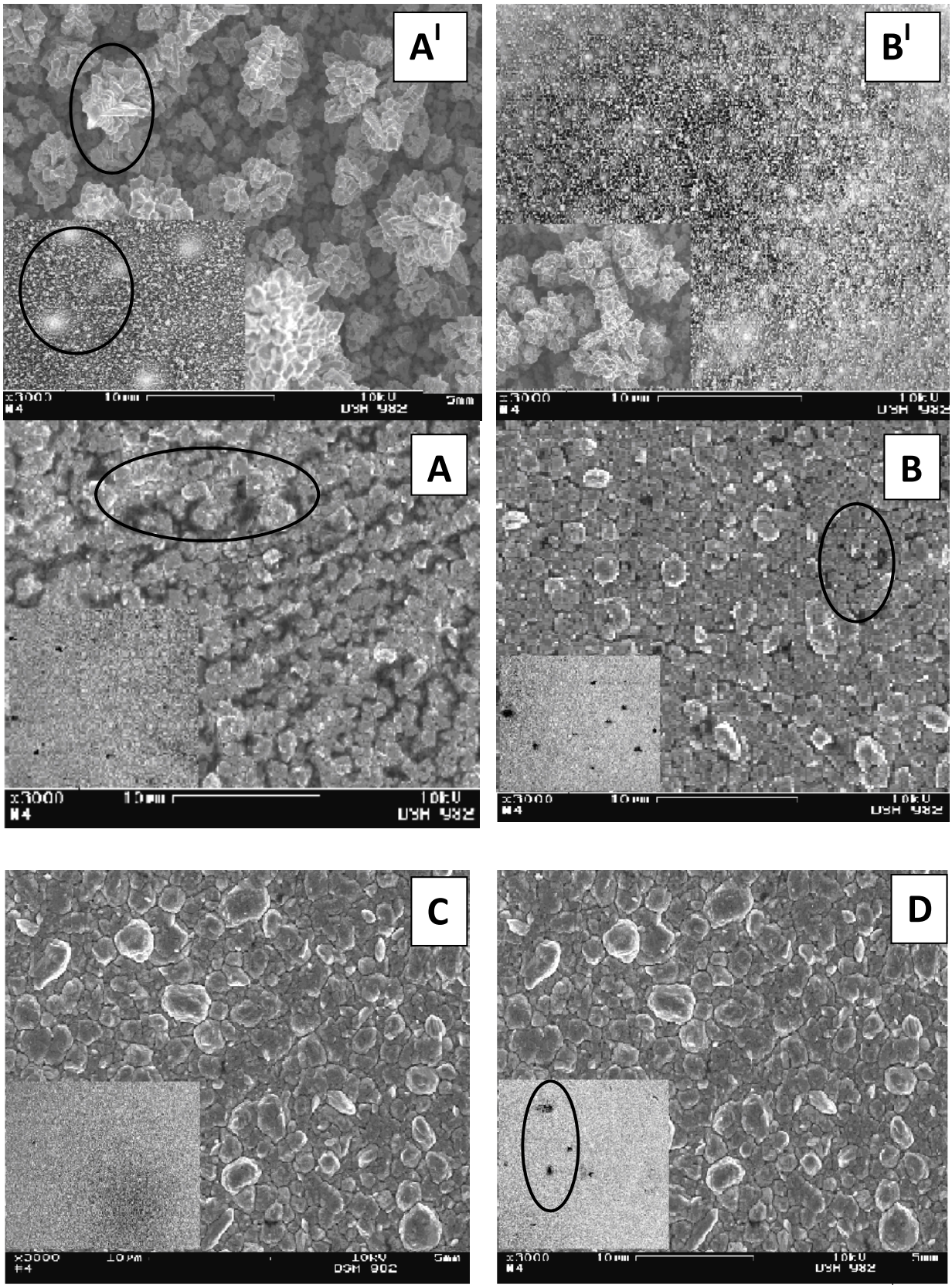

Figure 5.10 SEM micrographs showing the surface morphologies of Cu films obtained at i = 10 mA cm^{-2} (**A, A^I**), 20 mA cm^{-2} (**B, B^I**), 40 mA cm^{-2} (**C**), 80 mA cm^{-2} (**D**) with (2000 rpm: A, B, C and D) and without stirring (0 rpm: A^I and B^I)**.** (x 3000 respectively x 50 inset image)

From Figure 5.10 it can be seen that there are large differences between the deposits obtained with and without stirring the disk electrode. During electrodeposition, bubbles are visible on the cathode surface and dendritically features are produced in the deposits. Deposits of Cu obtained without stirring present crystals of well-defined morphology, some of them elongated with dendritically morphology [132].

On the other hand at the rotating the disk electrode, a good improvement of the morphology is observed and a smoother surface is obtained. Also, some dark black spots were observed on the surface, suggesting that the surface was not covered entirely by the deposit. Compared to the deposits obtained under static conditions, these deposits are more uniform. SEM micrographs of electrodeposited copper surfaces show that smoother surfaces are obtained with a current density of 40 mA cm^{-2}. These results are in accordance with literature [133].

5.2.3.2. Study of tin deposits

Electrodeposition of tin was performed only at rotating electrodes. In this study the tin deposits were obtained in a simple acidic bath containing 0.10 M $SnSO_4$ and 1M H_2SO_4. The SEM images obtained for tin electrodeposition at different current densities are presented in Figure 5.11.

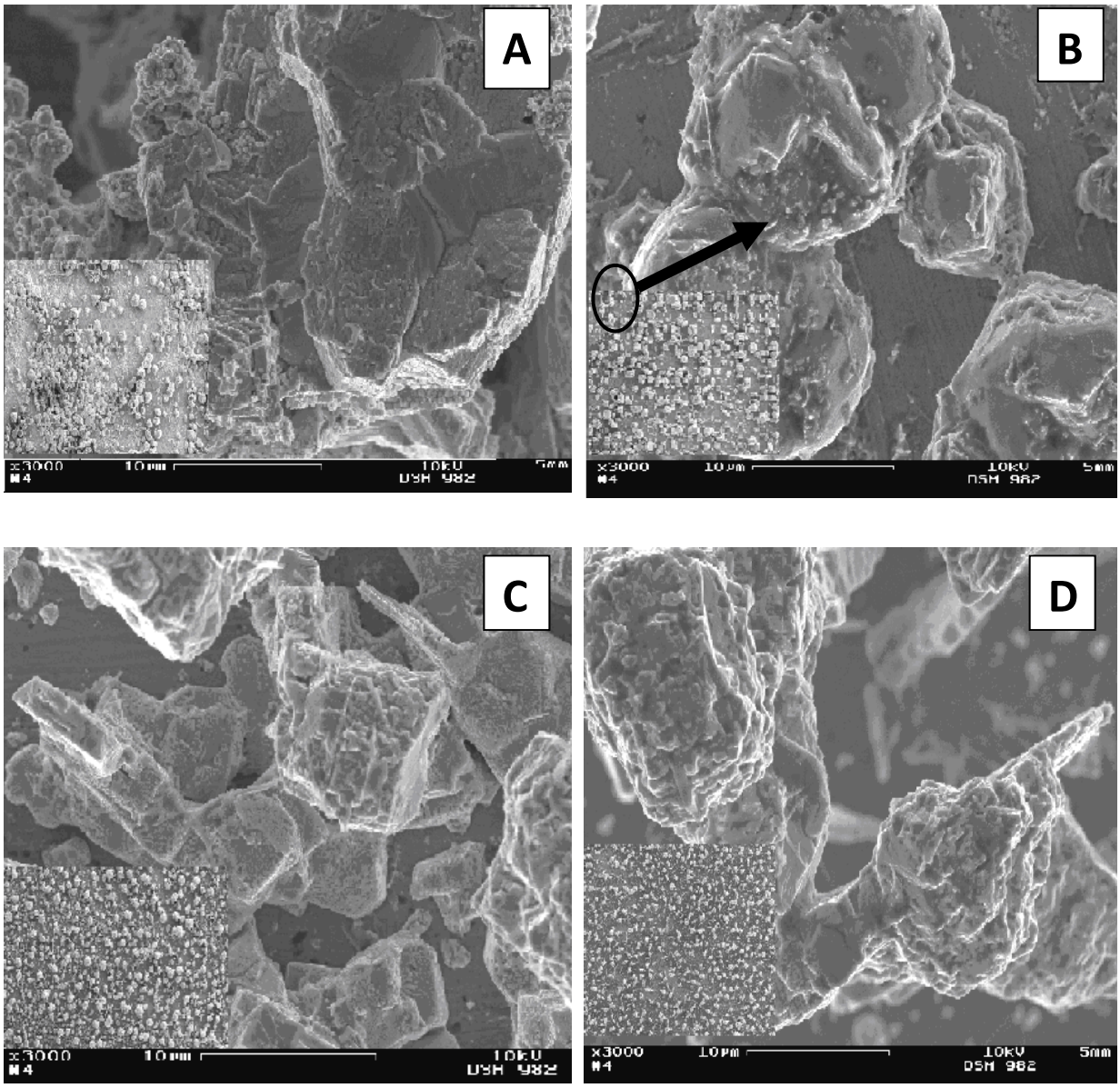

Figure 5.11 SEM micrographs showing the surface morphologies of Sn films obtained at i = 10 mA cm^{-2} (**A**), 20 mA cm^{-2} (**B**), 40 mA cm^{-2} (**C**), 80 mA cm^{-2} (**D**) with (2000 rpm) stirring. (x 3000 respectively x 50 inset image)

From the SEM micrographs (Fig. 5.11) it can be observed that by increasing the current density the shape of the grains is changing. Deposits obtained with agitation present crystals of well-defined morphology, some of them elongated with the characteristic tetragonal morphology of tin crystals [134]. Deposits made with agitation, present larger crystals and in most of the cases the large crystals show coalescence. The tin grains are much bigger than the copper grains obtained under the same conditions.

5.3. CuSn alloy electrodeposition

5.3.1. Voltammetry studies

Two types of baths were proposed for the electrodeposition of CuSn alloy (Table 5.4).

Table 5.4: Bath composition for CuSn alloy

Bath I	Bath II
$CuSO_4$	$CuSO_4$
$SnSO_4$	$SnSO_4$
H_2SO_4	H_2SO_4
	HBF_4

Tetrafluoroboric acid (HBF4) was chosen because it is known to keep the metal ions dissolved in the solution and to ensure a consistent deposition of CuSn alloy. In order to see where the electrodeposition of the two metals occurs, several cathodic sweeps were performed (Fig. 5.12).

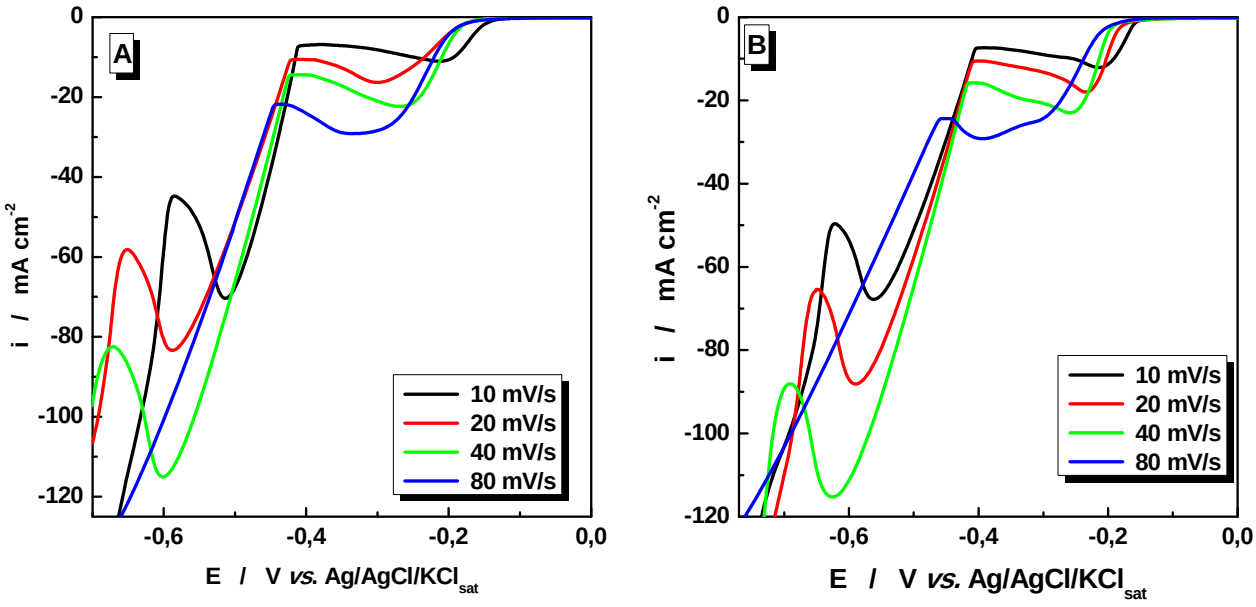

Figure 5.12 Cathodic sweeps of CuSn alloy deposition at different sweep rates recorded at a platinum disc electrode. The electrolyte was prepared at 296 K and contains: (**A**) $SnSO_4$ 0.4 M + $CuSO_4$ 0.1 M + H_2SO_4 1M and (**B**) $SnSO_4$ 0.4 M + $CuSO_4$ 0.1 M + HBF_4 0.2 M + H_2SO_4 1M

The copper deposition starts in the potential range -0.2 V ÷ -0.4V followed by tin deposition in the potential range -0.45 V ÷ -0.7V. Adding HBF_4 into the bath solution does not significantly modify the deposition potentials of the two metals.

5.3.2. Rotating disk electrode experiments

Fig. 5.13 shows the polarisation curves of CuSn electrodeposited under controlled rotation speeds from 0.1 M $CuSO_4$ + 0.1 M $SnSO_4$ + 1M H_2SO_4 bath. Electrode rotation speeds from 250 to 2000 rpm were investigated. The electrode potential was swept from 0.0 to −0.8V *vs.* $Ag/AgCl/KCl_{sat}$ at 10 mVs^{-1}.

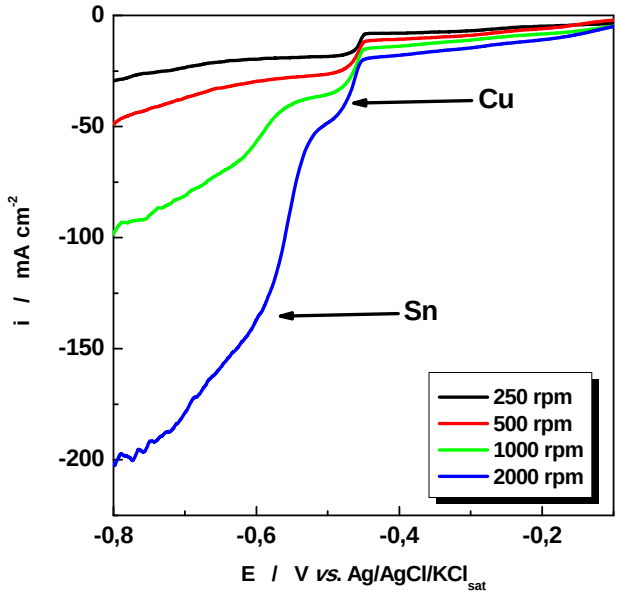

Figure 5.13 Influence of electrode rotation rate on CuSn deposition. The electrolyte contains 0.1 M $CuSO_4$ + 0.1 M $SnSO_4$ + 1M H_2SO_4. Scan rate: 10 mVs^{-1}.

The limiting current observed in the presence of CuSn ions (see Fig. 5.13) clearly depends on the electrode rotation speed (ω). Further, the effects regarding the quality and the performance of the alloy deposit towards ERN will be discussed.

Further on, the surface morphology of the deposits was studied. Potentiostatic and galvanostatic experiments were performed to study the influence of parameters on the electrodeposition of copper, tin and copper-tin alloys. Galvanostatic experiments were performed for depositing 5 μm of copper, tin and copper-tin alloys.

5.3.3. Study of copper-tin deposits

5.3.3.1. Deposits obtained by galvanostatic electrolysis

The desired composition for our CuSn alloy study is $Cu_{15}Sn_{85}$. In order to achieve this composition galvanostatic and potentiostatic measurements were performed. Figure 5.14 presents the SEM images obtained for Cu-Sn deposits, under different galvanostatic conditions from two types of baths. Information about baths composition is given in Figure caption 5.14.

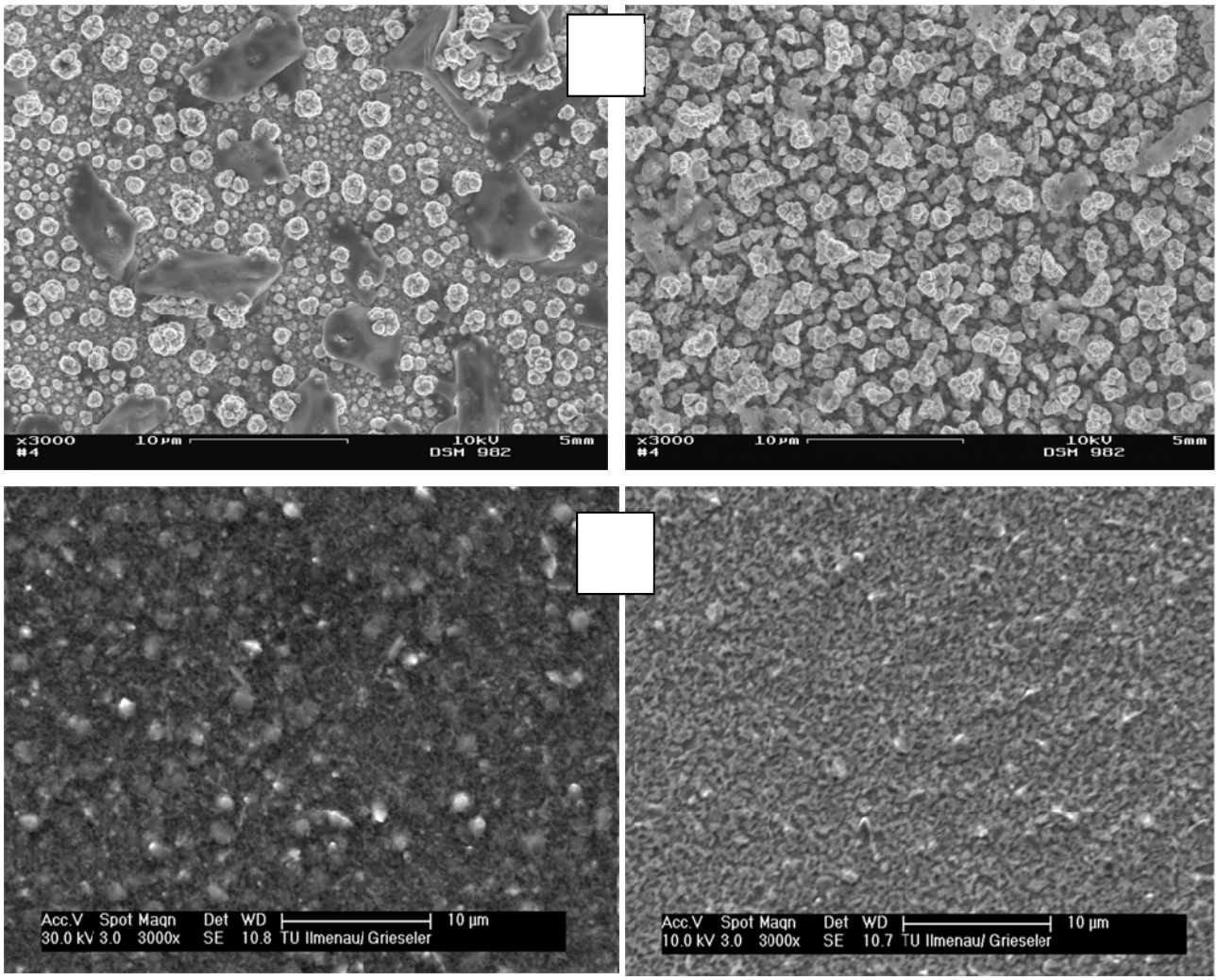

Figure 5.14 SEM micrographs showing the surface morphologies of Cu-Sn films obtained at i = 80 mA/cm^2 (**A**) and i = 120 mA/cm ^{2}(**B**), with stirring (2000 rpm). **Bath I** (0.1 M $CuSO_4$ + 0.4 M $SnSO_4$ + 1 M H_2SO_4) is presented in the left side and **Bath II** (0.1 M $CuSO_4$ + 0.4 M $SnSO_4$ + 1 M H_2SO_4 + 0.2 M HBF_4) in the right side, respectively.

As can be seen in Fig. 5.14 the CuSn alloys have a uniform surface morphology. A small difference between the two baths can be observed: Bath II reveals smoother deposits.

5.3.3.2. Deposits obtained by potentiostatic electrolysis

Based on the CV studies, we obtained CuSn deposits potentiostatically in the range between E = -0.5 V ÷ - 0.7 V. All the potentiostatic deposits had a thickness of 5μm. Information about baths composition is given in Figure caption 5.15.

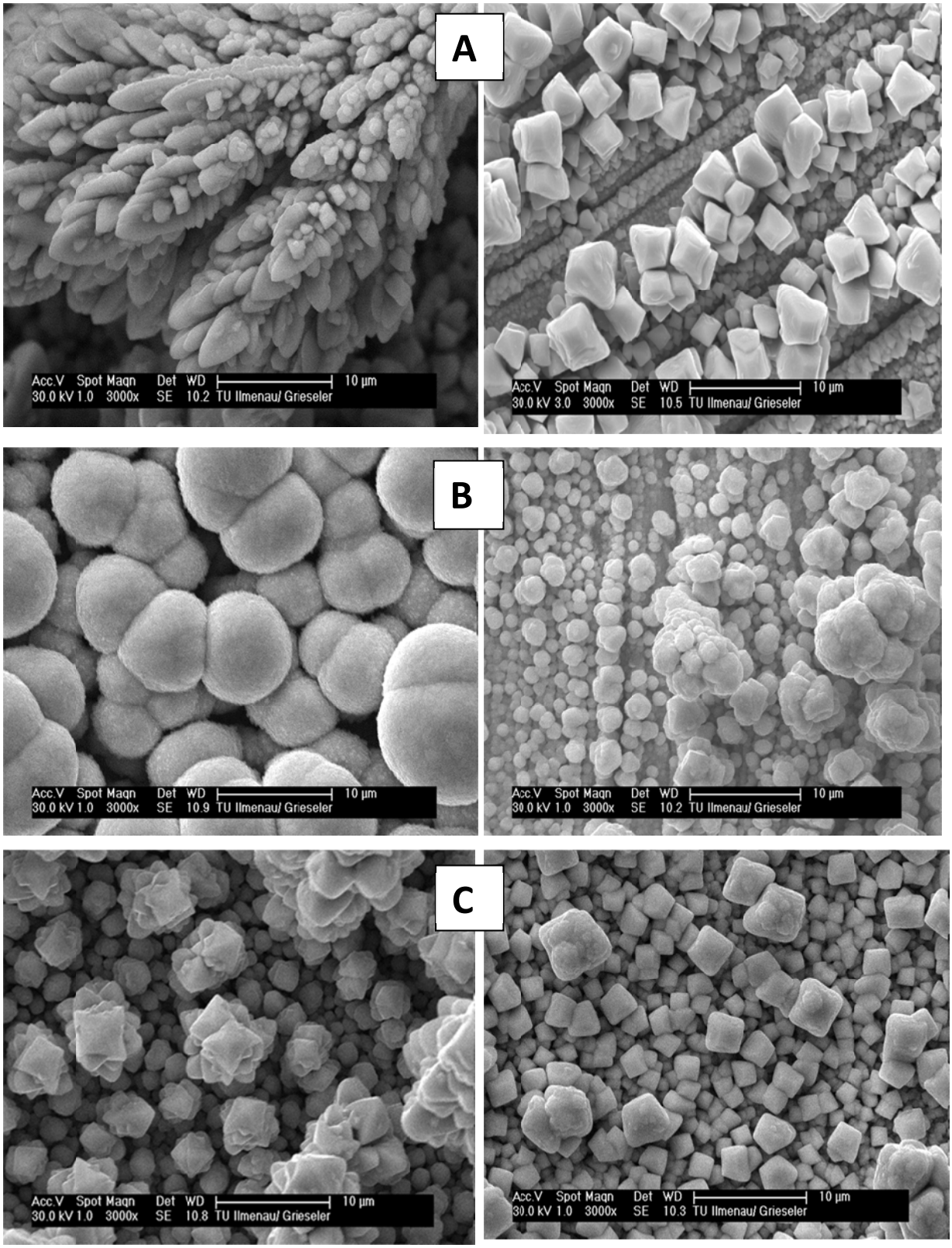

Figure 5.15 SEM micrographs showing the surface morphologies of CuSn films obtained at E = -0.5 V (**A**), E = -0.6 V (**B**) and E = -0.7 V (**C**) with stirring (2000 rpm). **Bath I** (0.1 M $CuSO_4$ + 0.4 M $SnSO_4$ + 1 M H_2SO_4) is presented in the left side and **Bath II** (0.1 M $CuSO_4$ + 0.4 M $SnSO_4$ + 1 M H_2SO_4 + 0.2 M HBF_4) in the right side, respectively.

As it can be seen from Fig. 5.15 for the potentiostatic deposition at E = -0.5 V vs. Ag/AgCl the surface morphology of the deposits looks very sharp and rough. This roughness could be related to the fact that, at E = -0.5V the deposition of tin just starts. This assumption is in correlation with the CV studies. As the potential increases (see E = -0.6 V and E = -0.7 V) uniform and dense deposits are obtained. Analyzing the insets, we can conclude that the deposits do not present any major differences. The CuSn grains are very small, indicating that the nucleation and growth of the crystals takes place uniformly.

5.4. EDX analysis

The relation between the metal ratio of the bath and the metal ratio of the deposit is one of the most important relations in alloy deposition. EDX analysis permits us to establish the correlation between the bath and alloy composition.

Table 5.5: Correlation between current density and copper and tin content for deposits obtained from the two types of baths **Bath I** and **Bath II**, estimated thickness of the deposits 5 μm.

i	**Cu**	**Sn**
(mA/cm^2)	(w/w %)	
Bath I 0.1 M $CuSO_4$ + 0.4 M $SnSO_4$ + 1 M H_2SO_4		
80	65	35
120	48	52
Bath II 0.1 M $CuSO_4$ + 0.4 M $SnSO_4$ + 1 M H_2SO_4 + 0.2 M HBF_4		
80	56	44
120	43	57

Analyzing the alloy deposits obtained under galvanostatic conditions (Table 5.5), we observed that by increasing the current density, in bath I the Cu content decreased and the Sn content of the deposit increased. Our results are in agreement with the one obtained by Bennett [135]. On the other hand analyzing the alloy deposits, obtained under galvanostatic conditions, using a bath containing HBF_4 we observed that with increasing current density the

Sn content increased. Therefore, in this stage we can conclude that when an increased current density is used the content of tin increases.

EDX analyses were performed also for the deposits obtained by potentiostatic electrolysis. Table 5.6 the composition of the alloys.

Table 5.6: Correlation between potential and CuSn content for deposits obtained from the two types of baths: **Bath I** and **Bath II**, estimated thickness of the deposits 5 μm.

E	**Cu**	**Sn**
(V vs. Ag/AgCl)	(Wt %)	
Bath I 0.1 M $CuSO_4$ + 0.4 M $SnSO_4$ + 1 M H_2SO_4		
-0.5	87	13
-0.6	58	42
-0.7	61	39
Bath II 0.1 M $CuSO_4$ + 0.4 M $SnSO_4$ + 1 M H_2SO_4 + 0.2 M HBF_4		
-0.5	85	15
-0.6	55	45
-0.7	57	43

At E = -0.5V, in both plating baths, the content of Sn is very small (Table 5.6). This is in correlation with the galvanostatic and voltammetry results, showing that at this potential the Sn electrodeposition just starts. As the potential increases, the Sn content also increases.

In order to achieve the alloy composition described above, we increased the tin concentration in the bath. Now, the baths have the following composition: 0.1 M $CuSO_4$ + 0.8 M $SnSO_4$ + 1 M H_2SO_4 (**Bath Ia**) and 0.1 M $CuSO_4$ + 0.8 M $SnSO_4$ + 1 M H_2SO_4 + 0.2 M HBF_4 (**Bath IIb**). When potentiostatic mode is used, experiments were performed for the ratio Cu:Sn = 1:8.

Table 5.7: Correlation between potential and CuSn content for deposits obtained from two types of baths **Bath Ia** and **Bath IIb**
estimated thickness of deposits 5 μm.

E	**Cu**	**Sn**
(V vs. Ag/AgCl)	(wt %)	
Bath Ia 0.1 M $CuSO_4$ + 0.8 M $SnSO_4$ + 1 M H_2SO_4		
-0.5	49	21
-0.6	33	67
-0.7	36	64
Bath IIb 0.1 M $CuSO_4$ + 0.8 M $SnSO_4$ + 1 M H_2SO_4 + 0.2 M HBF_4		
-0.5	42	58
-0.6	27	73
-0.7	29	71

When the concentration of tin was increased, we can observe that EDX analyses are in good correlation with this modification. The tin content increased as the potential increases. The highest tin percentage in the deposit (73%) was obtained at E = -0.6V, with bath IIb [136]. The EDX analyses (see Table 5.7) are in good correlation with the surface morphology analysis (see Fig. 5.15). An electrode material with high Sn content was obtained. Alloys with high Sn content have high electrocatalytic activity [45] and also CuSn alloy has the ability to control the ERN to nitrogen gas as final product [55]. Thus, we conclude that the deposit $Cu_{27}Sn_{73}$ is a suitable material for nitrate reduction due to its composition. This material will be investigated further for electrochemical reduction process (see Chapter 6 and 7).

5.5. Conclusions

Based on the above results we conclude:

The CV studies allowed us to establish the specific parameters concerning the electrodeposition of the individual metals and alloy respectively. Analyzing the voltammograms (see Fig. 5.5 and the data from Table 5.2) we can conclude that the anodic and cathodic copper and tin peaks do not represent the mirror image of each other they characterize a quasi-reversible process. For three different copper concentrations (0.12, 0.24

and 0.48 M) the number of transferred electrons was found to be 2.1 ± 0.15.In a similar way, for three different tin concentrations (0.10, 0.20 and 0.40 M), the number of transferred electrons (n =2.2 ± 0.06) was calculated. According to different possible pathways for the copper and tin electroreduction, only one reaction involves two electrons, which is the reduction of Cu^{2+} and Sn^{2+} to metallic Cu and Sn.

The reduction slopes log I vs. log v were ranged between 0.3 ÷ 0.5 (Table 5.3). the values were closed to 0.5 suggesting that the process is diffusion controlled.

SEM images taken for copper, tin and copper-tin alloy deposits indicate significant changes in their surface morphology by changing the electrodeposition parameters (see Fig. 5.10, 5.11, 5.14 and 5.15). Moreover, the rotational speed plays an important role in the process of electrodeposition, showing a significant improvement of deposits. 2000 rpm seems to be a suitable rotational speed for obtaining good deposits. Based on SEM measurements the Cu-Sn deposits are more uniform if potentiostatic deposition is used (see Fig. 5.15).

The highest tin percentage in the deposit (73%) was obtained at E = -0.6 V with bath IIb. The EDX analyses (see Table 5.7) are in good correlation with the surface morphology analyses (see Fig. 5.15). The performances of the obtained electrode materials will be further investigated (see Chapter 6 and 7).

6. ELECTROACTIVE SPECIES DETECTION RESULTING FROM ELECTROCHEMICAL REDUCTION OF NITRATE AT Cu AND CuSn ALLOYS

After synthesis and characterization of copper, tin and copper-tin alloy, the copper and copper-tin electrode material was chosen to be used as cathode materials for reduction of nitrate from model nitrate solutions.

The objective of this part of the thesis was to establish the optimal conditions for the detection of the electroactive species resulting from electrochemical reduction of nitrate (ERN). A simple and fast electrochemical methodology for determination of electroactive products resulting from nitrate reduction at a Cu and CuSn electrode in an alkaline media is proposed on the basis of cyclic hydrodynamic voltammetry (CHV) and square wave voltammetry (SWV). In our studies a modified CHV method was used for the detection of electroactive products resulting from ERN [137]. SWV method was used for the detection of electroactive products resulting from ERN [138]. The results of SWV were compared with those obtained through CHV. Our main purpose in this study is to obtain a fast and cheap analysis method of the electroactive products resulting from nitrate reduction.

The electrochemical measurements were carried out at relative high scan rates (500 mV/s) using a Pt/Cu and a Pt/Cu-Sn RRDE. Cyclic voltammetry combines the high scan rate with the controlled hydrodynamic mass transport. The SWV measurements were performed using the Pt ring as working electrode. After the polishing of the ring-disk electrodes they were pre-treated by repeated cycling between hydrogen and oxygen evolution regions -1.5 and +2.0 V vs. $Ag/AgCl/KCl_{sat}$. After the pre-treatment reproducible current-voltage curves were obtained. For each studied species, the electrochemical cell was first filled with 100 mL of 1 M Na_2SO_4 as supporting electrolyte. After that different amounts of NO_2^-, NH_2-OH and NH_4^+ stock solutions were added successively (resulting concentrations of 0.1, 0.5, 1.0, 2.0 g/L) and the pH was adjusted to 11.0 using 1 M NaOH.

6.1. Electroactive species detection in mono-component solutions

In order to evaluate the possibility of electrochemical detection of some electroactive products resulted from ERN in alkaline media, we performed preliminary studies in mono-component solutions using the standard addition method.

Figures 6.1A and 6.1B show the cyclic and square wave voltammograms recorded at the Pt ring electrode in 1 M Na_2SO_4 in the presence of different concentrations of NO_2^-. For clarity, figures present only the positive potential ranges from the corresponding anodic scan. Measurements were performed with the disk electrode disconnected; the detection of the individual species was carried out at the Pt ring electrode. In mono-component solutions, well defined oxidation peaks of nitrite (see Fig.6.1) were recorded using both techniques.

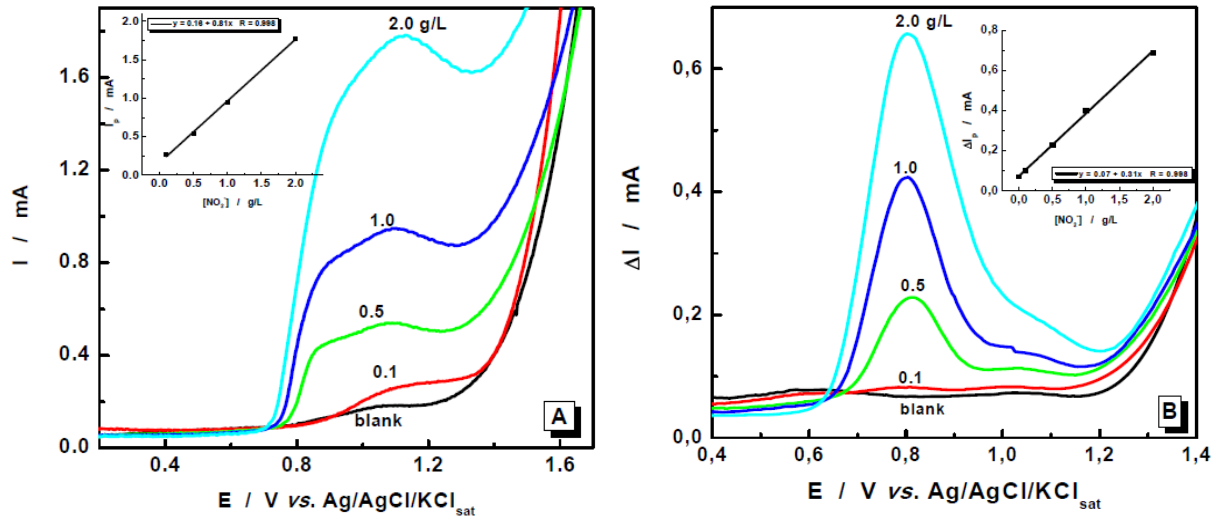

Figure 6.1 Anodic peak current dependence on the NO_2^- concentration by CHV (A) and SWV (B) Experimental conditions: Start potential = -1.5 V and end potential = 2.0 V, ω = 1000 rpm, disk electrode disconnected; CHV: v = 500 mV s^{-1}; SWV: wave amplitude = 50 mV; wave period = 10 ms; wave increment = 5 mV.

As it can be seen in Figure 6.1A, using CHV, the oxidation peaks of nitrite were detected close to + 1.1 V. In SWV (Figure 6.1B) experiments the oxidation peaks for nitrite can be observed at +0.8 V. The SWV measurements reveal well defined peaks and the peak potential does not vary with the concentration. The insets in Fig. 6.1A and 6.1B present the relationship between the peak current and the nitrite concentration. In both cases a good linear correlation (R = 0.998) can be observed.

Comparing the results obtained previously [139] and SWV for the nitrite oxidation, a ~ 300 mV difference between the peak potential values can be observed. This can be explained by the very poor reversibility of the nitrite oxidation process at Pt and also by the extremely large range of mixed control (kinetic and mass transport, resulting from the combination of the fast potential scan rate and the forced convection). Both factors inducing a positive shift of oxidation peak potential recorded by CHV. Contrarily, in SWV, where

roughly speaking the recorded curves can be considered, as the first order derivate of the cyclic voltammetric records, the observed peak potentials become closer to the equilibrium potential and also the influence of the mass transport is significantly reduced.

The electro-reduction of nitrite at a Pt electrode was explained by the group Piela et al. [140] where they observed that the nitrite electro-oxidation process strongly depends on the state of the electrode surface. The reaction is inhibited by the oxide layers formed at the platinum electrode surface.

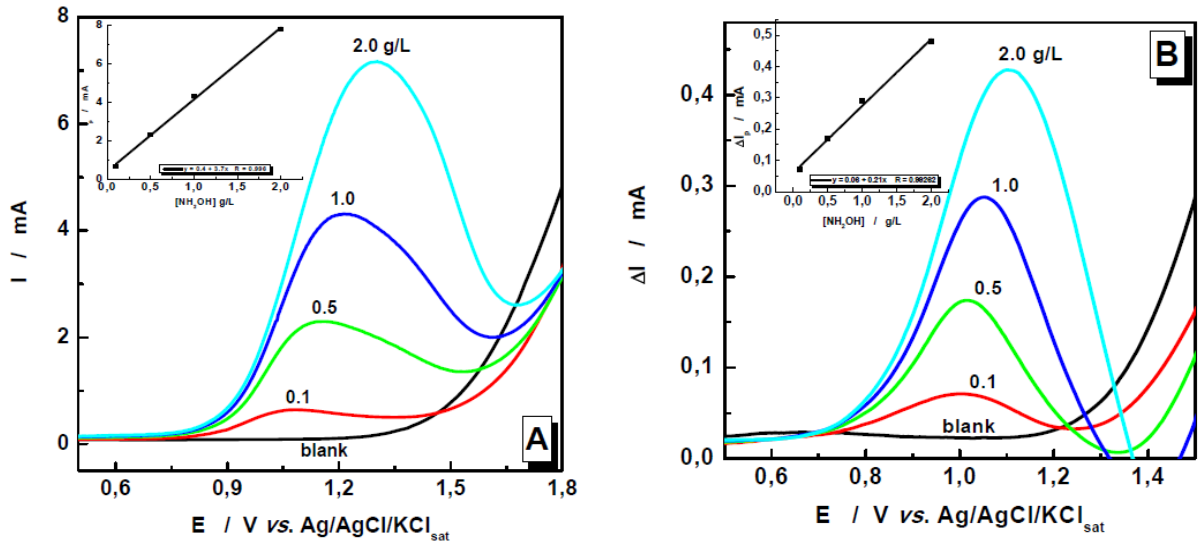

Figure 6.2 Anodic peak currents dependence with NH_2OH concentration by CHV (A) and SWV (B) at Pt ring electrode.

Figures 6.2A and 6.2B show CHV and SWV data for different concentrations of hydroxylamine and in the inset the relationship between the recorded peak currents and the hydroxylamine concentrations is presented. It is worth noting that for both techniques, a good linear correlation (R= 0.996) between the oxidation peak currents and the hydroxylamine concentration was obtained. In mono-component solutions, depending on the concentration, the oxidation peak potential of hydroxylamine was between +1.1 and +1.3 V for CHV and between +1.0 and +1.1 V for SWV, respectively. Compared to the nitrite oxidation, we observed only a relatively small difference (from 100 to 200 mV) between the peak potentials values evaluated by CHV and SWV. Taking into account that, the hydroxylamine oxidation process is faster at the Pt electrode, the decrease of this difference sustains the previous explanation.

A comparison between Fig. 6.1 and 6.2, when CHV method is used, was reported in [141].Gadde and Bruckenstein [142] studied the electro-oxidation of nitrite in 0.1M $HClO_4$ at a Pt electrode. Using RRDE technique, they showed that nitrite reduction is a convective-diffusion controlled process. On the other hand, their product analysis data indicate possible kinetic complications in the electrode reaction because of multiple product formation. Furthermore, Piela et al. [143] investigated the hydroxylamine oxidation in acidic media at the rotating platinum electrode. They showed that, an evidence for a kinetic hindrance of the reaction caused by the platinum oxide layer was present at the electrode surface. The process is hindered by the oxide, because the reaction is sensitive to all experimental conditions that influence the oxide formation process, *i.e.*, potential, time, and pH.

Anodic sweeps recorded in the presence of different concentrations of ammonium are presented in Figure 6.3.

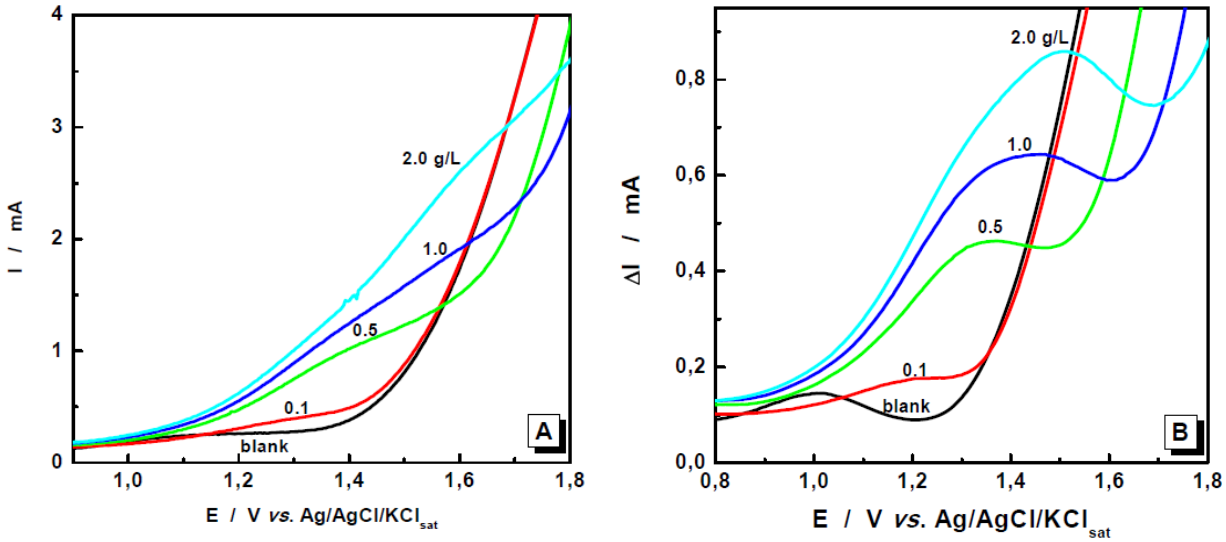

Figure 6.3 Anodic peak current dependence with NH_4^+ concentration by CHV (A) and SWV (B) at Pt ring electrode.

As a result of, at pH = 11 the ratio between NH_3 and NH_4^+ concentrations is 40[144] ammonium can be electrochemically detected by ammonia oxidation (see Fig.6.3.). The CHV measurements for different concentrations of ammonium reveal only poorly defined plateaus at ring potentials higher than +1.3 V. On the other hand, SWV measurements revealed well defined peaks for ammonia oxidation at ring potentials between +1.2 and +1.5 V, demonstrating that the SWV based method is more suitable for electrochemical detection of ammonia than CHV.

Due to the high sensitivity and the rejection of background currents (see Chapter 4.1.4), SWV can be successfully used for the individual detection of all the three involved species. Three different peak potentials were attributed: + 0.8 V for NO_2^- oxidation, +1.0 V for NH_2OH oxidation and at approximately +1.3 V for ammonia oxidation.

6.2. Experimental parameters selection

In order to evaluate the possibility of simultaneous electrochemical detection of electroactive products resulting from ERN in alkaline media, several experimental parameters were examined for developing a suitable analytical procedure for the determination of electroactive products, such as frequency (f), scan increment (E_{step}) and pulse height (ΔE_p). The study was done with 2 g/L NO_3^- in 1M Na_2SO_4 (pH 11.0). The peak current intensity increased linearly over the frequency range 10–100 Hz (see Fig. 6.4).

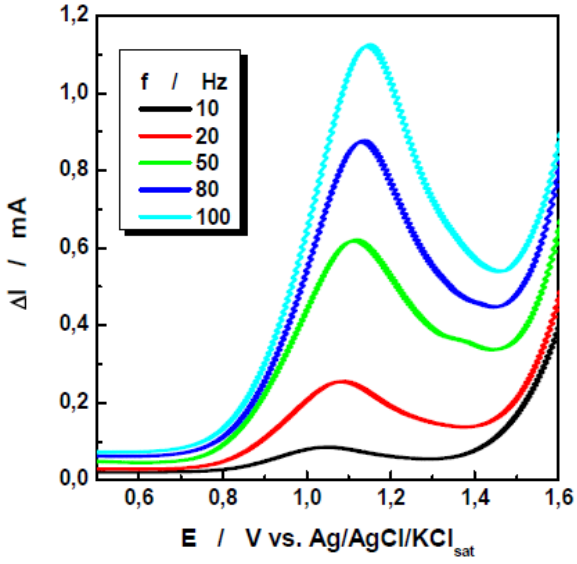

Figure 6.4 Anodic peak currents dependence with frequency (f) by SWV at Pt ring electrode.

The frequency of 100 Hz was chosen as suitable. At a frequency of 100 Hz, and pulse height of 50 mV, the peak current intensity increased linearly with the scan increment up to 5 mV. The scan increment of 5 mV was further applied. The increase of the wave amplitude increases the current intensity and linearity was observed up to 50 mV. The choice of ΔE_p = 50 mV yields optimum sensitivity with reasonable resolution [104]. The unusual high scan rate was selected based for two reasons: (i) at 500 mV/s a better sensitivity was obtained and (ii) the duration of the measurements for each cycle becomes short (~14 s), allowing us to

observe the very fast decrease of the Cu electrode electro-catalytic activity during the ERN process (see Chapter 6.3). A rotation of 1000 rpm gave reproducible limiting currents and was chosen for all the experiments.

A nitrate concentration of 2 g/L was chosen because it corresponds to the typical composition of some low level nuclear waste solutions, where the concentration of nitrate is about 1.80 M [13]. Taking into account that the homogeneous equilibrium between the $NH4^+$ and NH3 have a specific constant p*K*a = 9.25 [145], we chose a pH value of 11 in order to maintain the main amount of obtained ammonium in the form of ammonia (97.5 %). These results allow us to conclude that best results can be obtained using a 2 g/L NO_3^-solution containing 1 M Na_2SO_4 as supporting electrolyte, a rotation rate of 1000 rpm, a scan rate of 500 mV/s, pH 11.0 and thus these experimental conditions were used for all subsequent investigations.

6.3. Electrocatalytic stability of the electrode material

In order to evaluate the possibility of simultaneous electrochemical detection of electroactive products resulting from ERN in alkaline media, a working disk electrode of Cu or CuSn was used. This choice was based on the fact that this material has a well-known electrocatalytic activity for ERN and depending on the electrolyte composition and applied potential, a wide variety of species can be generated. For each set of measurements, the working disk electrode (Pt covered with Cu or CuSn) was polarised at a constant potential. Potentiohydrodynamic measurements were performed at the Pt ring electrode (between -1.5 and +2.0 V) and eight successive cycles were recorded without refreshing the Cu or CuSn layer.

For an accurate comparison, before each set of CHV and SWV measurements, the surface of the Pt disk electrode was covered with a thin layer (5 μm) of freshly electrodeposited Cu or CuSn. The experimental conditions for obtaining the electrode materials were presented at the previous section (see Chapter 5). The anodic currents recorded at the Pt ring electrode, corresponding to the oxidation of species generated at the disk, were investigated. Figure 6.5 presents three detailed examples of the currents recorded by SWV at the Pt ring electrode during the anodic scans, for different disk polarisation potentials. Only the anodic portions from the 1st, 2nd, 4th and 8th cycle, at a Cu electrode are presented in Figure 6.5. Depending on

the applied potential of the Cu and CuSn disk electrode, the currents recorded on the ring electrode correspond to different electroactive species.

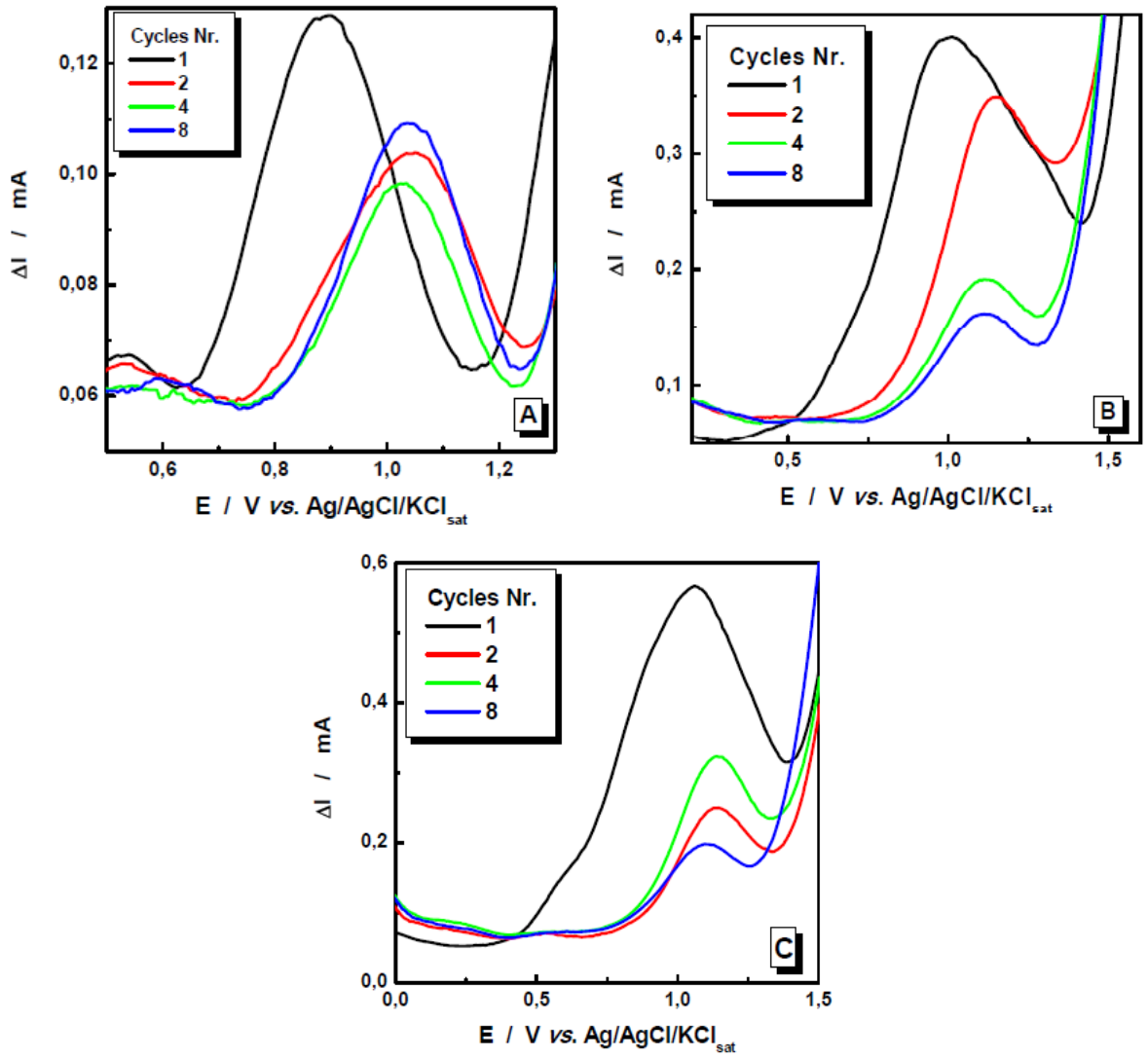

Figure 6.5 Current evolution on the Pt ring electrode at different Cu disk potentials: (**A**) -0.9 V, (**B**) - 1.3 V and (**C**) – 1.7 V in 2 g/L NO_3^- solution containing 1 M Na_2SO_4 (pH = 11) as supporting electrolyte.

Figure 6.6 presents details of the currents recorded at the Pt ring electrode during the anodic scans for two different disk polarization potentials. Measurements were performed by recording eight successive cycles without CuSn layer refreshing.

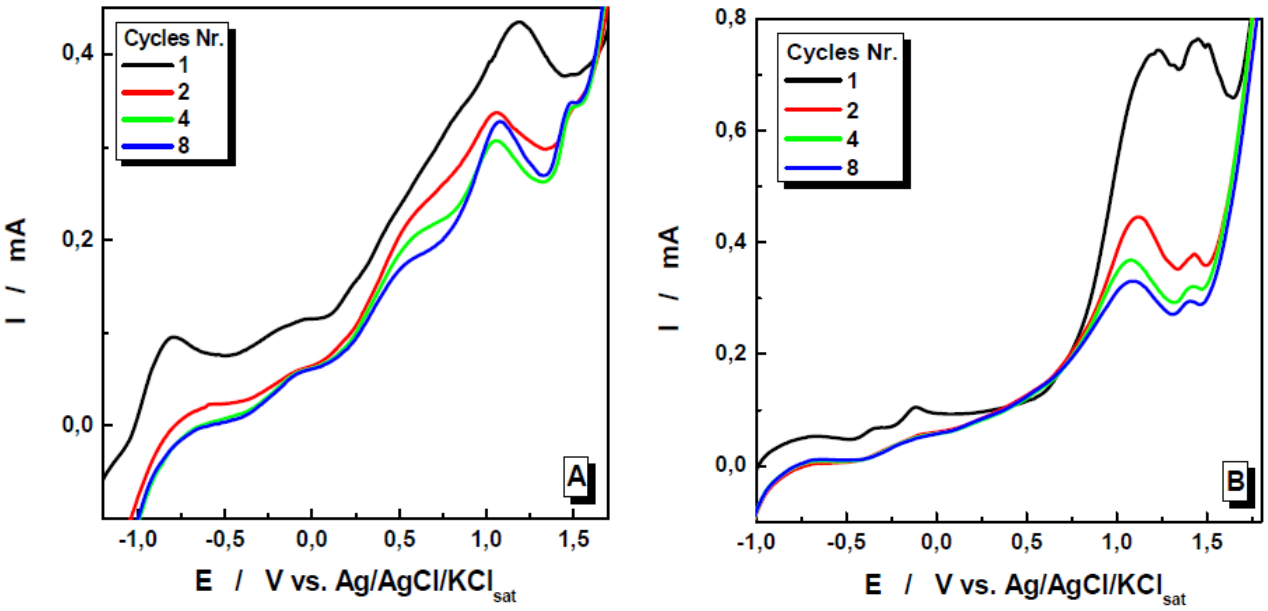

Figure 6.6 Current evolution on the Pt ring electrode at different CuSn disk potentials: (**A**) -1.0 V and (**B**) - 1.5 V in 2 g/L NO_3^- solution containing 1 M Na_2SO_4 (pH = 11) as supporting electrolyte.

It can be observed that for the selected potentials, every first cycle indicates a maximum electrocatalytic activity, which decreases rapidly in the following sweeps. Moreover, it can be observed that, after the first cycle, the peak potentials corresponding to the currents recorded at the Pt ring electrode are shifted to more positive values, suggesting a blocking of the surface. The decrease of the copper electrode electroactivity after the first cycle may be related to the adsorption of hydrogen and nitrate reduction products [146]. Reyter et al. [38] studied the electrocatalytic activity of the copper electrode in detail and reached the conclusion that the "deactivation" of the copper electrode observed during the first stage of the electrolysis may be related to the adsorption of N-containing species, limiting further nitrate reduction. As a solution, they propose a reactivation of the electrode by a periodic application of a square wave potential pulse of -0.5 V to desorb poisoning species. The same group [147] investigated the surface, electrochemical behavior and properties of the copper electrode. They concluded that, a simple and rapid electrochemical treatment consisting of a well-controlled procedure can activate an electrocatalytic material such as Cu. Cattarin et al. [37] observed variations of copper electrode behavior and attributed them to surface modifications affecting its catalytic behavior.

As a conclusion, the decrease of the Cu and CuSn electrode electroactivity during the first seconds may be related to the adsorption of hydrogen and nitrate reduction products. Hydrogen adsorption at step site inhibits the electrocatalytic activity of the electrode materials, since NO_3^- also adsorbs at the step sites during its electrocatalytic reduction. The

Cu and CuSn disk electrode surface can be rapidly poisoned by the reduced products which results in a poor stability, thus a periodic surface refreshing is required. Our experimental evidences come to support our statements and the literature data.

For a better understanding of the Cu electrode behavior, the electroreduction of nitrate at a freshly copper electrode was studied. Figure 6.7 presents the linear sweep voltammograms (LSV) at Cu electrode in the presence of nitrate. In order to see the freshly Cu electrode response a series of 4 cycles were performed in this potential range.

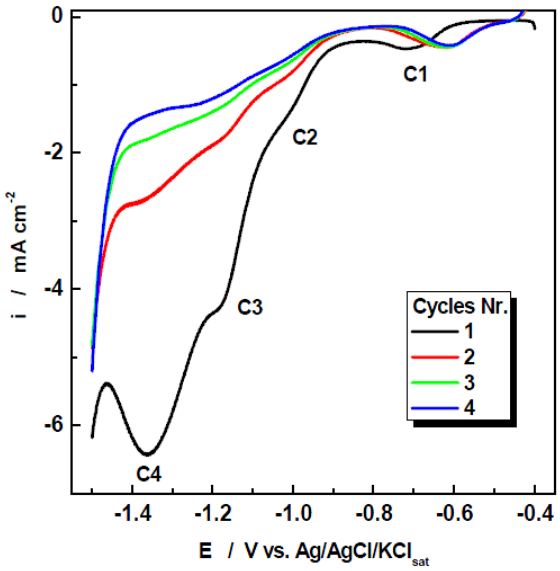

Figure 6.7 Linear sweep voltammograms of freshly Cu (1st cycle) and Cu_{cycled} (2nd, 3rd and 4th cycle) electrode in the presence of 0.1 M $NaNO_3$ in 1 M NaOH. Scan rate: 5 mV s^{-1}.

The LSV of copper in presence of 0.1M nitrate (NO_3^-) in 1M NaOH shows four reduction waves or peaks at *ca*. −0.7V (C1), −1.0V (C2), −1.2 V (C3) and −1.4 V (C4). The C1 peak is attributed to the adsorption of nitrate on Cu which is reduced further to nitrite at *ca*. -1.0V (C2). Reyter et al. [38] studied the behavior of nitrate reduction in an alkaline media at a Cu electrode and demonstrated that the C1 peak is related to the adsorption of nitrate to copper. Because of the complex nitrate reduction process, we attributed the C3 and C4 peaks to the reduction of nitrite to intermediate or final products of nitrate. Reyter et al. [38] showed that at *ca*. -1.1V nitrite is subsequently reduced to hydroxylamine (C3) and at potentials more negative then -1.3V only ammonia is formed as nitrate reduction product (C4). On the other hand, at the Cu_{cycled} electrodes (cycles 2, 3 and 4, respectively) the peak potential for the reduction of nitrate is shifted to more positive potentials, compared to the freshly Cu electrode (cycle 1). Additionally, a decrease of the current response from 1st to 4th cycle is observed.

This decrease is explained by the formation of intermediate N-adsorbed species which compete with hydrogen at the copper surface. The decrease of the electrocatalytic activity of the Cu electrode due to its poisoning by adsorbed hydrogen, blocking the electrode surface for further reduction of N-containing species was also mentioned by Reyter et al. [38] and by Petrii and Safonova [148].

In order to find out more details regarding the stability of the Cu electrode we performed measurements in the absence of nitrate. Figure 6.8 presents three detailed examples of the oxidation currents obtained in the same experimental conditions as in Figure 6.7. The anodic sweeps corresponding to the 1st, 2nd and 3th cycle are presented.

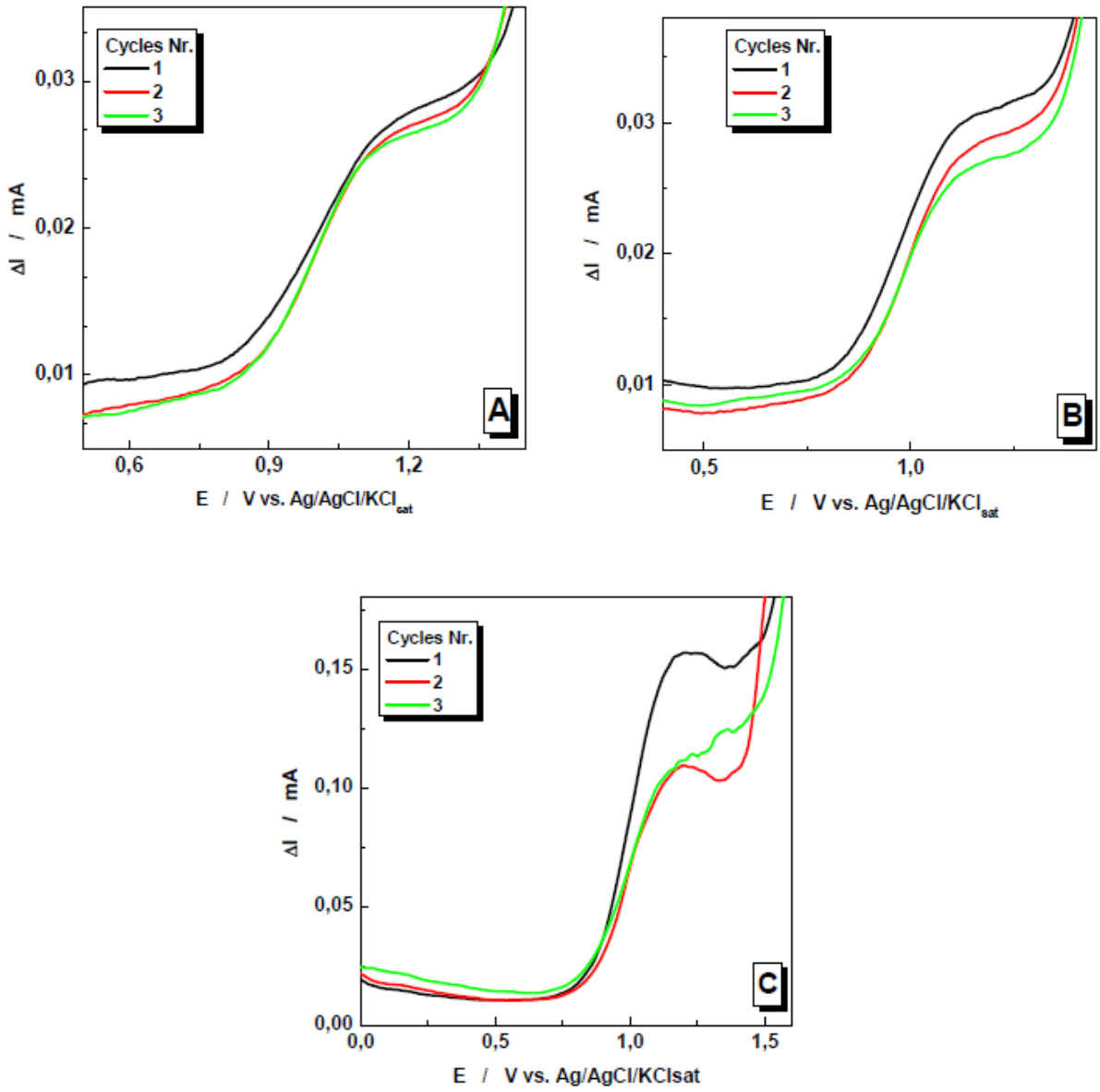

Figure 6.8 Current evolution on the Cu disk surface at different disk potentials: (**A**) -0.9 V, (**B**) - 1.3 V and (**C**) – 1.7 V in 1 M Na_2SO_4 (pH = 11) as supporting electrolyte.

The current increase (see Fig. 6.8A and 6.8B) could be explained by the oxidation of Pt surface due to the presence of oxygen and OH^- in the electrolyte. It can be seen that with the decreasing disk potential the ring current increases. The later observation (see Fig. 6.8C) could be attributed to H_2O_2 formation at the Cu electrode detected subsequently at Pt ring electrode. It is known that the O_2 reduction involves different stages including formation of O_2^-, HO_2, and HO_2^- as intermediates [149]. In order to confirm the influence of the dissolved oxygen containing species on the copper voltammetric behavior a set of measurements in deaerated solutions were carried out. The results showed no redox process in the investigated potential range.

To describe the electrochemical behavior of a freshly copper electrode in 1 M NaOH, a cyclic voltammetric curve (CV) was recorded between the hydrogen evolution reaction (HER) and the oxygen evolution reaction (OER) (Figure 6.9).

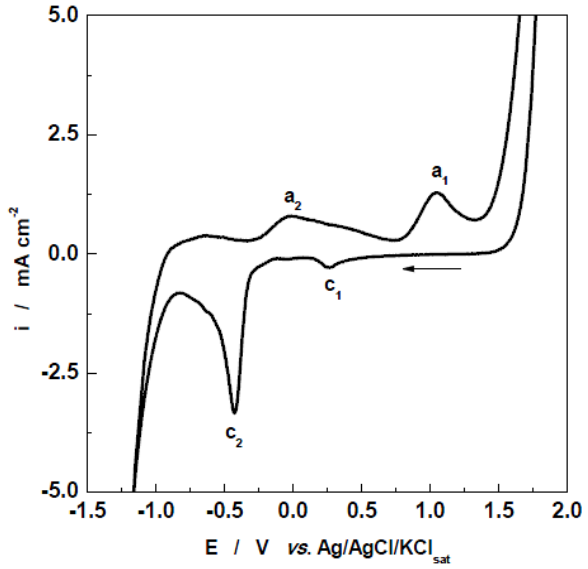

Figure 6.9 Cyclic voltammogram of a freshly copper electrode in 1 M NaOH. Scan rate: 25 mV s^{-1}.

The CV in Fig. 6.9 shows the successive anodic (a_1, a_2) and cathodic (c_1, c_2) peaks which were previously assigned to various redox processes [150, 151, 152]. Peaks a_1 and c_1 are assigned to the Cu(II)/Cu(I) redox couple just before the OER. Peak c_1 corresponds to the reduction of Cu(II) to Cu(0). Dong et al. [152] explain in detail the anodic and the cathodic processes that are taking place at the Cu electrode. The anodic peaks were found to correspond successively to the adsorption of oxygen, the formation of a surface layer of Cu_2O, the formation of a surface layer of $Cu(OH)_2$ or CuO. Similarly, a clear interpretation is

presented for the cathodic peaks which correspond successively to the reduction of CuO to Cu_2O, the reductions of Cu_2O to Cu and the soluble Cu(II) species to Cu. The behaviour of Cu electrode has been investigated also by Reyter et al. [147] showing a complex redox behavior of copper electrode in alkaline media.

6.4. Simultaneous detection of electroactive products

6.4.1. Simultaneous detection in mixed solution

Starting from the presented results, experiments were performed similar to CHV measurements in mixed solutions, containing different concentrations of NO_2^-, NH_2-OH and NH_4^+. An initial concentration of 0.5 g/L $NO_2^-$was used, followed by 0.2 g/L NH_2OH and 0.5 g/L NH_4^+. The obtained results showed that the involved species interact, making their individual detection difficult (Fig. 6.10).

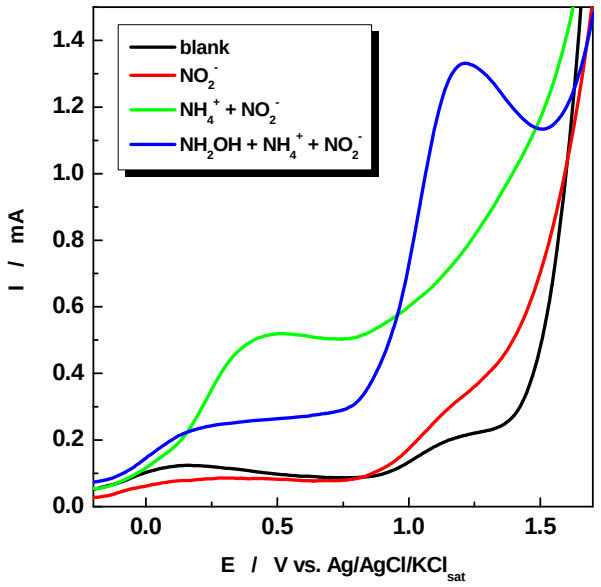

Figure 6.10 CHV in a mixed solution of NO_2^-, NH_2OH and NH_4^+ species at a Pt ring electrode.

Horyani *et al.* [153] studied the electrocatalytic reduction of nitrates in mixed solutions at a platinum electrode in alkaline media and concluded that in a system containing NO_2^- and NH_3 a mixed process occurs; this can be attributed to the adsorption competition between reacting species and the species present in the system, or formed under the experimental

conditions. Reaction mechanism and kinetics do not represent our objective in this study. Therefore this was not investigated further.

6.4.2. Simultaneous detection at Cu and CuSn electrodes

Based on the above discussed results and by reactivating the surface of the Cu and the CuSn electrode before each experiment, we started a detailed study concerning the influence of the polarization potential of the electrode on the ERN product composition. As shown in Fig. 6.11, only the anodic portions of every first cycle are presented, the decrease of the disk potential to more negative potentials causes an increase in the recorded ring currents. Depending on the disk potential, the currents recorded on the ring electrode correspond to the oxidation of different intermediate or final products of nitrate reduction.

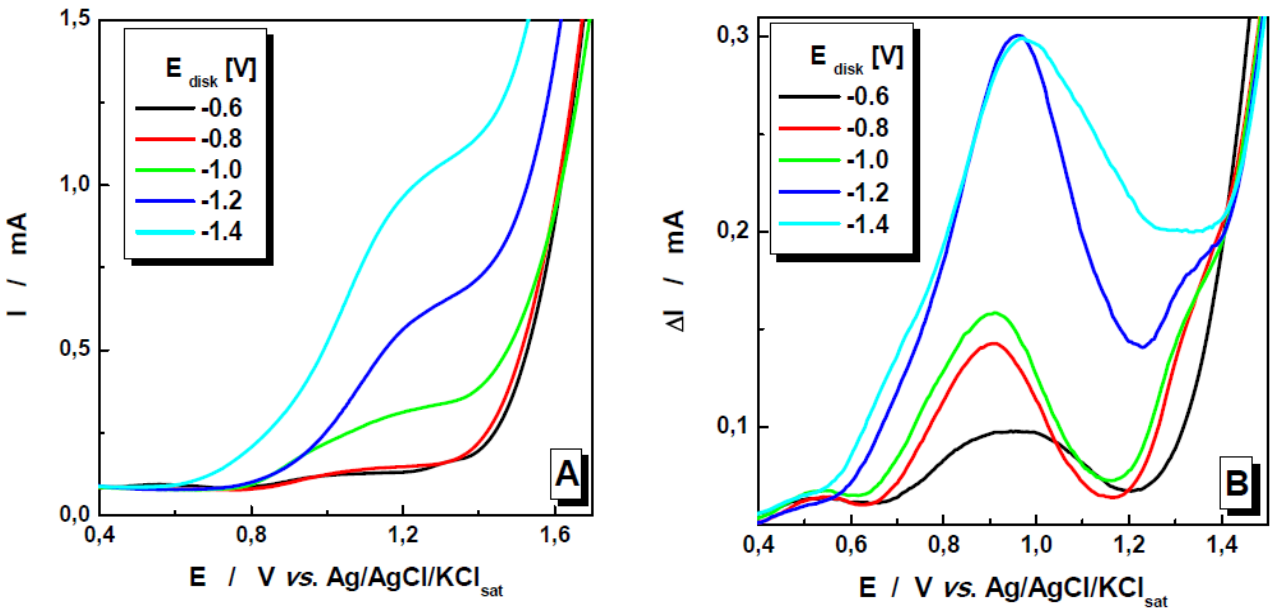

Figure 6.11 Influence of the polarization potential of the Cu disk surface on the oxidation currents recorded by CHV (A) and SWV (B). Experimental conditions: Start potential = -1.5 V and end potential = 2.0 V, ω = 1000 rpm, wave amplitude = 50 mV; wave period = 10 ms; wave increment = 5 mV. The Cu plated disk electrode was polarised at different constant potentials as indicated in the legends.

As discussed in the theoretical part of this study, NH_3 is one of the final products that is mainly obtained when a copper disk electrode is used. Therefore, for a better evaluation of the ERN pathway, the disk electrode was polarized at constant potential values between -0.6 V to -1.4 V with a 0.1 V increment. As can be seen from Fig. 6.11A, using CHV, only a poorly

defined oxidation plateau can be observed for ring potentials between + 1.0 V and + 1.4 V [154]. On the other hand, SWV measurements (see Fig. 6.11B) reveal two different oxidation processes. The voltammograms show that the SWV detection gave a well-defined anodic wave with a peak potential of 0.9 V in alkaline media. Based on the results obtained in mono-component solutions, the first anodic peak (positioned around 0.9 V) can be associated to nitrite and/or hydroxylamine oxidation. The oxidation peak of nitrite in mono-component solution has the maximum at 0.8 V and hydroxylamine at 1.0 V. An explanation for the peak displacement are the simultaneous oxidation processes (NO_2^- and NH_2OH) taking place. Due to that, the hydroxylamine oxidation process is faster than ofnitrite, the oxidationcurrentofhydroxylamineoverlaps partiallythe oxidation current of $NO_2^-$and as result the peak is shifted towardsmore positivevalues.

For disk potentials more negative than -0.8 V, a clear signal corresponding to ammonia oxidation, can be observed at ring potentials starting at 1.3 V. Since the ammonia oxidation peak is betterdefined and sufficiently separated from the oxygen evolution peak, it was exploited to confirm the presence of ammonium between the ERN products.

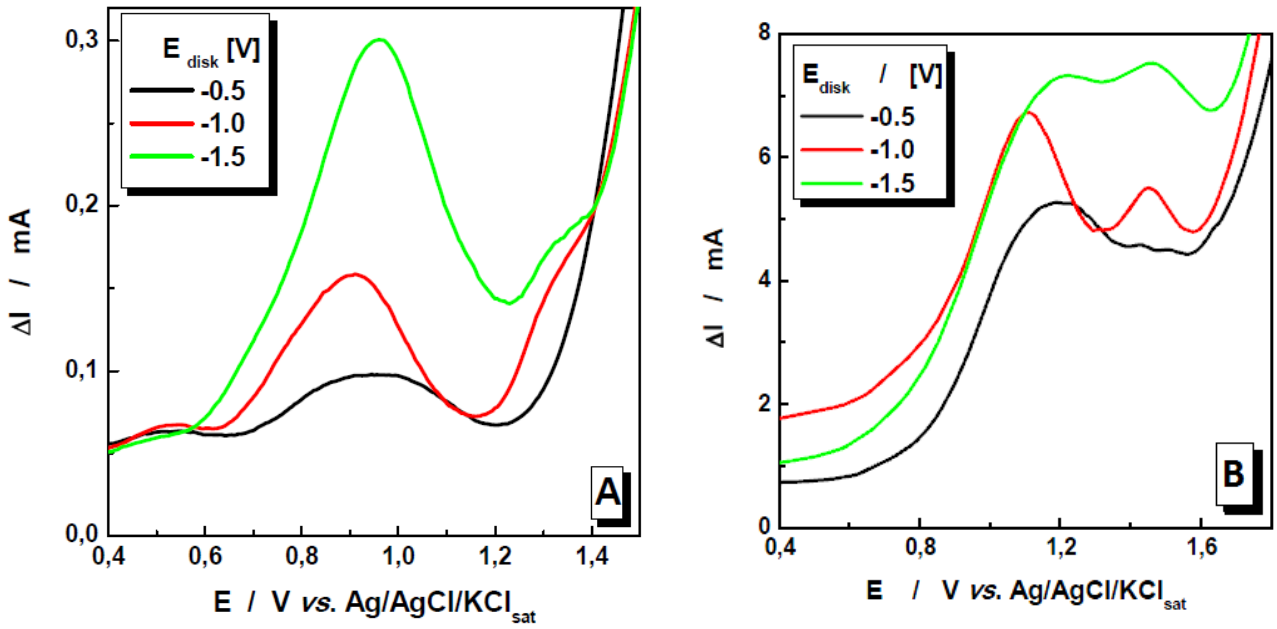

Figure 6.12 Influence of the polarization potential on the oxidation currents recorded by SWV at a Cu (A) and CuSn (B) disk electrode. Experimental conditions as in Figure 6.11.

In the case of the CuSn electrode (Fig. 6.12) the electrocatalytic activity of the electrode material is improved. Two distinct signals (peaks) are observed. Based on the results obtained in mono-component solutions, the first one (~ 1.0V) can be attributed to nitrite (see Fig. 6.1)

and hydroxylamine (see Fig. 6.2) oxidation. For disk potentials more negative than -0.5V, a clear signal, corresponding to ammonia oxidation, can be observed at ring potentials starting at 1.3 V. In comparison with the Cu electrode, the CuSn electrode presents an improved electrochemical activity [155].

Bouzek et al.[39] and J. F. E. Gootzen et al. [61] reached the conclusions that, from all possible products that are formed during the nitrate reduction only nitrite and hydroxylamine are sensitive towards oxidation at the platinum ring electrode and other possible products like NH_4^+, N_2 and N_2O are not susceptible towards oxidation at the platinum ring electrode. Contrarily, Endo *et al.*[156] studied the oxidation of ammonia on a disk electrode and concluded from RRDE experiments that, two kinds of intermediates involved in the anodic oxidation of ammonia on platinum could be detected in situ; one can then be reduced (probably NO_x) and another can be further oxidized (such as NH_2OH).

In our experimental conditions the possibility of electrochemical detection of ammonia via the ammonia oxidation at a Pt ring electrode was demonstrated. From the above discussion it was shown that, at least three electroactive products resulting from ERN at a copper plated Pt electrode in alkaline media can be detected by the SWV technique. The difference between the results obtained by the SWV and CHV were found to be significant, proving the superiority of the SWV based method. Comparing the two techniques, it is worth to note that, if the electrochemical processes have reasonable differences between the characteristic potentials, only SWV allows accurate evaluation of peak potentials and currents. Moreover, using the cyclic SWV for the detection of the resulting products we can obtain a more detailed picture of the global chemical and electrochemical processes that take place at the disk electrode. The results obtained with CHV and SWV allow a fast evaluation in real-time (or in situ) of the electrocatalytic properties for the electrode materials, proving the possibility of quantitative evaluation of individual electroactive species. In comparison to pure Cu electrode material, an enhancement of the electrocatalytic activity of Cu by alloying with Sn was observed. The optimal conditions for the voltammetric detection of electroactive species resulting from nitrate reduction were established, which provides useful information for the optimization of the ERN process.

6.5. Conclusions

It was demonstrated that the electroactive products resulting from ERN in alkaline media can be detected precisely by the SWV technique at a Cu and CuSn plated Pt electrode. CHV and SWV allowed us to detect simultaneously the involved species resulting from ERN. Moreover, using SWV ammonium can be electrochemically detected with good accuracy. The measurements performed in mono-component solutions prove the fact that, combining cyclic and square wave voltammetry at high scan rates with hydrodynamic techniques and using an adequate pH value, at least three different electroactive species generated from the NO_3^- reduction (NO_2^-, NH_2-OH and NH_4^+) can be electrochemically detected. The results obtained with the CHV and SWV techniques allow a real-time evaluation of the electrocatalytic properties of the used electrode material. Using both techniques, the optimal conditions for the voltammetric detection of electroactive species resulting from nitrate reduction were established. In this study some features of CHV and SWV were compared, the resolution of cyclic voltammetry scan was lower than that of the square wave voltammetry. The voltammograms, recorded successively without Cu layer refreshing, demonstrated that the electrocatalytic activity of this electrode material decreases, requiring additional studies concerning the preparation of novel electrode materials with increased stability and/or the periodic reactivation of the electrode surface.

7. DIRECT REDUCTION IN AN ELECTROCHEMICAL FLOW REACTOR

7.1. Description of the electrochemical reactor

An electrochemical flow reactor as presented in Fig. 7.1 was used for the electroreduction of nitrates. The cell was operated in a divided configuration to avoid possible interferences such as nitrite oxidation at the anode. A model electrolyte ($NaNO_3$, NaOH) was used in the cathodic compartment. In both compartments a volume of 300 mL of solution was circulated. The anolyte was 1.0 M NaOH. Constant current electrolysis tests were performed using various cathode materials. The cathode and anode chambers were separated by a Nafion® 324 (DuPont) cation selective – membrane (separator). Among the ionic species present in the anolyte and catholyte, the separator allows only the passage of sodium ions. Besides sodium ions, water is transported across the membrane due to electroosmotic drag. Therefore, only the transport of sodium and water across the separator needs to be considered.

The cathode materials investigated were copper (Cu) and a copper-tin alloy (detailed aspects for the preparation of the alloy can be found in Chapter 5). An oxygen evolving dimensionally stable anode (DSA) was used. The anodic and cathodic compartments were of equal volume (10 mL). The tightness of the cell was achieved by using rubber frames, specially designed for the reactor. The geometrical area of the cathode and the anode was 10 cm^2 and the distance between the two electrodes was 1 cm. The flow cell design is shown schematically in Figure 7.2. The electrolytes were circulated through the cell compartments with a double channel peristaltic pump with a monitored flow rate. In order to analyse the nitrate and nitrite concentration samples were taken from the cathode compartment at specific time intervals by using a syringe. They were analyzed after the appropriate dilution (section 4.1.7). The determination of nitrate and nitrite was performed by ion chromatography (Dionex DX 100 with an anion column for AG 14A/AS14 A) (see Chapter 4.1.7).

Figure 7.1 Electrochemical flow reactor for nitrate removal

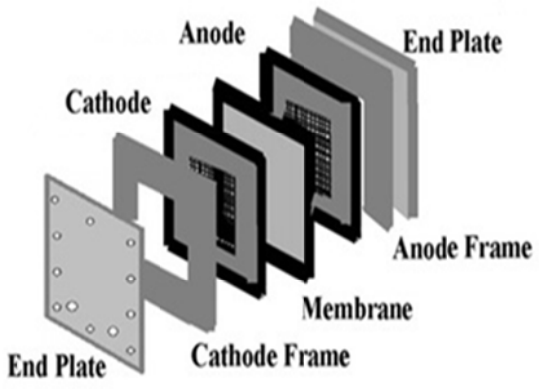

Figure 7.2 Schema of the electrochemical flow cell

The electrochemical reduction of nitrate is complicated due to the existence of a large number of stable compounds and unstable intermediates; for example in an earlier work [41] it was suggested by Li *et al.* that the nitrate reduction might involve many parallel reactions.

The main reactions occurring at the cathode are given below [5, 157]:

$NO_3^- + H_2O_{(l)} + 2e^- \rightarrow NO_2^- + 2OH^-$, $\varepsilon^0 = 0.01$ V vs SHE (7.1)

$NO_2^- + 5H_2O_{(l)} + 6e^- \rightarrow NH_{3(g)} + 7OH^-$, $\varepsilon^0 = -0.165$ V vs SHE (7.2)

$2NO_2^- + 4H_2O_{(l)} + 6e^- \rightarrow N_{2(g)} + 8OH^-$, $\varepsilon^0 = 0.406$ V vs SHE (7.3)

$2NO_2^- + 3H_2O_{(l)} + 4e^- \rightarrow N_2O_{(g)} + 6OH^-$ $\varepsilon^0 = 0.15$ V vs SHE (7.4)

In a divided cell (for example with a cation-selective membrane) the evolution of oxygen is the reaction taking place at the anode [76]:

$4OH^- \rightarrow O_{2(g)} + 2H_2O_{(l)} + 4e^-$, $\varepsilon^0 = 0.401$ V vs SHE (7.5)

Nitrite is an intermediate of the nitrate reduction and is further reduced to ammonia or nitrogen. The mechanism of nitrite reduction in alkaline solutions is not clearly understood [158]. The successive reduction reactions of nitrate/nitrite can generate nitrogen or ammonia, two products with a minimal environmental impact [159]. The yield for ammonia or nitrogen is dependent on the electrocatalytic effect of the electrode material (see Chapter 3.1).

7.2. Electroreduction of nitrate at Cu and CuSn alloy cathodes

7.2.1. Voltammetric analysis

As a part of the evaluation of electrode materials, cyclic voltammetry experiments were performed on two electrode materials. The materials tested along with their specifications are described in Chapter 5. Linear sweep voltammetry (LSV) measurements were performed at a Cu and CuSn ($Cu_{27\%}Sn_{73\%}$) electrodes in the absence and presence of nitrate (Fig. 7.3A and 7.3B). The difference between these two voltammograms was attributed to the electrocatalytic effects specific of the electrode material. The potential was swept in the cathodic range until hydrogen evolution occurred.

The LSV at a Cu electrode in presence of 0.1M NO_3^- shows an onset of the cathodic current at -0.6V which is followed by a continuous increase in the current which is clearly attributed (see also Chapter 6) to nitrate electroreduction (Figure 7.3A). It appears that two different potential regions need to be explored for the electroreduction of nitrate. The first one is near the rising part of the reduction peak of the LSV around -0.9 V which would be favourable to nitrite production and the second near -1.4 V where nitrate reduction would mostly yield ammonia. The hydrogen evolution reaction (HER) takes place only for potentials more negative than -1.5V. The results are in agreement with the studies performed by Reyter *et al*. [38], who observed the first peak around -1.0V, attributed to nitrite production and the second near -1.4V, attributed to ammonia.

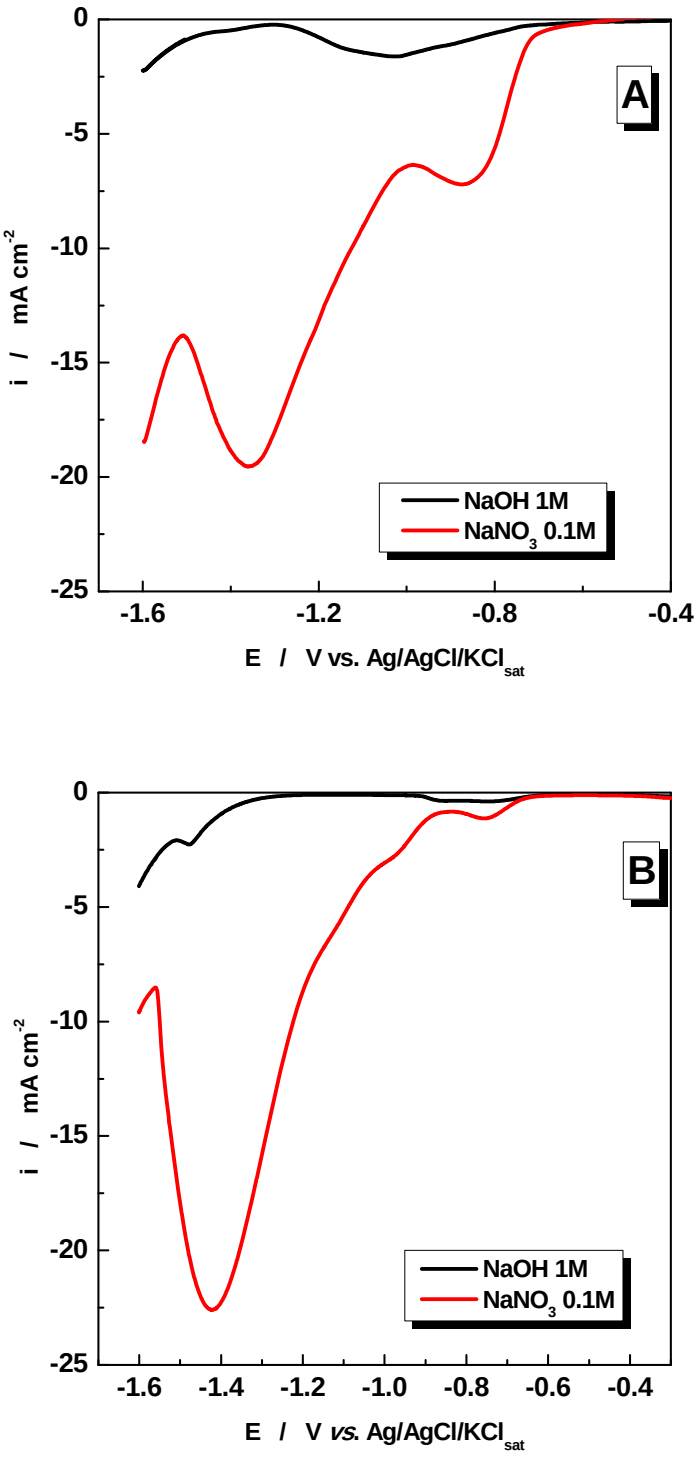

Fig.7.3 Linear sweep voltammograms at a Cu (A) and CuSn (B) electrode in 1M NaOH (black line) in presence of 0.1M $NaNO_3$ (red line). Scan rate: 10 mV s^{-1}.

In analogy with the Cu electrode, LSV was performed at a CuSn electrode (Figure 7.3B). In the same potential range two reduction peaks are observed. The first peak is around -0.7 V and the second near -1.4 V. The HER was observed only for potentials more negative

than -1.6 V. Based on these results, the two potential regions were further used for the reduction of nitrate.

Based on the above discussed voltammetric studies, current density ranges were chosen in order to monitor the nitrate concentration. Moreover, the concentration of nitrite was monitored as well.

7.2.2. Effect of applied current density and flow rate on the ERN

In order to investigate the nitrate reduction process, prolonged electrolyses were carried out at different current densities. In the electrochemical reduction process, the nitrate removal rate is proportional to the concentration of nitrate and to the hydrogen concentration. The kinetic equation for nitrate removal is [160]:

$$\frac{-d[NO_3^-]}{dt} = k[NO_3^-] \quad (7.6)$$

The apparent kinetic rate constant was estimated for the reduction process by plotting log $[C_i/C_t]$ vs. time, where C_t is the concentration of nitrate at time t and C_i is the initial nitrate concentration. The plot gives a straight line which indicates that the reaction follows a pseudo first order kinetics [160]. From the slope of the plot:

$$\log_{10}[C_t/C_i] = -kt/2.303 \quad (7.7)$$

the apparent rate constant, k, was determined.

Moreover, the influence of the flow rate on the electrochemical reduction of nitrate was investigated.

Figure 7.4 displays the evolution of the nitrate and nitrite concentration during prolonged electrolyses at different flow rates and current densities (A) 10 mA cm^{-2} and (B) 5 mA cm^{-2}.

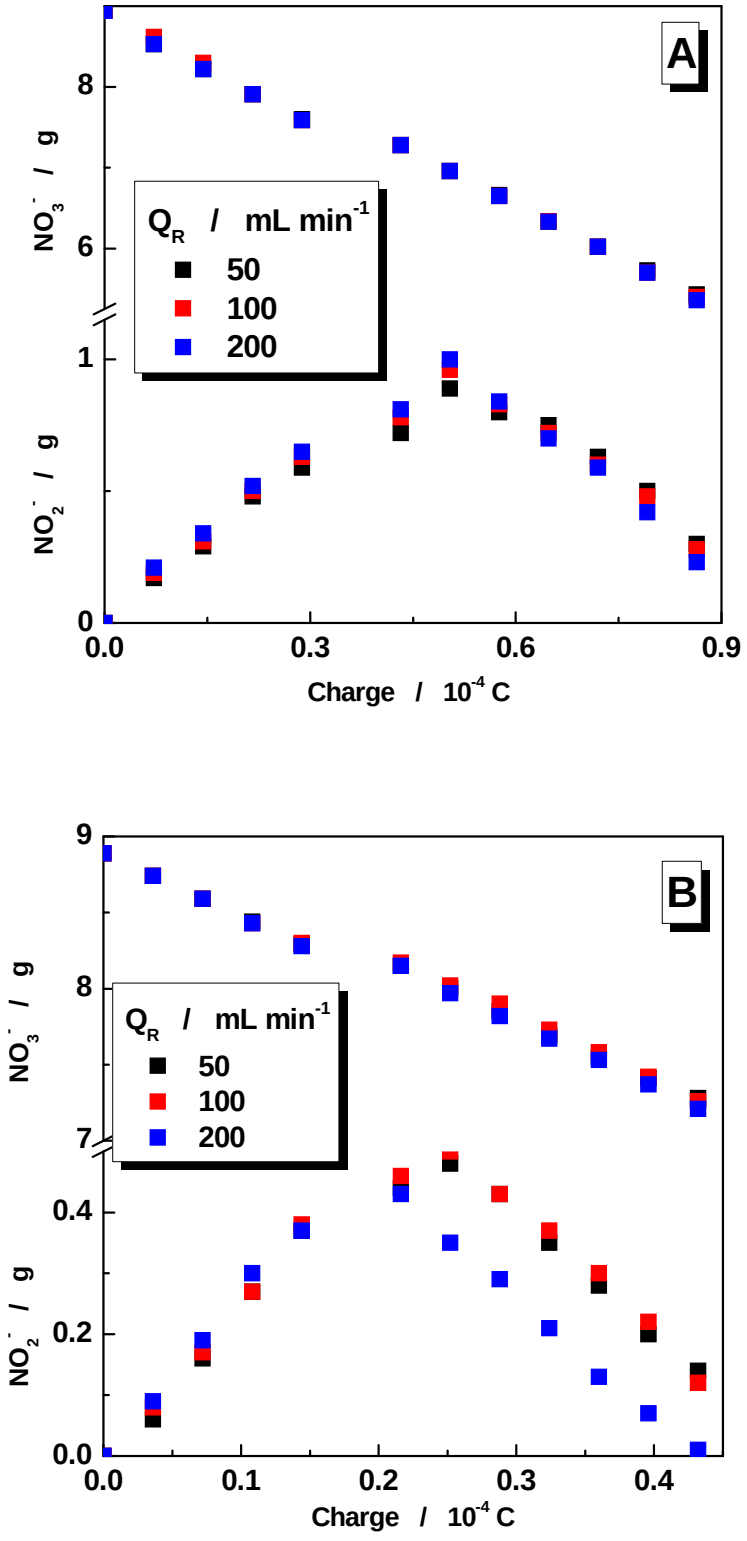

Figure 7.4 Evolution of the concentration of NO_3^- and NO_2^- *vs* charge. Experimental conditions: 0.1M $NaNO_3$ in 1M NaOH electrolyte solution; (A) -10 mA cm^{-2} at a Cu electrode and (B) -5 mA cm^{-2} at a CuSn electrode.

Figure 7.4 shows the destruction of nitrate at Cu (Fig. 7.4A) and CuSn (Fig. 7.4B) cathodes. With both electrodes, nitrate levels decrease continuously. The concentration of nitrite initially increases, reaches a maximum and then decreases (Fig. 7.4). The form of this curve is characteristic for an intermediate product generated in a consecutive reaction mechanism:

$$NO_3^- \rightarrow NO_2^- \rightarrow Products \quad (7.8)$$

This suggests that the conversion of nitrite to other reduction products is the slow step in the reaction mechanism. At CuSn, after a slight increase in nitrite concentration, both nitrite and nitrate decrease throughout the experiment. Overall, Cu and CuSn present the same rate of removal of NO_3^-/NO_2^-. After a period of 24 h of electrolysis a nitrate conversion of 40% was achieved at a Cu cathode (see Fig. 7.4A) and, on the other side, a conversion of 20% is achieved at a CuSn cathode (see Fig. 7.4B). Given that the current density used in the case of Cu electrode is two times higher than on CuSn electrode, the proportionality observed in our experiments sustains the above results. On the other hand, it can be seen that, at these small current densities, the flow rates have a minimal influence on the reduction process (Fig. 7.4).

The apparent rate constant, k, of the reaction was calculated (Fig. 7.5) based on pseudo first order kinetics described above (Eq. 7.7). The mean k values were ≈ 3.3 min^{-1} for Cu and ≈ 1.4 min^{-1} for CuSn, respectively. Moreover, at these small current densities, charge transfer occurs slowly and, therefore, the influence of the mass transport is minor (Fig. 7.5).

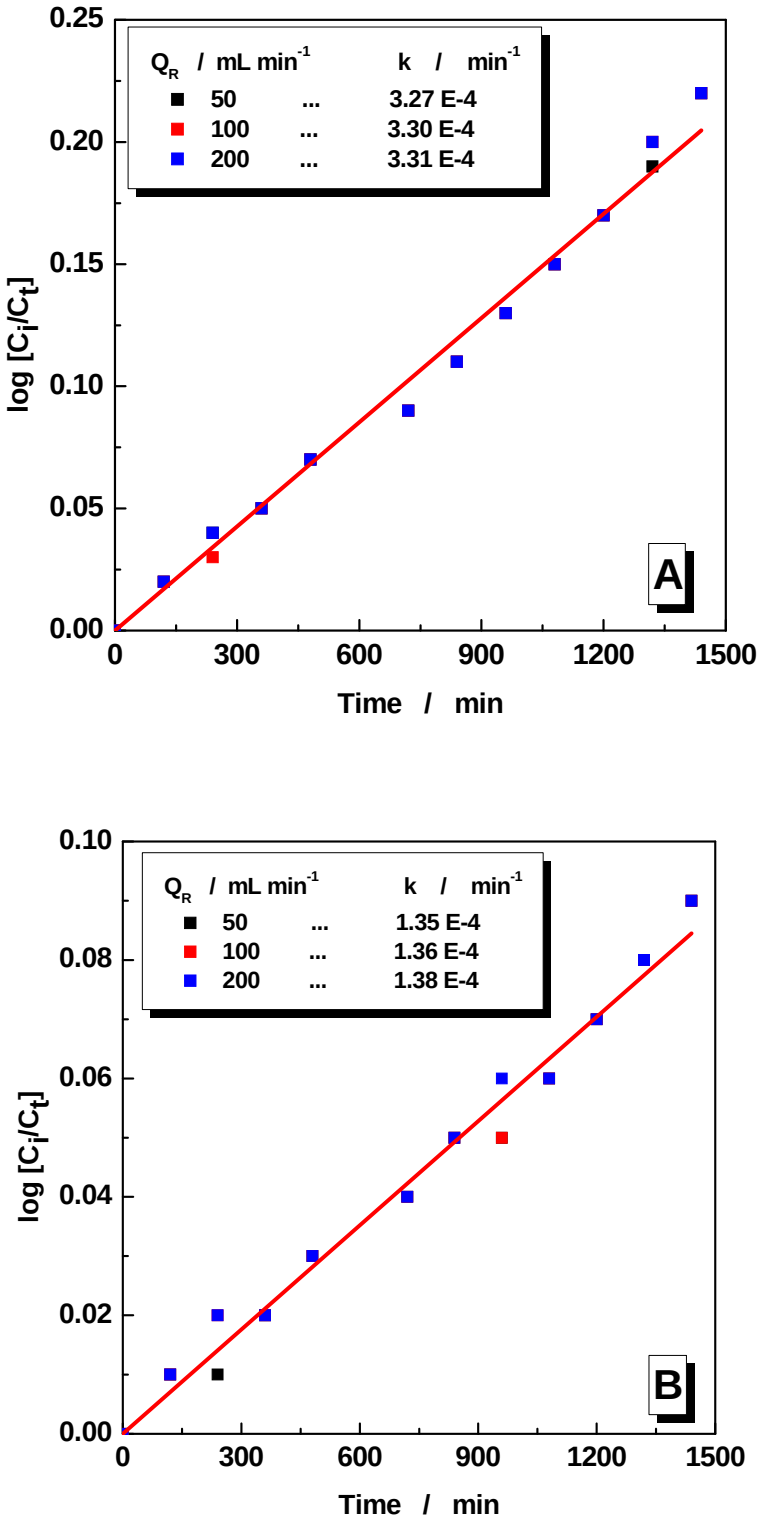

Figure 7.5 Logarithmic conversion of nitrate vs. time for apparent rate constant evaluation. Experimental conditions: 0.1M $NaNO_3$ in 1M NaOH electrolyte solution; (A) -10 mA cm^{-2} at a Cu electrode and (B) -5 mA cm^{-2} at a CuSn electrode.

In order to analyse the reaction evidenced by the appearance of the second peak (obtained in the voltammetry analysis, see Fig. 7.3) measurements involving prolonged electrolysis were performed at higher current densities: (A) -20 mA cm^{-2} at a Cu electrode and (B) -25 mA cm^{-2} at a CuSn electrode. The experimental data are presented in Figure 7.6.

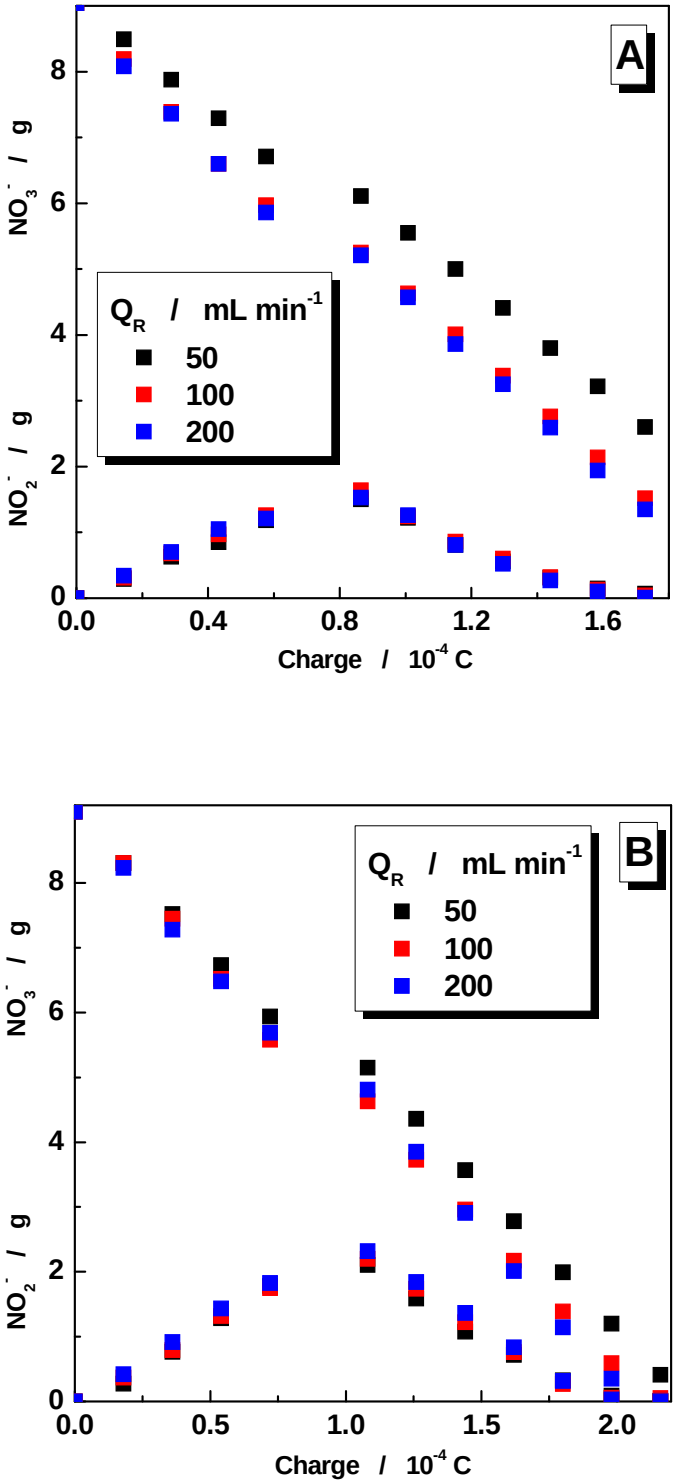

Figure 7.6 Evolution of the concentration of NO_3^- and NO_2^- *vs* charge. Experimental conditions: 0.1M $NaNO_3$ in 1M NaOH electrolyte solution; (A) -20 mA cm^{-2} at a Cu electrode and (B) -25 mA cm^{-2} at a CuSn electrode.

As can be seen, after 24 h of electrolysis, at the Cu cathode the final concentration of nitrate reaches 1 g/L and it is totally eliminated at the CuSn cathode. Given that the current density at the CuSn electrode is somewhat higher (0.05 mA cm^{-2}), the electroreduction of nitrate is more effective at the CuSn electrode, the maximum concentration limit (MCL, Section 1.3) being achieved.

The nitrite concentration increases at the Cu electrode (Figure 7.6A) and, after that, is further diminished under the MCL after 24 h of electrolysis.

In the case of the CuSn electrode (Figure 7.6B) the nitrite content increases up to a charge of $1.0 \cdot 10^{-4}$ C and then decreases below the MCL. The *k* values could not be calculated for the above experimental conditions (see Fig. 7.6) because the reaction does not follow a pseudo first order kinetics (Fig. 7.7). This could be explained by changes in the reaction mechanism these current densities (Fig. 7.6).

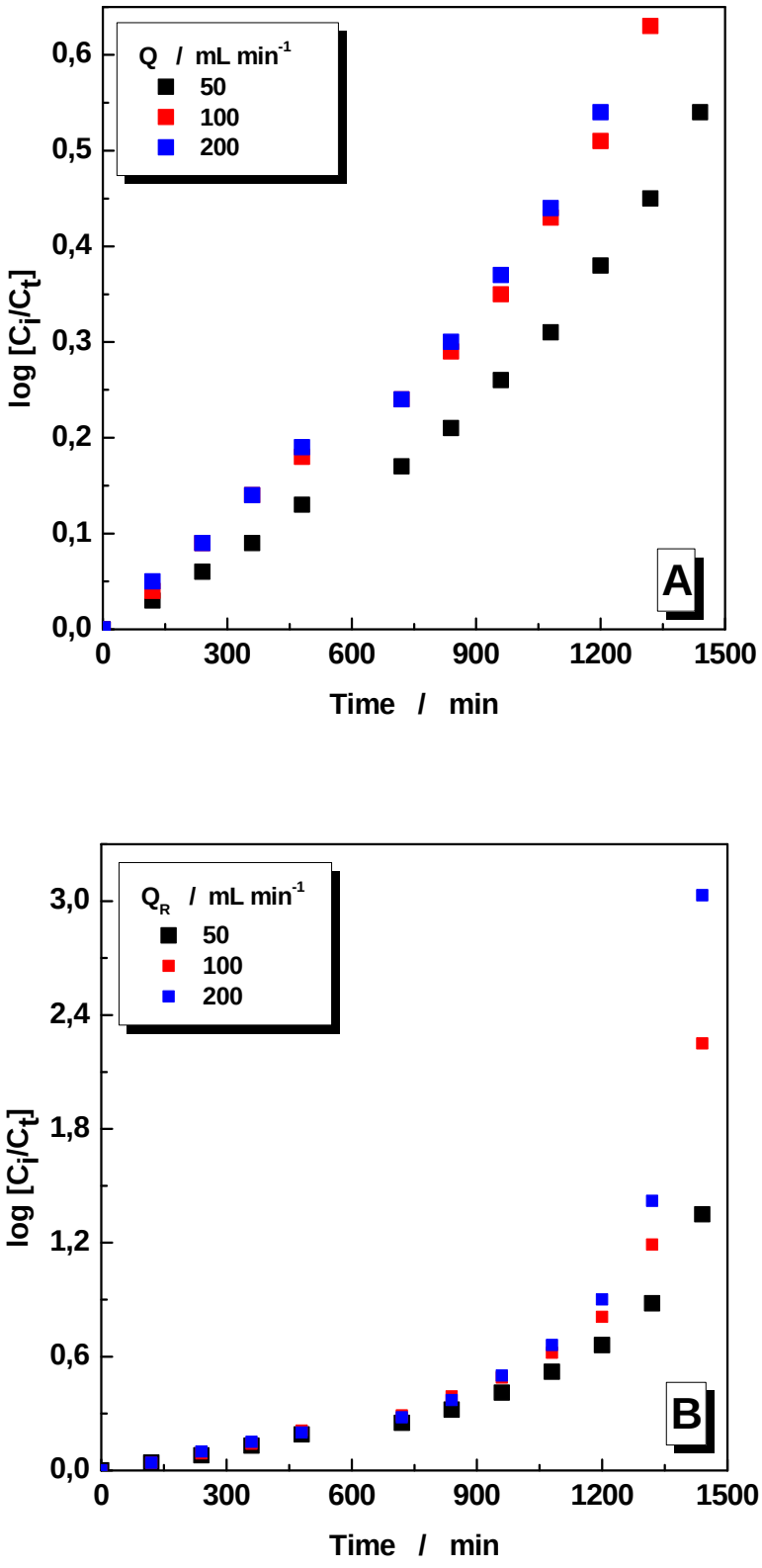

Figure 7.7 Logarithmic conversion of nitrate vs. time. Experimental conditions: 0.1M $NaNO_3$ in 1M NaOH electrolyte solution; (A) -20 mA cm^{-2} at a Cu electrode and (B) -25 mA cm^{-2} at a CuSn electrode.

Since the mechanism of the reaction changes at the previously studied current densities (Figure 7.6 and 7.7) ERN was further investigated at even higher current densities in order to establish optimized working parameters. For this purpose, prolonged electrolyses were carried out at (A) -40 mA cm^{-2} at a Cu electrode and (B) -50 mA cm^{-2} and CuSn electrode. The data obtained using the same electrolyte (0.1M $NaNO_3$ in 1M NaOH) are presented in Figure 7.8.

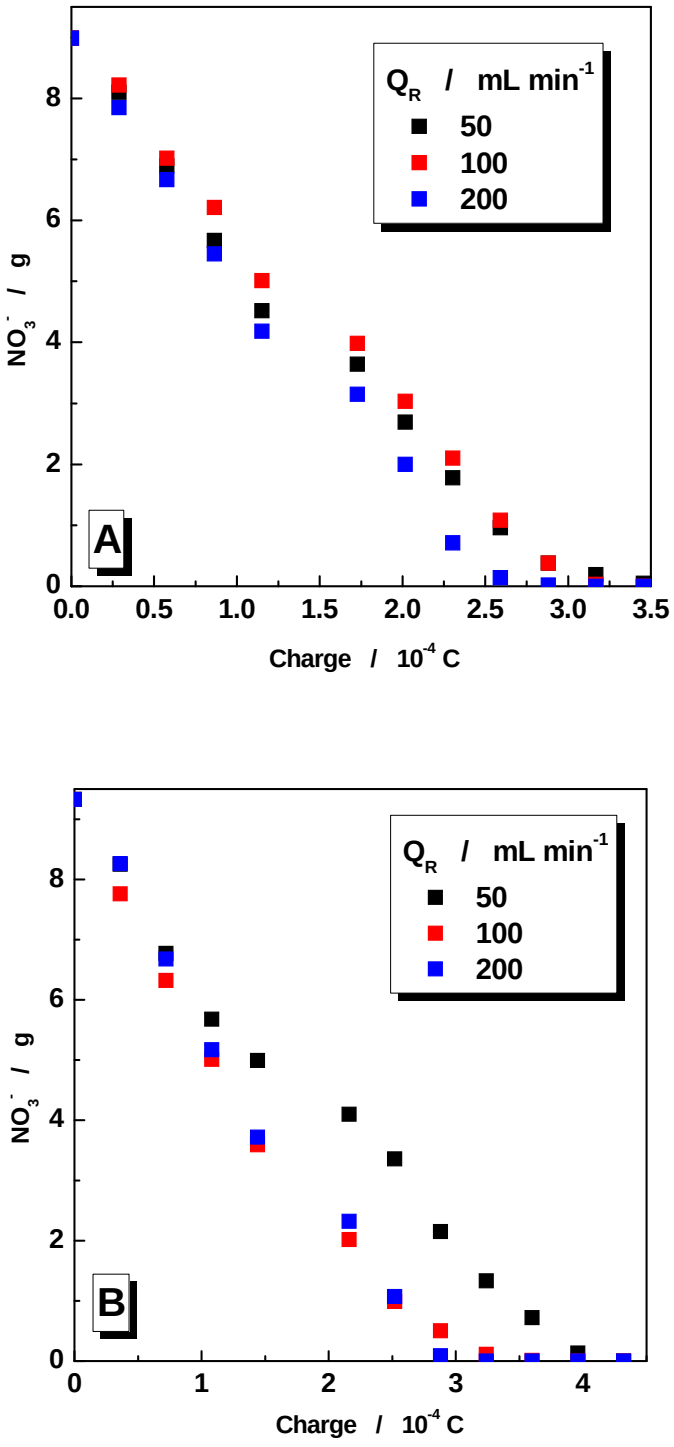

Figure 7.8 Evolution of the concentration of NO_3^- *vs* charge. Experimental conditions: 0.1M $NaNO_3$ in 1M NaOH electrolyte solution; (A) -40 mA cm^{-2} at a Cu electrode and (B) -50 mA cm^{-2} at a CuSn electrode.

As can be seen from Figure 7.8, the conversion of nitrate to a value under MCL (50 mg/L), at Cu and CuSn electrode materials, was achieved. The results obtained show that at the same charge (~ $0.29 \cdot 10^{-4}$ C·cm^{-2}) and flow rate (200 mL·min^{-1}), for the Cu electrode, a period of 18 h is sufficient to reduce the nitrate below the MCL, while for the CuSn electrode, after 14 h the ERN is completed. Thus, we can conclude that at higher current density values, the ERN is more effective at the CuSn electrode.

In this case, the *k* value was not calculated for the above experimental conditions (see Figure 7.8). A more complicated reaction mechanism than discussed above (see Eq. 7.7) seems to apply at high current densities. As can be seen from Fig. 7.9, the rate of the reaction has an exponential behaviour. At these high current densities, the hydrogen evolution reaction (HER) is intense and the evolved hydrogen participates in the nitrate and/or nitrite reduction. This behaviour was also observed in the paper of Katsouranos *et al*. [81] who explained that the produced hydrogen participates in the nitrate reaction mechanism, even though it is difficult to explicitly decide which steps of the reduction involve. Moreover, the HER increases the mass transport by increasing the convection in the reactor.

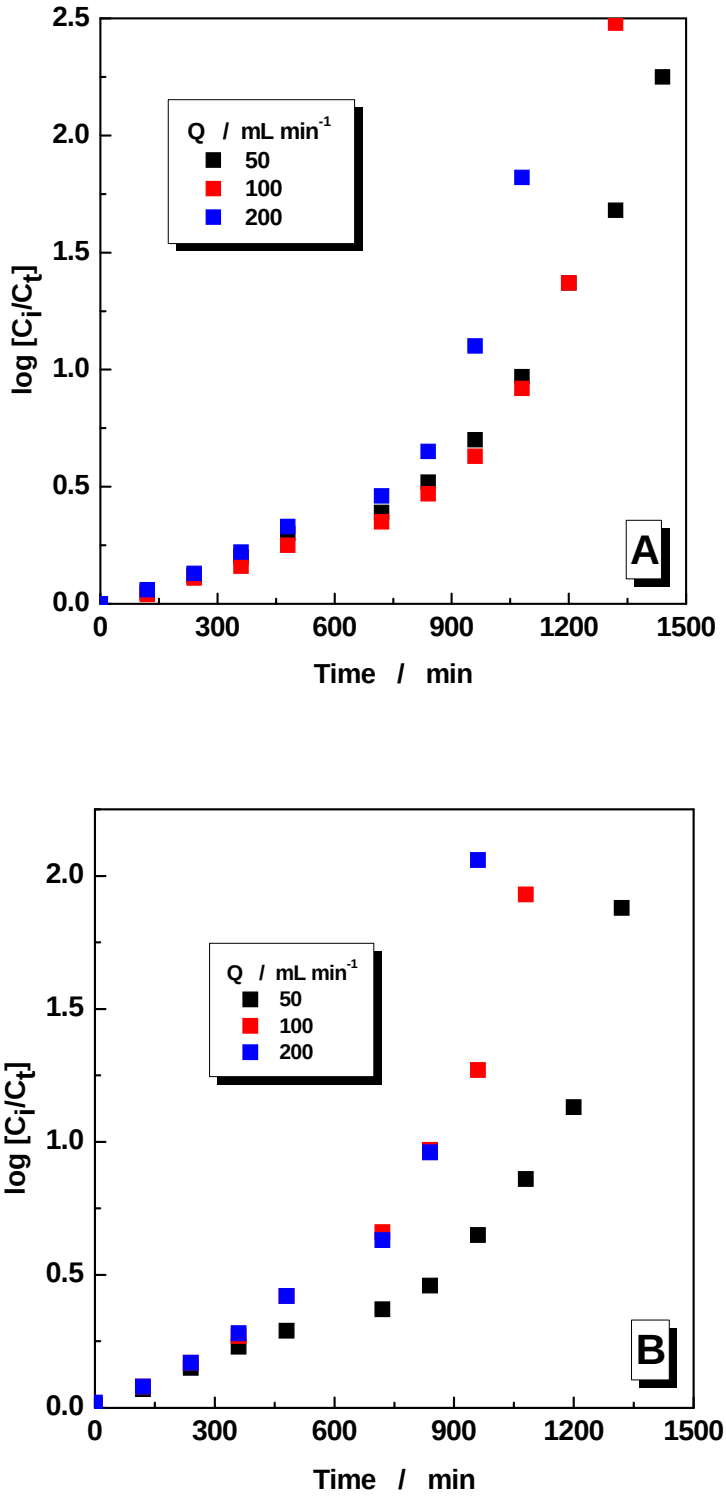

Figure 7.9 Logarithmic conversion of nitrate vs. time. Experimental conditions: 0.1M $NaNO_3$ in 1M NaOH electrolyte solution; (A) -40 mA cm^{-2} at a Cu electrode and (B) -50 mA cm^{-2} at a CuSn electrode.

In conclusion, the experiments showed that at small current densities, the charge transfer is slow and therefore, the mass transport only has a minor influence on the ERN process. The process follows a pseudo first order kinetics at small current densities, while at high current densities the process follows a complex mechanism. The HER is intense and the evolved hydrogen participates in the nitrate and/or nitrite reduction. Moreover, the prolonged electrolysis performed at high current densities is more efficient. Therefore, the MCL of nitrate is achieved in shorter time. The electroreduction of nitrate is more effective at the CuSn electrode.

Contrarily to Prasad et al. [160] and Koparal et al. [161] that conclude that higher current densities cannot be used for the treatment of nitrate in order to achieve better treatment efficiency, our results show an opposite effect, that is in our case higher current densities can be used combined with a high flow rate.

7.3. Performances of the electrochemical reactor

The energy consumption for the removal of nitrate and nitrite presents an essential parameter in the evaluation of the process performance. For cost evaluation of the ERN process, is important to identify the most efficient electrode material. Fig. 7.14A and B show the concentration decrease of nitrate at Cu and CuSn electrodes, respectively, obtained at a flow rate of 200 ml min^{-1}, from a solution containing 0.1M $NaNO_3$ in 1M NaOH, at three current densities.

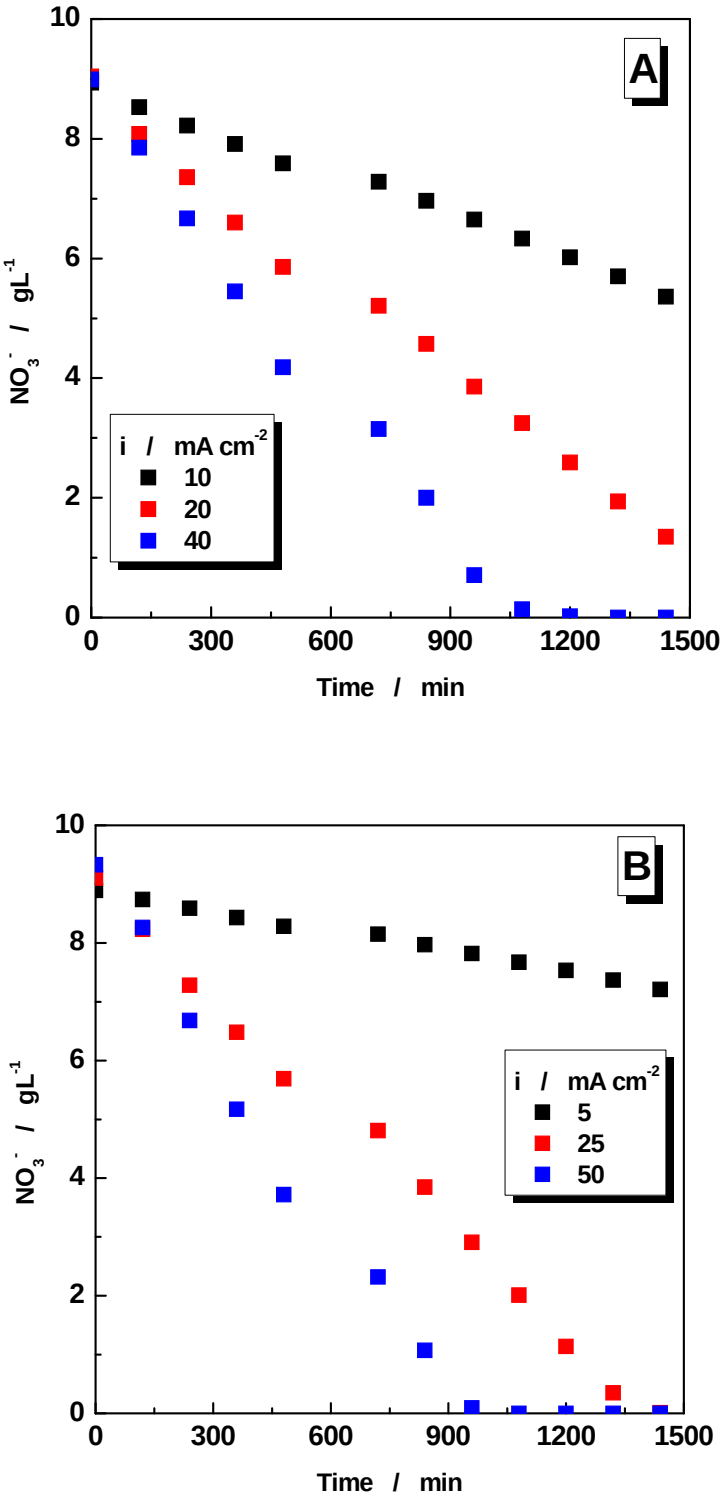

Figure 7.10 Concentration profile of nitrate vs. time at a Cu (A) and CuSn (B) electrode. Experimental conditions: flow rate of 200 mL·min^{-1}; electrolyte: 0.1M $NaNO_3$ + 1M NaOH.

In order to reach the MCL, the prolonged electrolyses need to perform a conversion degree for nitrate of at least 99.5%. As can be seen above (Fig. 7.10) at the Cu electrode the MCL was achieved just at -40 $mA \cdot cm^{-2}$ after 20 h. On the other hand, for the CuSn electrode, at -25 $mA \cdot cm^{-2}$, the MCL was achieved after 22 h, while at the highest current density (-50 $mA \cdot cm^{-2}$) the MCL was reached after 18 h.

Based on the experimental results (see Fig. 7.10) it can be stated that the CuSn electrode exhibits a better performance for the ERN process, illustrated by shorter reaction times and lower energy consumption. Moreover, the performance of the CuSn electrode does not improve at higher current densities (-50 $mA \cdot cm^{-2}$) in comparison to the cases where low current densities are used.

The key parameters which describe the ERN process were evaluated based on the experimental results and are presented in Table 7.2. The time values from Table 7.2 represent the duration of electrolysis until the MCL was reached. All the values were calculated at a flow rate of 200 $mL \cdot min^{-1}$.

Table 7.2: Current efficiency (r_F) and energy consumption (W_s) values for the ERN at Cu and CuSn electrodes, obtained in synthetic nitrate solutions.

Electrode material	**i (mA/cm^2)**	**E_{cell} (V)**	**Time (h)**	**r_F (%)**	**W_s (kWh/kg $NaNO_3$)**
Cu	10	2.9	24*	48	4
	20	4.8	24*	35	9
	40	6.5	20	21	15
CuSn	5	2.4	24*	74	2
	25	2.9	22	34	4
	50	5.5	18	22	16

*the MCL was not reached in the given time period

Based on the energy consumption values (Table 7.2) the following conclusions were formulated:

In the studied current density ranges, for treatment of the same volume of solution, the ERN process needs less energy when a CuSn alloy cathode is used. This could be explained by the higher electrocatalytic activity (see Chapter 6) of the alloy material, which is in agreement with the kinetic data, obtained for small current densities (see Section 7.2.2).

The calculated W_s values (at higher current densities) are in accordance with those obtained by Katsouranos et al. [13], who succeeded to remove nitrate from an alkaline medium at an energy consumption value of 16.5 kWh/kg $NaNO_3$ at a Sn electrode. Similarly, Reyter et al. [162] studied the electroreduction of nitrate at a Cu electrode and obtained an energy consumption value of 25 kWh/kg $NaNO_3$.

The energy consumption values shown in Table 7.2 depend largely on the pilot unit configuration and they could be significantly decreased by a better design of the electrochemical reactor. Therefore, we can conclude that the CuSn alloy is a suitable electrode material for ERN because it can be used in a large range of current densities and has a higher electrocatalytic activity compared to the Cu cathode. At low current densities, the energy consumption is similar for both materials. However, when increasing the cell current density, the energy consumption is higher for Cu than for CuSn. This is illustrated by an increase in the nitrate destruction time and a larger cell voltage.

7.4. Conclusions

Electrochemical destruction of nitrate and nitrite has been demonstrated in an engineering laboratory scale flow reactor under different operating conditions. In the used flow reactor the nitrate/nitrite destruction efficiency was improved with an increase in the current density and operation of the cell in a divided configuration. On the two investigated types of cathode materials (Cu and CuSn), the concentration of nitrate was reduced electrochemically to the maximum permissible limit (50 mg/L in drinking water). An identical quantity of nitrate (8.5 g) was reduced at the CuSn cathode, below the permissible limit (99.5% conversion), in 18 h, and at the Cu cathode in 20 h. In both cases, as the current density increases the removal efficiency increases, less time being needed to reduce nitrate successfully.

A comparison between apparent rate constants *vs.* current densities (at low values) at Cu and CuSn cathodes was performed (Fig. 7.5). Moreover, the electroreduction of nitrate was investigated at several flow rates (see Section 7.2.2). The results show that, at small

current densities charge transfer occurs slowly and, therefore, the mass transport does not have a significant influence on the ERN process. Comparisons between these two electrodes indicate definite advantages in using the CuSn alloy for nitrate and nitrite destruction. The energy consumption values, estimated in this thesis are comparable and even smaller compared to literature data.

8. GENERAL CONCLUSIONS

The electrochemical method used within this doctoral thesis was focused on the removal of nitrate and nitrite from alkaline model nitrate solutions. This method is the most advantageous among all the proposed alternative methods (Chapter 2 and 3).

The first part of the thesis (Chapters 1 - 3) is dedicated to literature review. It has been explained that the application of electrochemical reduction of nitrate (ERN) is useful also at high concentrations of nitrate where the biological methods cannot be applied (Section 2.3). Moreover, a comparison with other methods was presented (Chapter 2). By applying the electrochemical methods, nitrates can be reduced to nitrite, hydroxylamine, ammonia, nitrogen oxides and molecular nitrogen; products that depend strongly on the nature of the electrode material (Chapter 3). An overview on the specific parameters of ERN processes are presented in Table 3.1. This table contains information about the electrochemical reactors, detailed aspects of the electrode materials, electrolyte composition, pH, electrochemical parameters (current density, electrode potential) which are essential for a better knowledge of the ERN process. The study of the ERN has been described extensively in Section 3.3.

Chapter 5 deals with the synthesis of the electrode materials (Cu and CuSn alloy) used for ERN. The CV studies allowed us to establish the specific parameters concerning the electrodeposition of the individual metals and their alloy (see Fig. 5.3 and 5.4). For the synthesis of the Cu, Sn and CuSn electrode materials three different concentrations (Fig. 5.5A and B) were investigated.

SEM images taken for copper, tin and copper-tin alloy deposits indicate significant changes in their surface morphology by changing the electrodeposition parameters (Fig. 5.10-5.15). Moreover, the RDE tests showed that the rotational speed (intensified mass transport) plays an important role in the process of electrodeposition, showing a significant improvement of deposits. In order to obtain uniform deposits, the 2000 rpm seems to be a suitable rotational speed. Based on SEM measurements the CuSn deposits are more uniform if potentiostatic deposition is applied (Section 5.3.3.2).

The EDX analyses showed that a CuSn alloy was obtained with a content of 27% Cu and 73 % Sn, respectively ($Cu_{27}Sn_{73}$). This alloy electrode material had the highest content of Sn obtained and based on the literature study it is a suitable electrode material for nitrate reduction (Table 5.6).

The electrocatalytic properties of the synthesized electrode materials were further investigated in Chapter 6. For this purpose the detection of the electroactive species resulting from ERN was investigated.

A simple and fast electroanalytical methodology for determination of electroactive products resulting from nitrate reduction in alkaline media is proposed on the basis of cyclic hydrodynamic voltammetry (CHV) and square wave voltammetry (SWV). These methods allowed us to detect simultaneously the involved species resulting from ERN (Section 6.4.2). It was demonstrated that the electroactive products resulting from ERN in alkaline media can be detected by the SWV technique at Cu and CuSn plated Pt electrodes (see Section 6.4.2). Moreover, using SWV ammonium can be electrochemically detected (see Fig. 6.12 and 6.13) with good accuracy. In this work for the first time it was achieved the detection of ammonium using SWV method.

The measurements performed in mono-component solutions prove that, combining CV and SWV at high scan rates with hydrodynamic techniques and using an adequate pH value, at least three different electroactive species generated from the NO_3^- reduction (NO_2^-, NH_2-OH and NH_4^+) can be electrochemically detected (Fig. 6.1 - 6.3).

Using both techniques, the optimal conditions for the voltammetric detection of electroactive species resulting from nitrate reduction were established (Section 6.2). The results obtained with the CHV and SWV techniques allow a real-time evaluation of the electrocatalytic properties of the electrode materials.

The electrocatalytic activity of the Cu and CuSn electrodes was investigated in Section 6.3. The voltammograms, recorded successively without Cu layer refreshing, demonstrated that the electrocatalytic activity of the electrode material decreased (Figure 6.6 - 6.8). This decrease is explained with the electrode poisoning by adsorbed hydrogen, blocking the electrode surface for further reduction of N-containing species.

Electrochemical destruction of nitrate and nitrite has been demonstrated in a laboratory scale flow reactor under different operating conditions (Chapter 7). On the two investigated types of cathode materials (Cu and CuSn), the concentration of nitrate was reduced electrochemically to the maximum permissible limit (50 mg/L in the EU).

A comparison between apparent rate constants *vs.* current densities at Cu and CuSn cathodes was performed (Fig. 7.5). Moreover, the electroreduction of nitrate was investigated at several flow rates (Section 7.2.2). The results show that, at small current densities, charge

transfer occurs slowly and, therefore, the mass transport does not have a significant influence on the ERN process.

An identical quantity of nitrate, was reduced at the CuSn cathode below the permissible limit (99.5% conversion), in 18 h while at the Cu cathode the process needed 20 h. In both cases, as the current density increases the conversion efficiency increases, less time being needed to successfully reduce the nitrate.

Comparisons between the two electrode materials indicate definite advantages of the CuSn alloy for nitrate and nitrite destruction. The energy consumption, estimated for the tests performed in this thesis, are comparable and even smaller compared to literature data.

In the used flow reactor the nitrate/nitrite destruction efficiency was improved with an increase in the current density and operation of the cell in a divided configuration.

9. CONFERENCE CONTRIBUTIONS AND PAPERS

Parts of this work have been published in refereed journals or have been presented at international conferences:

1. Bălaj, F. M.; Imre-Lucaci, F.; Dorneanu, S. A.; Ilea, P., Detection of electroactive products resulted from electrochemical nitrate reduction in alkaline media. International conference *Journees d'Electrochimie*, Sinaia, Romania, **2009**, (Poster).
2. Bălaj, F. M.; Dorneanu, S. A.; Ilea, P., Depoluarea electrochimică a apelor reziduale cu continut de nitrati. International conference *Corrosion and Anti-Corrosion Protection*, Cluj Napoca, Romania, **2009** (oral Presentation).
3. Bălaj, F. M.; Dorneanu, S. A.; Ilea, P., Workshop: *Doctoral studies: science towards society ID 5216 POSDRU/6/1.5/S/3*, Cluj Napoca, Romania, **2009** (oral Presentation).
4. Bălaj, F. M.; Imre-Lucaci, F.; Dorneanu, S. A., Ilea, P., Detection of electroactive products resulted from electrochemical nitrate reduction in alkaline media. *Studia Universitatis Babes-Bolyai Chemia,* **2009**, (SPEC. ISSUE 1), 127-134.
5. Bălaj, F. M.; Dorneanu, S. A.; Ispas, A.; Bund, A.; Ilea, P., Detection of products resulting from nitrate reduction in alkaline media by square wave voltammetry. International conference *Electrochemistry - From microscopic understanding to global impact*, Bochum, Germany, **2010** (Poster).
6. Bălaj, F. M.; Imre-Lucaci, F.; Dorneanu, S. A.; Ilea, P., Synthesis and characterisation of some metallic materials for nitrate reduction. *The 61st Annual Meeting of ISE – Electrochemistry from Biology to Physics*, Nice, France, **2010**, (Poster).
7. Cuibus, F. M.; Ispas, A.; Bund, A.; Ilea, P., Square Wave Voltammetry for the Detection of Electroactive Products Resulting from Nitrate Reduction at a Copper-Tin Alloy Electrode. International conference *Engineering of Functional Interfaces*, Linz, Austria, **2011** (Poster).
8. Cuibus, F. M.; Dorneanu, S. A.; Ispas, A.; Bund, A.; Ilea, P., Square Wave Voltammetry for the detection of electroactive products resulting from nitrate reduction at a Cu-Sn Alloy electrode. International conference *The 220th ECS Meeting*, Boston, MA, USA, **2011** (oral Presentation).
9. Cuibus, F. M.; Ispas, A.; Bund, A.; Ilea, P., Square wave voltammetric detection of electroactive products resulting from electrochemical nitrate reduction in alkaline media. *Journal of Electroanalytical Chemistry* **2012**, accepted for publication, DOI: 10.1016/j.jelechem.2012.04.015.

10. Cuibus, F. M.; Ivanov, S. D.; Bund, A.; Ilea, P., Electroreduction of nitrate in an electrochemical flow reactor. *Manuscript in preparation*.

10. REFERENCES

[1] Hudak, P. F.; Regional trends in nitrate content of Texas groundwater. *Journal of Hydrology* **2000,** 228, (1-2), 37-47.

[2] Agrawal, G. D.; Lunkad, S. K.; Malkhed, T., Diffuse agricultural nitrate pollution of groundwaters in India. *Water Science and Technology* **1999,** 39, (3), 67-75.

[3] Almasri, M. N.; Kaluarachchi, J. J., Assessment and management of long-term nitrate pollution of ground water in agriculture-dominated watersheds. *Journal of Hydrology* **2004,** 295, (1-4), 225-245.

[4] Canter, L.; Nitrates in groundwater, Lewis, New York, **1997.**

[5] Bockris, J. O. M.; Kim, J., Electrochemical treatment of low-level nuclear wastes. *Journal of Applied Electrochemistry* **1997,** 27, (6), 623-634.

[6] Agency, U. E. P., Drinking water standards and health advisories. In Office of Water: **2000**.

[7] Gray, N. F., „Drinking Water Quality: Problems and Solutions", J. Wiley & Sons Ltd. Chichester, **1994**.

[8] Wolfe, A. H.; Patz, J. A., Reactive nitrogen and human health: Acute and long-term implications. *Ambio* **2002,** 31, (2), 120-125.

[9] Gibson, Q. H.; The reduction of methemoglobin in red blood cells and studies on the cause of idiophatic methemoglobinemia. *The Biochemical Journal* **1948,** 42, (1), 13-23.

[10] Soares, M. I. M.; Biological denitrification of groundwater. *Water, Air, and Soil Pollution* **2000,** 123, (1-4), 183-193.

[11] Schoeman, J. J.; Steyn, A., Nitrate removal with reverse osmosis in a rural area in South Africa. *Desalination* **2003,** 155, (1), 15-26.

[12] Hiscock, K. M.; Lloyd, J. W.; Lerner, D. N., Review of natural and artificial denitrification of groundwater. *Water Research* **1991,** 25, (9), 1099-1111.

[13] Katsounaros, I.; Dortsiou, M.; Kyriacou, G., Electrochemical reduction of nitrate and nitrite in simulated liquid nuclear wastes. *Journal of Hazardous Materials* **2009,** 171, (1-3), 323-327.

[14] Huang, C. P.; Wang, H. W.; Chiu, P. C., Nitrate Reduction by Metal Iron. *Water Research* **1997,** 32, (8), 2257-2264.

[15] Cyplik, P.; Grajek W. „Removal of nitrates from drinking water by ion exchange", Proceedings of the XV-th Intern. Simposium on Phisica-Chemical Methods of the Mixtures separation "ARC Separatoria 2000" Borowno, Bydgoszcz, June 14 – 17, **2000**, pp. 173 – 174.

[16] Panyor, L.; Fabiani, C., Anion rejection in a nitrate highly rejecting reverse osmosis thin-film composite membrane. *Desalination* **1996,** 104, (3), 165-174.

[17] Milhano, C.; Pletcher D., The electrochemistry and electrochemical technology of nitrate, in R. E. White (Ed.) Modern Aspects of Electrochemistry, Vol. 45, Springer, New York, **2009**, pp. 105.

[18] Haque, I. U.; Wahid, S., Electroreduction of nitric acid to hydroxylamine (a review). *Science International (Lahore)* **2008,** 20, (1), 25-28.

[19] Haque, I. U.; Bano, K., Voltammetric determination of hydroxylamine at platinum. *The Electrochemical Society Transactions* **2007,** 6, (6), 57-65.

[20] Haque, I. U.; Khan, A.; Waheed, S., Electropolymerization at solid electrodes. *Science International (Lahore)* **2007,** 19, (3), 199-202.

[21] Bard, A. J.; L. R. Faulkner, Electrochemical Methods, Fundamentals and Applications, Wiley, New Jersey, **2001**.

[22] Li, H. L.; Robertson, D. H.; Chambers, J. Q.; Hobbs, D. T., Electrochemical reduction of nitrate and nitrite in concentrated sodium hydroxide at platinum and nickel electrodes. *Journal of the Electrochemical Society* **1988,** 135, (5), 1154-1158.

[23] Rajeshwar, K.; Ibanez J. Environmental Electrochemistry: Fundamentals and Applications in Pollution Abatement, San Diego: Academic Press, Inc., **1997.**

[24] Pletcher, D; Walsh FC. “Industrial Electrochemistry” 2nd ed. London: Blackie Academic and Professional, **1993**.

[25] Stucki, S.; Switzerlad N., Winkler D., "Process for complete removal of nitrites and nitrates from an aqueous solution", Patent Lauchringen, Fed. Rep. Of Germany, **1990.**

[26] Mani, K. N., Electrodialysis water splitting technology. *Journal of Membrane Science* **1991,** 58, (2), 117-138.

[27] Brett, C. M. A.; Brett A. M. O., Electrochemistry Principles, Methodes, and Applications, Oxford University Press, Oxford, UK, **1994**.

[28] Wang, J., *Analytical Electrochemistry, 2nd ed.* Wiley & Sons Inc., New York, USA, **2001**.

[29] Denuault, G.; Milhano, C.; Pletcher, D., Mesoporous palladium - The surface electrochemistry of palladium in aqueous sodium hydroxide and the cathodic reduction of nitrite. *Physical Chemistry Chemical Physics* **2005,** 7, (20), 3545-3551.

[30] Dima, G. E.; De Vooys, A. C. A.; Koper, M. T. M., Electrocatalytic reduction of nitrate at low concentration on coinage and transition-metal electrodes in acid solutions. *Journal of Electroanalytical Chemistry* **2003,** 554-555, (1), 15-23.

[31] Da Cunha, M. C. P. M.; De Souza, J. P. I.; Nart, F. C., Reaction pathways for reduction of nitrate ions on platinum, rhodium, and platinum-rhodium alloy electrodes. *Langmuir* **2000,** 16, (2), 771-777.

[32] Taguchi, S.; Feliu, J. M., Electrochemical reduction of nitrate on Pt(S)[n(1 1 1) × (1 1 1)] electrodes in perchloric acid solution. *Electrochimica Acta* **2007,** 52, (19), 6023-6033.

[33] Brylev, O.; Sarrazin, M.; Roué, L.; Bélanger, D., Nitrate and nitrite electrocatalytic reduction on Rh-modified pyrolytic graphite electrodes. *Electrochimica Acta* **2007,** 52, (21), 6237-6247.

[34] Tucker, P. M.; Waite, M. J.; Hayden, B. E., Electrocatalytic reduction of nitrate on activated rhodium electrode surfaces. *Journal of Applied Electrochemistry* **2004,** 34, (8), 781-796.

[35] Brylev, O.; Sarrazin, M.; Bélanger, D.; Roué, L., Rhodium deposits on pyrolytic graphite substrate: Physico-chemical properties and electrocatalytic activity towards nitrate reduction in neutral medium. *Applied Catalysis B: Environmental* **2006,** 64, (3-4), 243-253.

[36] Ohmori, T.; El-Deab, M. S.; Osawa, M., Electroreduction of nitrate ion to nitrite and ammonia on a gold electrode in acidic and basic sodium and cesium nitrate solutions. *Journal of Electroanalytical Chemistry* **1999,** 470, (1), 46-52.

[37] Cattarin, S., Electrochemical reduction of nitrogen oxyanions in 1 M sodium hydroxide solutions at silver, copper and CuInSe2 electrodes. *Journal of Applied Electrochemistry* **1992,** 22, (11), 1077-1081.

[38] Reyter, D.; Bélanger, D.; Roué, L., Study of the electroreduction of nitrate on copper in alkaline solution. *Electrochimica Acta* **2008,** 53, (20), 5977-5984.

[39] Bouzek, K.; Paidar, M.; Sadílková, A.; Bergmann, H., Electrochemical reduction of nitrate in weakly alkaline solutions. *Journal of Applied Electrochemistry* **2001,** 31, (11), 1185-1193.

[40] Xiang, Y.; Zhou, D. L.; Rusling, J. F., Electrochemical conversion of nitrate to ammonia in water using Cobalt-DIM as catalyst. *Journal of Electroanalytical Chemistry* **1997,** 424, (1-2), 1-3.

[41] Li, H. L.; Chambers, J. Q.; Hobbs, D. T., Electroreduction of nitrate ions in concentrated sodium hydroxide solutions at lead, zinc, nickel and phthalocyanine-modified electrodes. *Journal of Applied Electrochemistry* **1988,** 18, (3), 454-458.

[42] Katsounaros, I.; Kyriacou, G., Influence of the concentration and the nature of the supporting electrolyte on the electrochemical reduction of nitrate on tin cathode. *Electrochimica Acta* **2007,** 52, (23), 6412-6420.

[43] De, D.; Englehardt, J. D.; Kalu, E. E., Cyclic voltammetric studies of nitrate and nitrite ion reduction at the surface of iridium-modified carbon fiber electrode. *Journal of the Electrochemical Society* **2000,** 147, (11), 4224-4228.

[44] Ureta-Zañartu, S.; Yáñez, C., Electroreduction of nitrate ion on Pt, Ir and on 70:30 Pt: Ir alloy. *Electrochimica Acta* **1997,** 42, (11), 1725-1731.

[45] Mácová, Z.; Bouzek, K.; Šerák, J., Electrocatalytic activity of copper alloys for NO3- Reduction in a weakly alkaline solution: Part 2: Copper-tin. *Journal of Applied Electrochemistry* **2007,** 37, (5), 557-566.

[46] De Vooys, A. C. A.; Van Santen, R. A.; Van Veen, J. A. R., Electrocatalytic reduction of NO-3 on palladium/copper electrodes. *Journal of Molecular Catalysis A: Chemical* **2000,** 154, (1-2), 203-215.

[47] Dou, D.; Liu, D. J.; Williamson, W. B.; Kharas, K. C.; Robota, H. J., Tin promoted palladium catalysts for nitrate removal from drinking water. *Applied Catalysis B: Environmental* **2001,** 30, (1-2), 111-122.

[48] Lemaignen, L.; Tong, C.; Begon, V.; Burch, R.; Chadwick, D., Catalytic denitrification of water with palladium-based catalysts supported on activated carbons. *Catalysis Today* **2002,** 75, (1-4), 43-48.

[49] Shimazu, K.; Kawaguchi, T.; Tada, K., Preparation of binary metal electrocatalysts by self-assembly of precursor ionic species on gold and reduction of nitrate ions. *Journal of Electroanalytical Chemistry* **2002,** 529, (1), 20-27.

[50] Mácová, Z.; Bouzek, K., Electrocatalytic activity of copper alloys for NO3- reduction in a weakly alkaline solution: Part 1: Copper-zinc. *Journal of Applied Electrochemistry* **2005,** 35, (12), 1203-1211.

[51] Gootzen, J. F. E.; Lefferts, L.; Van Veen, J. A. R., Electrocatalytic nitrate reduction on palladium based catalysts activated with germanium. *Applied Catalysis A: General* **1999,** 188, (1-2), 127-136.

[52] Szpyrkowicz, L.; Daniele, S.; Radaelli, M.; Specchia, S., Removal of NO3- from water by electrochemical reduction in different reactor configurations. *Applied Catalysis B: Environmental* **2006,** 66, (1-2), 40-50.

[53] Duncan, H.; Lasia, A., Mechanism of hydrogen adsorption/absorption at thin Pd layers on Au(1 1 1). *Electrochimica Acta* **2007,** 52, (21), 6195-6205.

[54] Casella, I. G.; Gatta, M., Electrochemical reduction of NO3- and NO 2- on a composite copper thallium electrode in alkaline solutions. *Journal of Electroanalytical Chemistry* **2004,** 568, (1-2), 183-188.

[55] Polatides, C.; Kyriacou, G., Electrochemical reduction of nitrate ion on various cathodes - Reaction kinetics on bronze cathode. *Journal of Applied Electrochemistry* **2005,** 35, (5), 421-427.

[56] Genders, J. D.; Hartsough, D.; Hobbs, D. T., Electrochemical reduction of nitrates and nitrites in alkaline nuclear waste solutions. *Journal of Applied Electrochemistry* **1996,** 26, (1), 1-9.

[57] Moorcroft, M. J.; Davis, J.; Compton, R. G., Detection and determination of nitrate and nitrite: A review. *Talanta* **2001,** 54, (5), 785-803.

[58] Andrade, F. V.; Deiner, L. J.; Varela, H.; De Castro, J. F. R.; Rodrigues, I. A.; Nart, F. C., Electrocatalytic reduction of nitrate over palladium nanoparticle catalysts: A temperature-dependent study. *Journal of the Electrochemical Society* **2007,** 154, (9), F159-F164

[59] Scharifker, B. R.; Mostany, J.; Serruya, A., Catalytic reduction of nitrate during electrodeposition of thallium from Tl3+ solution. *Electrochemistry Communications* **2000,** 2, (6), 448-451

[60] Gauthard, F.; Epron, F.; Barbier, J., Palladium and platinum-based catalysts in the catalytic reduction of nitrate in water: Effect of copper, silver, or gold addition. *Journal of Catalysis* **2003,** 220, (1), 182-191

[61] Gootzen, J. F. E.; Peeters, P. G. J. M.; Dukers, J. M. B.; Lefferts, L.; Visscher, W.; Van Veen, J. A. R., The electrocatalytic reduction of NO-3 on Pt, Pd and Pt + Pd electrodes activated with Ge. *Journal of Electroanalytical Chemistry* **1997,** 434, (1-2), 171-183.

[62] Tada, K.; Shimazu, K., Kinetic studies of reduction of nitrate ions at Sn-modified Pt electrodes using a quartz crystal microbalance. *Journal of Electroanalytical Chemistry* **2005,** 577, (2), 303-309.

[63] Tada, K.; Kawaguchi, T.; Shimazu, K., High electrocatalytic performance of Pd/Sn/Au electrodes for nitrate reduction. *Journal of Electroanalytical Chemistry* **2004,** 572, (1), 93-99.

[64] De Groot, M. T.; Koper, M. T. M., The influence of nitrate concentration and acidity on the electrocatalytic reduction of nitrate on platinum. *Journal of Electroanalytical Chemistry* **2004,** 562, (1), 81-94.

[65] Wang, Y.; Qu, J.; Wu, R.; Lei, P., The electrocatalytic reduction of nitrate in water on Pd/Sn-modified activated carbon fiber electrode. *Water Research* **2006,** 40, (6), 1224-1232.

[66] Piao, S.; Kayama, Y.; Nakano, Y.; Nakata, K.; Yoshinaga, Y.; Shimazu, K., Nitrate reduction on tin-modified rhodium, ruthenium, and iridium electrodes. *Journal of Electroanalytical Chemistry* **2009,** 629, (1-2), 110-116.

[67] Li, M.; Feng, C.; Zhang, Z.; Sugiura, N., Efficient electrochemical reduction of nitrate to nitrogen using Ti/IrO2-Pt anode and different cathodes. *Electrochimica Acta* **2009,** 54, (20), 4600-4606.

[68] Badea, G. E., Electrocatalytic reduction of nitrate on copper electrode in alkaline solution. *Electrochimica Acta* **2009,** 54, (3), 996-1001.

[69] Polatides, C.; Dortsiou, M.; Kyriacou, G., Electrochemical removal of nitrate ion from aqueous solution by pulsing potential electrolysis. *Electrochimica Acta* **2005,** 50, (25-26 SPEC. ISS.), 5237-5241.

[70] Trinidad, P.; Walsh, F.; Gilroy, D., Conversion expressions for electrochemical reactors which operate under mass transport controlled reaction conditions, part I: Batch reactor, PFR and CSTR. *International Journal of Engineering Education* **1998,** 14, (6), 431-441.

[71] Hobbs, D. T., In *Electrochemical treatment of liquid wastes*, Efficient separations and crosscutting program, technical exchange meeting, Gaithersburg, MD, USA, 1997; Gaithersburg, MD, USA, **1997**.

[72] Lin, S. H.; Wu, C. L., Electrochemical removal of nitrite and ammonia for aquaculture. *Water Research* **1996,** 30, (3), 715-721.

[73] Lu, C.; Lu, S.; Qiu, W.; Liu, Q., Electroreduction of nitrate to ammonia in alkaline solutions using hydrogen storage alloy cathodes. *Electrochimica Acta* **1999,** 44, (13), 2193-2197.

[74] Paidar, M.; Bouzek, K.; Bergmann, H., Influence of cell construction on the electrochemical reduction of nitrate. *Chemical Engineering Journal* **2002,** 85, (2-3), 99-109.

[75] Kuroda, M.; Watanabe, T.; Umedu, Y., Simultaneous COD removal and denitrification of wastewater by bio-electro reactors. *Water Science and Technology* **1997,** 35, 161-168.

[76] Jha, K.; Weidner, J. W., Evaluation of porous cathodes for the electrochemical reduction of nitrates and nitrites in alkaline waste streams. *Journal of Applied Electrochemistry* **1999,** 29, (11), 1305-1315.

[77] Ranjit, K. T.; Viswanathan, B., Photoelectrochemical reduction of nitrite ions to ammonia on CdS photocatalysts. *Journal of Photochemistry and Photobiology A: Chemistry* **2003,** 154, (2-3), 299-302.

[78] Sakakibara, Y.; Araki, K.; Watanabe, T.; Kuroda, M., The denitrification and neutralization performance of an electrochemically activated biofilm reactor used to treat nitrate-contaminated groundwater. *Water Science and Technology* **1997,** 36, 61-68.

[79] Feleke, Z.; Araki, K.; Sakakibara, Y.; Watanabe, T.; Kuroda, M., Selective reduction of nitrate to nitrogen gas in a biofilm-electrode reactor. *Water Research* **1998,** 32, (9), 2728-2734.

[80] Chen, S. M., Bicatalyst electrocatalytic reduction and oxidation of nitrite by Fe(II) and Cu(II) complexes in the same solution. *Journal of Electroanalytical Chemistry* **1998,** 457, (1-2), 23-30.

[81] Katsounaros, I.; Kyriacou, G., Influence of nitrate concentration on its electrochemical reduction on tin cathode: Identification of reaction intermediates. *Electrochimica Acta* **2008,** 53, (17), 5477-5484.

[82] Bradbury, D., "Method for the combined removal and destruction of nitrate ions", European Patent specification, **1994**.

[83] Katsounaros, I.; Ipsakis, D.; Polatides, C.; Kyriacou, G., Efficient electrochemical reduction of nitrate to nitrogen on tin cathode at very high cathodic potentials. *Electrochimica Acta* **2006,** 52, (3), 1329-1338.

[84] Shimazu, K.; Goto, R.; Piao, S.; Kayama, R.; Nakata, K.; Yoshinaga, Y., Reduction of nitrate ions on tin-modified palladium thin film electrodes. *Journal of Electroanalytical Chemistry* **2007,** 601, (1-2), 161-168.

[85] Hörold, S.; Vorlop, K. D.; Tacke, T.; Sell, M., Development of catalysts for a selective nitrate and nitrite removal from drinking water. *Catalysis Today* **1993,** 17, (1-2), 21-30.

[86] Cheng, H.; Scott, K.; Christensen, P. A., Application of a solid polymer electrolyte reactor to remove nitrate ions from wastewater. *Journal of Applied Electrochemistry* **2005,** 35, (6), 551-560.

[87] Hiro, M.; Kouchi, Koizumi T., Rakuma T., "Nitrogen treating method", Sanyo Electric Co., Ltd., Moriguchishi (JP) **2007.**

[88] Kaczur, J. J.; Cawlfield D. W., Woodard K. E., "Process for the removal of oxynitrogen species for the aqueous solution", Olin Corporation Stamford, Conn. **1994.**

[89] Vorlop, K-D.; Tacke T., Sell M., Strauss G., "Process for removing the nitrite and/or nitrate content in water", Umweltschutztechnologie GmbH GUTEC: Gesellschaft zur Entwicklung von, Hanover, Fed. Rep. of Germany, **1991.**

[90] Yamada A.; Ikematsu, M.; Iseki M.; Takaoka D., Ogawa Y., Kurokawa Y., "Method for treating for-treatment water containing organic matter and nitrogen compound", Sanyo Electric Co., Ltd., Osaka (JP), **2007**.

[91] Velin, A.; Resbeut, S., "Process and apparatus for removal and destruction of dissolved nitrate", **2004.**

[92] Velzen, D. V.; Langenkamp H., Moryoussef A., „Process for removing nitrogen compounds from a liquid", European Atomic Energy Community, **1994**.

[93] Orlebeke, D. N.; „Electrolytic treatment of aqueous media", Aquatic Tehnologies, McMinnville, OR, US, **2004**.

[94] Mindler, A. B., Princeton S. B., Baldwin T., "Electrolytic reduction of nitrate from solutions of alkali metal hydroxides", Hydronics Corporation, Metuchen, N.J., US, **1970**.

[95] Adams, R. N., *Electrochemistry at Solid Electrodes*. Marcel Dekker: New York, USA, **1969**.

[96] Bruckenstein, S.; Miller, B., Unraveling reactions with rotating electrodes. *Accounts of Chemical Research* **1977,** 10, (2), 54-61

[97] Oniciu, L.; Mureşan, L., *Electrochimie aplicată*. Presa Universitară Clujeană: Cluj-Napoca, Romania, **1998.**

[98] Gorton, L.; Dominguez, E., Electrochemistry of NAD (P)+/NAD (P) H. In *Bioelectrochemistry*, Wilson, G. S., Ed. Wiley: New York, USA, **2002**.

[99] O'Dea, J. J.; Osteryoung, J.; Osteryoung, R. A., Theory of square wave voltammetry for kinetic systems. *Analytical Chemistry* **1981,** 53, (4), 695-701.

[100] O'Dea, J.; Wojciechowski, M.; Osteryoung, J.; Aoki, K., Square wave voltammetry at electrodes having a small dimension. *Analytical Chemistry* **1985,** 57, (4), 954-955.

[101] Whelan, D. P.; O'Dea, J. J.; Osteryoung, J.; Aoki, K., Square wave voltammetry at small disk electrodes.Theory and experiment. *Journal of Electroanalytical Chemistry* **1986,** 202, (1-2), 23-36.

[102] Aoki, K.; Tokuda, K.; Matsuda, H.; Osteryoung, J., Reversible square-wave voltammograms independence of electrode geometry. *Journal of Electroanalytical Chemistry* **1986**, 207, (1-2), 25-39.

[103] Henze, G., Analytical Voltammetry and Polarography, Wiley-VCH Verlag GmbH & Co. KGaA, Weinheim, Germany, **2008**.

[104] Osteryoung, J.; O'Dea, J. J., Square-WaveVoltammetry. In *Electroanalytical Chemistry*, Bard, A. J., Ed. Marcel Dekker: New York, USA, **1986**.

[105] Goldstein, J. I.; Newburg, D. E.; Echlin, P.; Joy, D. C.; Fiori, C.; Lifshin, E., *Scanning Electron Microscopy and X-Ray Microanalysis, 2nd ed.* Plenum Press: New York and London, USA and UK, **1984**.

[106] Wells, O. C.; Boyde A., E. Lifshin, A. Rezanowich, *Scanning Electron Microscopy* McGraw-Hill Book Company, Columbus, OH, USA, **1974**.

[107] Lawes, G., *Scanning Electron Microscopy and X-Ray Microanalysis* Ed. John Wiley & Sons, Chichester, UK, **1987**.

[108] Jackson, P. E., Ion Chromatography in Environmental Analysis in Encyclopedia of Analytical Chemistry edited byR.A. Meyers,John Wiley & Sons Ltd, Chichester, UK, **2000.**

[109] Milli-Q® Direct Water purification system Brochure, www.millipore.com

[110] Shams El Din, A. M.; Abd El Wahab, F. M., The Behaviour of copper-tin alloys in alkaline solutions upon alternate anodic and cathodic polarization. *ElectrochimicaActa* **1965,** 10, (11), 1127-1140.

[111] Huttunen-Saarivirta, E.; Tiainen, T., Characterising the quality of chemical tin coatings on copper by electrochemical current noise method. *Applied Surface Science* **2002,** 191, (1-4), 106-117.

[112] Padhi, D.; Gandikota, S.; Nguyen, H. B.; McGuirk, C.; Ramanathan, S.; Yahalom, J.; Dixit, G., Electrodeposition of copper-tin alloy thin films for microelectronic applications. *Electrochimica Acta* **2003,** 48, (8), 935-943.

[113] Hassoun, J.; Panero, S.; Scrosati, B., New electrochemical process for the in situ preparation of metal electrodes for lithium-ion batteries. *Electrochemistry Communications* **2007,** 9, (6), 1239-1241.

[114] Huttunen-Saarivirta, E., Observations on the uniformity of immersion tin coatings on copper. *Surface and Coatings Technology* **2002,** 160, (2-3), 288-294.

[115] Galdikiené, O.; Mockus, Z., Cathodic process in copper-tin deposition from sulphate solutions. *Journal of Applied Electrochemistry* **1994,** 24, (10), 1009-1012.

[116] Low, C. T. J.; Walsh, F. C., The stability of an acidic tin methanesulfonate electrolyte in the presence of a hydroquinone antioxidant. *Electrochimica Acta* **2008,** 53, (16), 5280-5286.

[117] Yan, J. W.; Wu, J. M.; Wu, Q.; Xie, Z. X.; Mao, B. W., Competitive adsorption and surface alloying: Underpotential deposition of Sn on sulfate-covered Cu(111). *Langmuir* **2003,** 19, (19), 7948-7954.

[118] Carlos, I. A.; Souza, C. A. C.; Pallone, E. M. J. A.; Francisco, R. H. P.; Cardoso, V.; Lima-Neto, B. S., Effect of tartrate on the morphological characteristics of the copper-tin electrodeposits from a noncyanide acid bath. *Journal of Applied Electrochemistry* **2000,** 30, (8), 987-994.

[119] Survila, A.; Mockus, Z.; Kanapeckaite, S.; Jasulaitiene, V.; Juškenas, R., Codeposition of copper and tin from acid sulphate solutions containing polyether sintanol DS-10 and micromolar amounts of halides. *Electrochimica Acta* **2007,** 52, (9), 3067-3074.

[120] Anuar, K.; Tan, W. T.; Atan, M. S.; Dzulkefly, K.; Ho, S. M.; Jelas, H.; Saravanan, N., Cyclic Voltammetry Study of Copper Tin Sulfide Compounds. *The Pacific Journal of Science and Technology* **2007,** 8, (2), 252-260.

[121] Kim, K. Y.; Yang, B. Y., Electrochemical study on Zn-Sn-alloy-coated steel sheets deposited by vacuum evaporation. Part I. *Surface and Coatings Technology* **1994,** 64, (2), 99-110.

[122] Vitkova, S.; Ivanova, V.; Raichevsky, G., Electrodeposition of low tin content zinc-tin alloys. *Surface and Coatings Technology* **1996,** 82, (3), 226-231.

[123] Latimer W. M. *The oxidation States of the Elements and their Potentials in Aqueous solutions*, *2nd ed*., Prentice-Hall, New Jersey, USA, **1952**, pp. 392.

[124] Schlesinger, M.; Paunovic, M., *Modern Electroplating, 4th ed.* John Wiley and Sons: New Jersey, USA, **2000**.

[125] Pourbaix, M., *Atlas of Electrochemical Equilibria in Aqueous Solutions*. Pergamon: New York, USA, **1966**.

[126] He, A.; Liu, Q.; Ivey, D. G., Electrodeposition of tin: A simple approach. *Journal of Materials Science: Materials in Electronics* **2008,** 19, (6), 553-562

[127] Kremann, R.; Suchy, C. T.; Lorber, J.; Maas, R., Zur elektrolytischen Abscheidung von Legierungen und deren metallographische und mechanische Untersuchung. II. Mitteilung: über Versuche zur Abscheidung von Kupfer-Zinnbronzen. *Monatshefte für Chemie* **1914,** 35, (3), 219-288.

[128] Vaid, J.; Rama Char, T. L., Electrodeposition of Copper-Tin Alloys from the Pyrophophate Bath. *Curent Science* **1953,** 22, 170-171.

[129] Strow, H., Brass and Bronze Electroplating. In *Metal Finishing, 68th Guidebook & Directory*, **2001**.

[130] Finazzi, G. A.; de Oliveira, E. M.; Carlos, I. A., Development of a sorbitol alkaline Cu-Sn plating bath and chemical, physical and morphological characterization of Cu-Sn films. *Surface and Coatings Technology* **2004,** 187, (2-3), 377-387.

[131] Juškenas, R.; Mockus, Z.; Kanapeckaite, S.; Stalnionis, G.; Survila, A., XRD studies of the phase composition of the electrodeposited copper-rich Cu-Sn alloys. *Electrochimica Acta* **2006,** 52, (3), 928-935.

[132] Grujicic, D.; Pesic, B., Electrodeposition of copper: The nucleation mechanisms. *Electrochimica Acta* **2002,** 47, (18), 2901-2912.

[133] Quemper, J. M.; Dufour-Gergam, E.; Frantz-Rodriguez, N.; Gilles, J. P.; Grandchamp, J. P.; Bosseboeuf, A., Effects of direct and pulse current on copper electrodeposition through photoresist molds. *Journal of Micromechanics and Microengineering* **2000,** 10, (2), 116-119.

[134] Torrent-Burgués, J.; Guaus, E.; Sanz, F., Initial stages of tin electrodeposition from sulfate baths in the presence of gluconate. *Journal of Applied Electrochemistry* **2002,** 32, (2), 225-230.

[135] Bennett, S., The electrodeposition of tin cadmium alloys. *Journal of the Electrodepositors' Technical Society* **1950,** 26, 107-118.

[136] Bălaj, F. M.; Imre-Lucaci, F.; Dorneanu, S. A.; Ilea, P., Synthesis and characterisation of some metallic materials for nitrate reduction. *The 61st Annual Meeting of ISE – Electrochemistry from Biology to Physics*, Nice, France, **2010**, (Poster).

[137] Bălaj, F. M.; Imre-Lucaci, F.; Dorneanu, S. A.; Ilea, P., Detection of electroactive products resulted from electrochemical nitrate reduction in alkaline media. *Studia Universitatis Babes-BolyaiChemia* **2009**, (SPEC. ISSUE 1), 127-134.

[138] Cuibus, F. M.; Ispas, A.; Bund, A.; Ilea, P., Square wave voltammetric detection of electroactive products resulting from electrochemical nitrate reduction in alkaline media. *Journal of Electroanalytical Chemistry* **2012**, submitted, under review.

[139] Bălaj, F. M.; Imre-Lucaci, F.; Dorneanu, S. A.; Ilea, P., Detection of electroactive products resulted from electrochemical nitrate reduction in alkaline media. International conference *Journees d'Electrochimie*, Sinaia, Romania, **2009**, (Poster).

[140] Piela, B.; Wrona, P. K., Oxidation of nitrites on solid electrodes I. Determination of the reaction mechanism on the pure electrode surface. *Journal of the Electrochemical Society* **2002,** 149, (2), E55-E63.

[141] Bălaj, F. M.; Dorneanu, S. A.; Ilea, P., Depoluarea electrochimică a apelor reziduale cu continut de nitrati. International conference *Corrosion and Anti-Corrosion Protection*, Cluj Napoca, Romania, **2009** (oral Presentation).

[142] Gadde, R. R.; Bruckenstein, S., The electroreduction of nitrite in 0.1 M HClO4 at platinum. *Journal of Electroanalytical Chemistry* **1974,** 50, (2), 163-174.

[143] Piela, B.; Wrona, P. K., Oxidation of Hydroxylamine on the Rotating Solid Electrodes: I. Oxidation of Hydroxylamine in Protonated Form. *Journal of the Electrochemical Society* **2004,** 151, (2), E69-E79.

[144] Kelter, P.; Mosher, M.; Schott, A., *Chemistry: The practical Science, Media Enhanced Edition*. Cengage Learning Inc., USA, **2009.**

[145] Lower, S. K., *Acid-Base equilibria and calculations. A Chem1 Reference Text*, **1996.**

[146] Cuibus, F. M.; Ispas, A.; Bund, A.; Ilea, P., Square Wave Voltammetry for the Detection of Electroactive Products Resulting from Nitrate Reduction at a Copper-Tin Alloy Electrode. International conference *Engineering of Functional Interfaces*, Linz, Austria, **2011** (Poster).

[147] Reyter, D.; Odziemkowski, M.; Ɓlanger, D.; Roú, L., Electrochemically activated copper electrodes: Surface characterization, electrochemical behavior, and properties for the electroreduction of nitrate. *Journal of the Electrochemical Society* **2007,** 154, (8), K36-K44.

[148] Petrii, O. A.; Safonova, T. Y., Electroreduction of nitrate and nitrite anions on platinum metals: A model process for elucidating the nature of the passivation by hydrogen adsorption. *Journal of Electroanalytical Chemistry* **1992,** 331, (1-2), 897-912.

[149] Kreizer, V.; Marshakov, I. K.; Tutukina, N. M.; Zartsyn, I. D., The Effect of Oxygen on Copper Dissolution during Cathodic Polarization. *Protection of Metals* **2003,** 39, (1), 30-33.

[150] Marchiano, S. L.; Elsner, C. I.; Arvia, A. J., The anodic formation and cathodic reduction of cuprous oxide films on copper in sodium hydroxide solutions. *Journal of Applied Electrochemistry* **1980,** 10, (3), 365-377.

[151] Abd El Haleem, S. M.; Ateya, B. G., Cyclic voltammetry of copper in sodium hydroxide solutions. *Journal of Electroanalytical Chemistry* **1981,** 117, (2), 309-319.

[152] Dong, S.; Xie, Y.; Cheng, G., Cyclic voltammetric and spectroelectrochemical studies of copper in alkaline solution. *Electrochimica Acta* **1992,** 37, (1), 17-22.

[153] Horanyi, G.; Rizmayer, E. M., Electrocatalytic reduction of NO2- and NO3- ions at a platinized platinum electrode in alkaline medium. *Journal of Electroanalytical Chemistry* **1985,** 188, (1-2), 265-272.

[154] Bălaj, F. M.; Dorneanu, S. A.; Ispas, A.; Bund, A.; Ilea, P., Detection of products resulting from nitrate reduction in alkaline media by square wave voltammetry. International conference *Electrochemistry - From microscopic understanding to global impact*, Bochum, Germany, **2010** (Poster).

[155] Cuibus, F. M.; Dorneanu, S. A.; Ispas, A.; Bund, A.; Ilea, P., Square Wave Voltammetry for the detection of electroactive products resulting from nitrate reduction at a Cu-Sn Alloy electrode. International conference *The 220th ECS Meeting*, Boston, MA, USA, **2011** (oral Presentation).

[156] Endo, K.; Katayama, Y.; Miura, T., A rotating disk electrode study on the ammonia oxidation. *Electrochimica Acta* **2005,** 50, (11), 2181-2185.

[157] Coleman, D. H.; White, R. E.; Hobbs, D. T., A parallel plate electrochemical reactor (PPER) model for the destruction of nitrate and nitrite in alkaline waste solutions. *Journal of the Electrochemical Society* **1995,** 142, (11), 1152-1161.

[158] Bockris, J. O. M.; Kim, J., Electrochemical reductions of Hg(II), ruthenium-nitrosyl complex, chromate, and nitrate in a strong alkaline solution. *Journal of the Electrochemical Society* **1996,** 143, (12), 3801-3808.

[159] Kuwabata, S.; Uezumi, S.; Tanaka, K.; Tanaka, T., Assimilatory and dissimilatory reduction of NO3- and NO2- with an (n-Bu4N)3[Mo2Fe6S 8(SPh)9] modified glassy-carbon electrode in water. *Inorganic Chemistry* **1986,** 25, (17), 3018-3022.

[160] Prasad, P. K. R.; Priya, M. N.; Palanivelu, K., Nitrate removal from groundwater using electrolytic reduction method. *Indian Journal of Chemical Technology* **2005,** 12, (2), 164-169.

[161] Koparal, A. S.; Öütveren, U. B., Removal of nitrate from water by electroreduction and electrocoagulation. *Journal of Hazardous Materials* **2002,** 89, (1), 83-94.

[162] Reyter, D.; Bélanger, D.; Roué, L., Optimization of the cathode material for nitrate removal by a paired electrolysis process. *Journal of Hazardous Materials* **2011,** 192, (2), 507-513.